ÉCOLE DE TECHNOLOGIE SUPÉRIEURE
UNIVERSITÉ DU QUÉBEC

THESIS PRESENTED TO
ÉCOLE DE TECHNOLOGIE SUPÉRIEURE

IN PARTIAL FULFILLMENT OF THE REQUIREMENTS FOR
THE DEGREE OF DOCTOR OF PHILOSOPHY
Ph. D.

BY
Axaykumar RANA

DEVELOPMENT OF HIGHLY SENSITIVE MULTIMODAL TACTILE SENSOR

MONTREAL, "OCTOBER 7TH, 2015"

BOARD OF EXAMINERS

THIS THESIS HAS BEEN EVALUATED

BY THE FOLLOWING BOARD OF EXAMINERS:

Mr. Vincent Duchaine, thesis director
Département de génie de la production automatisée

Mr. Pascal Bigras, co-advisor
Département de génie de la production automatisée

Mr. Ricardo Zednik, committee president
Département de génie mécanique

Mr. Guy Gauthier, invited examiner
Département de génie de la production automatisée

Mr. Shahbaz Youssefi, external examiner
Kinova Robotics, QC, Canada

THIS THESIS WAS PRESENTED AND DEFENDED

IN THE PRESENCE OF A BOARD OF EXAMINERS AND THE PUBLIC

ON "OCTOBER 5TH, 2015"

AT ÉCOLE DE TECHNOLOGIE SUPÉRIEURE

ACKNOWLEDGEMENTS

My Ph. D thesis would be not be complete without an elucidation of the efforts of those who have supported me. It is my honor to capture this esteemed opportunity for acknowledging all my mentors and colleagues for their assistance and encouragement.

I begin with my supervisor, Professor Vincent Duchaine, whose visionary guidance, intuitive advice and efficient management have provided many of the ingredients that turned this Ph.D. from an idea into an achievement! Also, I would like to thank my colleagues for guiding me in brainstorming the solutions, rejuvenating the engineering concepts, and relieving my stress through our enjoyable talks. Jean-Baptiste, Reza, Rachid, Kate, Long-Fei, Jean-Philippe, Deen, Salman; all of my 'CoRo'mates are the influential geeks who have reinforced my spirit and ideas with their positive sarcasm and tireless endorsement.

My earliest teachers were of course my parents, Ashwin Rana and Lalita Rana, who have molded me into a character for procuring my dreams. I am thankful to my family and friends from all stages of my life, who have educated and nourished me to achieve the pinnacle of my academic career thus far. My wife, Anita, deserves the most credit for accompanying me in my all the challenging times and supporting me at every instance with her abilities to keep me motivated. Her remarkable strength, dedication and enthusiasm never fails to astonish me.

I, Axaykumar Rana, heart-fully appreciate all the people who have contributed to help me achieve the goal of my PhD with their supportive efforts!

Thank you!

DEVELOPMENT OF HIGHLY SENSITIVE MULTIMODAL TACTILE SENSOR

Axaykumar RANA

ABSTRACT

The sense of touch is crucial for interpreting exteroceptive stimuli, and for moderating physical interactions with one's environment during object grasping and manipulation tasks. For years, tactile researchers have sought a method that will allow robots to achieve the same tactile sensing capabilities as humans, but the solution has remained elusive. This is a problem for people in the medical and robotics communities, as prosthetic and robotic limbs provide little or no force feedback during contact with objects. During object manipulation tasks, the inability to control the force (applied by the prosthetic or robotic hand to the object) frequently results in damage to the object. Moreover, amputees must compensate for the lack of tactility by paying continuous visual attention to the task at hand, making even the simplest task a frustrating and time-consuming endeavor. We believe that these challenges of object manipulation might best be addressed by a closed feedback loop with a tactile sensory system that is capable of detecting multiple stimuli. To this end, the goal of our research is the development of a tactile sensor that mimics the human sensory apparatus as closely as possible.

Thus far, tactile sensors have been unable to match the human sensory apparatus in terms of simultaneous multimodality, high resolution, and broad sensitivity. In particular, previous sensors have typically been able to sense either a wide range of forces, or very low forces, but never both at the same time; and they are designed for either static or dynamic sensing, rather than multimodality. These restrictions have left them unsuited to the needs of robotic applications. Capacitance-based sensors represent the most promising approach, but they too must overcome many limitations. Although recent innovations in the touch screen industry have resolved the issue of processing complexity, through the replacement of clunky processing circuits with new integrated circuits (ICs), most capacitive sensors still remain limited by hysteresis and narrow ranges of sensitivity, due to the properties of their dielectrics.

In this thesis, we present the design of a new capacitive tactile sensor that is capable of making highly accurate measurements at low force levels, while also being sensitive to a wide range of forces. Our sensor is not limited to the detection of either low forces or broad sensitivity, because the improved soft dielectric that we have constructed allows it to do both at the same time. To construct the base of the dielectric, we used a geometrically modified silicone material. To create this material, we used a soft-lithography process to construct microfeatures that enhance the silicone's compressibility under pressure. Moreover, the silicone was doped with high-permittivity ceramic nanoparticles, thereby enhancing the capacitive response of the sensor. Our dielectric features a two-stage microstructure, which makes it very sensitive to low forces, while still able to measure a wide range of forces. Despite these steps, and the complexity of the dielectric's structure, we were still able to fabricate the dielectric using a relatively simple process.

In addition, our sensor is not limited to either static or dynamic sensing; unlike previous sensors, it is capable of doing both simultaneously. This multimodality allows our sensor to detect fluctuating forces, even at very low force levels. Whereas past researchers have used separate technologies for static and dynamic sensing, our dynamic sensing unit is formed with same capacitive technology as the static one. This was possible because of the high sensitivity of our dielectric. We used the entire surface area effectively, by integrating the single dynamic-sensing taxel on the same layer as the static sensing taxels. Essentially, the dynamic taxel takes the shape of the lines of a grid, filling in the spaces between the individual static taxels. For further optimization, the geometry of the dynamic taxel has been redesigned by fringing miniature traces of the dynamic taxel within the static taxels. In this way, the entire surface of the sensor is sensitive to both dynamic and static events. While this design slightly reduces the area that is covered by the static taxels, the trade-off is justified, as the capacitive behavior is boosted by the edge effect of the capacitor.

The fusion of an innovative dielectric with a capacitive sensing IC has produced a highly sensitive tactile sensor that meets our goals regarding resolution, noise immunity, and overall performance. It is sensitive to forces ranging from 1 mN to 15 N. We verified the functionality of our sensor by mounting it on several of the most popular mechanical hands. Our grasp assessment experiments delivered promising results, and showed how our sensor might be further refined so that it can be used to accurately estimate the outcome of an attempted grasp. In future, we believe that combining an advanced robotic hand with the sensor we have developed will allow us to meet the demand for human-like tactile sensing abilities.

Keywords: multimodal tactile sensor, Capacitive tactile sensing, Soft dielectric tactile sensor, Double layer Micro-structured dielectric, Dynamic tactile sensing

LE DÉVELOPPEMENT DE CAPTEUR TACTILE MULTIMODAL HAUTEMENT SENSIBLE

Axaykumar RANA

SOMMAIRE

Le sens du toucher est crucial pour l'interprétation des stimuli extéroceptifs, et pour modérer les interactions physiques avec son environnement au cours de la préhension d'objets et des tâches de manipulation. Pendant des années, les chercheurs dans le domaine du tactile ont cherché une méthode qui permettra aux robots d'atteindre les mêmes capacités de détection tactile que les humains, mais la solution est resté incomplète. Ceci est un problème pour les gens dans les communautés médicale et robotique, puisque les prothèses robotiques offrent peu ou pas de retour de force lors d'un contact avec des objets. Au cours des tâches de manipulation d'objets, l'incapacité de contrôler la force (appliquée par la prothèse ou la main robotique sur l'objet) entraîne souvent des dommages à l'objet. En outre, les personnes amputées doivent compenser le manque de tactilité en accordant une attention visuelle continue à la tâche, rendant la tâche la plus simple frustrante et chronophage. Nous croyons que ces défis de la manipulation d'objets pourraient être mieux traitées par une boucle de rétroaction fermée avec un système sensoriel tactile qui est capable de détecter de multiples stimuli. À cet effet, le but de notre recherche est le développement d'un capteur tactile qui imite l'appareil sensoriel humain aussi étroitement que possible.

Jusqu'à présent, les capteurs tactiles ont été incapables de faire correspondre l'appareil sensoriel humain en termes de multimodalité simultanée, d'haute résolution et de grande sensibilité. En particulier, les capteurs précédents ont généralement été capable de détecter soit, une large gamme de forces, ou des forces très faibles, mais jamais les deux en même temps ; et ils sont conçus pour la détection soit statique ou dynamique, plutôt que multimodale. Ces restrictions ont laissé ces capteurs inadaptés aux besoins des applications robotiques. Les capteurs capacitifs représentent la méthode la plus prometteuse, mais ils doivent aussi surmonter de nombreuses limitations. Bien que les innovations récentes dans l'industrie de l'écran tactile ont résolu la question de la complexité de traitement par le remplacement des circuits de traitement maladroit avec de nouveaux circuits intégrés (IC), la plupart des capteurs capacitifs restent encore limités par l'hystérésis et des plages étroites de sensibilité en raison des propriétés de leurs diélectriques.

Dans cette thèse, nous présentons la conception d'un nouveau capteur tactile capacitif qui est capable de faire des mesures très précises à des niveaux de faible force, tout en étant sensible à un large éventail de forces. Notre capteur ne se limite pas à la détection de forces à faible ou large sensibilité, car le diélectrique souple amélioré que nous avons construit lui permet de faire les deux à la fois. Pour construire la base du diélectrique, nous avons utilisé un matériau de silicone modifié géométriquement. Pour créer cette matière, nous avons utilisé un processus de lithographie molle pour construire des microcaractéristiques qui améliorent la compressibilité

du silicone sous pression. En outre, le silicone a été dopé avec des nanoparticules de céramique à haute permittivité, ce qui améliore la réponse du capteur capacitif. Notre diélectrique dispose d'une microstructure en deux étapes, ce qui le rend très sensible à de faibles forces, tout en étant capable de mesurer un large éventail de forces. Malgré ces nombreuses étapes et la complexité de la structure du diélectrique, nous étions encore en mesure de le fabriquer en utilisant un processus relativement simple.

En outre, notre capteur ne se limite pas à des données statiques ou dynamiques de détection. Contrairement aux capteurs antérieurs, il est capable de faire les deux simultanément. Cette multimodalité permet à notre capteur de détecter la fluctuation des forces, même à des niveaux de force très faible. Alors que les chercheurs ont utilisé des technologies distinctes pour la détection statique et dynamique, notre unité de détection dynamique est formé avec la même technologie capacitive que celui statique. Cela a été possible en raison de la grande sensibilité de notre diélectrique. Nous avons utilisé la totalité de la surface de manière efficace, en intégrant le seule taxel dynamique de détection sur la même couche que les taxels de détection statiques. Essentiellement, le taxel dynamique prend la forme des lignes d'une grille, en remplissant les espaces entre les taxels statiques individuels. Pour plus d'optimisation, la géométrie du taxel dynamique a été redessinée en insérant des traces miniatures du taxel dynamique au sein des taxels statiques. De cette façon, toute la surface du capteur est sensible à la fois à des événements dynamiques et statiques. Bien que cette conception réduit légèrement la zone qui est couverte par les taxels statiques, le compromis est justifiée puisque le comportement capacitif est augmenté par l'effet de bord du condensateur.

La fusion d'un diélectrique innovateur avec une détection capacitive IC à produit un capteur tactile très sensible qui répond à nos objectifs en ce qui concerne la résolution, l'immunité au bruit et la performance globale. Il est sensible aux forces allant de 1mN à 15 N. Nous avons vérifié la fonctionnalité de notre capteur en le montant sur plusieurs mains mécaniques populaires. Nos expériences d'évaluation de préhension ont livrés des résultats prometteurs et ont montré comment notre capteur pourrait être raffinée afin qu'il puisse être utilisé pour estimer avec précision le résultat d'une tentative de prise. À l'avenir, nous pensons que la combinaison d'une main robotique de pointe avec le capteur que nous avons développé nous permettra de répondre à la demande de capacités tactiles similaire à celle des humains.

Mots clés: Capteur multimodal tactile, capacitif de détection tactile, capteur tactile diélectrique souple, Double couche de micro-structuré diélectrique, détection tactile dynamique

CONTENTS

Page

LIST OF TABLES

Page

LIST OF FIGURES

Page

LIST OF ABBREVIATIONS

ADC	Analog to Digital Converter
ASIC	Application Specific Integrated Circuit
BaTiO3	Barium Titanate
CCD	Charge Coupled Deceives
CCTO	Calcium Copper Titanate
CDCs	Capacitance to Digital Converters
CGDB	Columbia Grasp DataBase
DC	Direct Current
DMA	Direct Memory Access
DPI	Dots Per Inches
EIT	Electrical Impedance Tomography
ETS	École de Technologie Supérieure
EVA	Ethyl Vinyl Acetate
FA	Fast Adaptive
FFT	Fast Fourier Transform
FPGAs	Field Programming Gate Arrays
GPS	Global Positioning System
GUI	Graphic User Interface
IC	Integrated Circuits

ITO	Indium Titanium Oxide
MCU	Micro-Controller Unit
MEMS	Micro Electro Mechanical Systems
PCB	Printed Circuit Board
PDMS	PolyDiMethylSiloxane
PGA	Programmable Gain Amplifier
PMNPT	Lead Magnesiun Niobate-Lead Titanate
PPS	Pressure Profile Systems
PSoC	Programmable System on Chip
PTFE	PolyTetraFluoroEthylene
PU	PolyUrethane
PVDF	PolyVinylideneDiFluoride
QTC	Qunatum Tunneling Composites
ROS	Robot Operating System
SA	Slow Adaptive
SEM	Scanning Electron Microscope
SNR	Signal to Noise Ratio
SoC	System on Chip
Taxel	Tactile Pixel
TIA	Trans Impedance Amplifier

UR5	Universal Robot 5
VDC	Voltage Direct Current
VLSI	Very Large Scale Integration

LIST OF SYMBOLS AND UNITS OF MEASUREMENTS

A	Ampere
cm	centimeters
F	Farad
Hz	Hertz
KHz	Kilo Hertz
KPa	Kilo Pascal
mm	millimeter
N	Newton
nm	Nano-meter
μm	Micro-meter
V	Volts

CHAPTER 1

INTRODUCTION TO THE HUMAN SENSE OF TOUCH

The sense of touch is the key anatomic element that allows us to understand the tactile stimulations that are generated during events such as grasping, object manipulation, gripping, and recognizing surface properties. Wang *et al.* (2006) described tactility as a set of sensational cognitive processes of the brain. Tactility occurs in the sensation layer that detects and receives touch information when contact between an object and an area of the body's surface occurs. This contact can be in the form of heat, pressure, weight, texture or pain. Human skin is the only tactile sensory apparatus that consists of multiple mechanoreceptors that act as sensory cells to deliver the tactile modality to the human. To mimic same functionalities in artificial hands by tactile sensors, this chapter will elaborate the detailed view for the human sense of touch in section 1.1 by explaining its core elements as mechanoreceptors in section 1.1.1, properties for ideal tactile sensor according to the needs in the section 1.2. Following that introductory knowledge, the chapter will proceed for a comprehensive sketch of the tactile forms namely static tactile sensing in section 1.4 and dynamic tactile sensing in the section 1.5.

The human body possesses five senses: vision, hearing, taste, smell and tactility (Jaimes and Sebe, 2007). As illustrated in Fig.1.1, most of the senses have their own dedicated organs, such as eyes for vision and ears for hearing, that are localized at a certain point on the human body. However, the sense of touch is different from the others in that its corresponding organ, skin, is spread over the entire body. When attempting to restore this modality to those who have lost it, such as amputees, the first challenge is to conceive of an artificial sensory apparatus that can cover a wide area, so that it will be as similar as possible to human skin (Lee and Nicholls, 1999). Another challenge stems from the fact that the human sense of touch involves several forms of perception, including static forces, dynamic forces, heat, and moisture. With this information, the human nervous system interprets the complex tactile events of contact localization, friction, slippage, excessive force, adaptive grasp, surface recognition, and temperature changes.

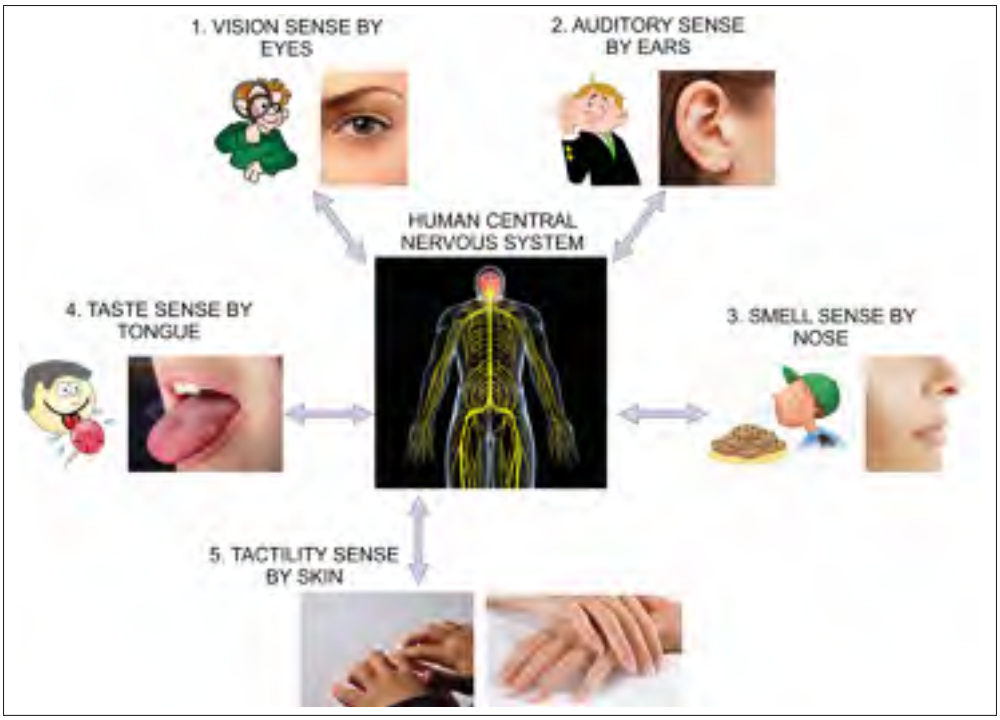

Figure 1.1 5 different senses of human body and their localizing organs

Tactile sensing is part of the somatosensory system, as described by Burgess and Perl (1973), where it is classified under a variety of sensory types such as proprioception, exteroception and kinaesthetic events. Fig. 1.2 displays the classification of the sensory modalities and their elements.

1.1 Human body's tactile perception

Human body's tactile ability is classified mainly into 2 types of sensing scenarios.

a. Kinaesthetic sensing and

b. Cutaneous sensing.

The tactile sensing abilities of the human body are divided into two categories: kinesthetic sensing and cutaneous sensing. Kinesthetic perception provides details about the relative posi-

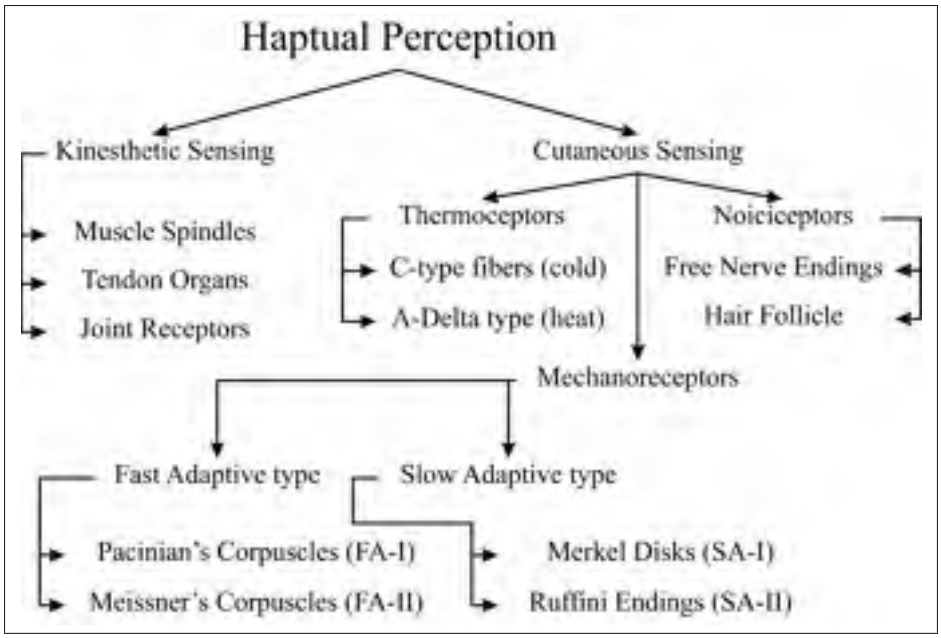

Figure 1.2 Haptic perception receptors in human body

tion of one's organs/limbs in reference to one's other limbs and joints (Loomis and Lederman, 1986). Conceptually, it defines the muscles and joints as they are co-related to the position of human limbs within the body. Such information helps the brain with the position and posture of the body. Walsh *et al.* (2014) explains that kinesthetic sensations usually collect the afferent information that originates within the muscles, joints and tendons. This information is conveyed by the muscle spindles, tendon organs, and joint receptors, respectively. The muscle spindles give details about the length of muscle and the speed of changes in that length. The tendon organs are responsible for generating information about tension in the muscle and changes in tension. Finally, the joint receptors provide information on the positions of the joints of human limbs.

Humans require a complete proprioceptive feedback loop in order to accurately control the movement of their limbs. The reflex of pulling away from something as soon as the skin senses pain is also important for avoiding injury. The kinesthetic controls in the human body can be compared to existing technologies in robotics: advanced robotic arms feature joint encoders, and motion and positioning sensors, that operate in similar ways to the human system.

Cutaneous sensing is defined by Koskinen (2008) as the stimulation of the outer surface of the body by means of mechanoreceptors within the skin and the associated nervous system. A study by Stillman (2002) further classifies the cutaneous receptors according to the nature of their stimuli. The two types of cutaneous sensing are known as proprioception and exteroception.

Proprioception is defined by Stillman (2002) as the sense of the position, movement, posture or balance of the limbs given by the deep tissue mechanoreceptors in the musculoskeletal environment. Exteroception is defined as the sense of a stimulus given by the external environment, such as stimuli in the form of pressure, skin stretch, or vibration. According to (Halata and Baumann, 2008), there are around 17000 cutaneous receptors in a healthy human hand, and they are concentrated more densely in certain areas like the palm and fingers of the hand. Exteroceptive stimuli also exist in the form of pressure, vibration, shear stress, temperature, and humidity, and can include the sensation of pain and fatigue.

Fig. 1.2 shows the exteroceptive stimuli, divided into three categories according to their transducing functionalities. The cells that interpret mechanical force events are called mechanoreceptors. Other set of cells, called thermoreceptors, detect heat properties. The last set of cells measures excessive stress and temperature when they leads to the fatigue and eventual rupture of the skin. These cells, which comprise free nerve endings called nociceptors, respond via pain. For most object manipulation and grasping tasks, mechanoreceptors dominate the tactile sensing response. A detailed study of their functionality and performance has been abstracted from Halata and Baumann (2008), Dargahi and Najarian (2004), Nghiem *et al.* (2015), Lederman and Klatzky (2009) and Schmidt *et al.* (2006b) which has given us an overview of the ideal tactile sensing capabilities during object manipulation.

1.1.1 Mechanoreceptors in human skin

Inside human skin, four types of mechanoreceptors are responsible for detecting different force activities. They are categorized according to their adaptive response time, as either Fast Adapt-

ing (FA) or Slow Adapting (SA) mechanoreceptors. Meissner's corpuscles and Pacinian's corpuscles are FA cells, and they typically detect dynamic events such as initial touch, vibration, friction, and slippage. Merkel disks and Ruffini endings are SA cells, and they record static exteroceptive events like normal pressure, shear, stable grasp and grip control. Fig. 1.3 displays their distribution within the skin layers.

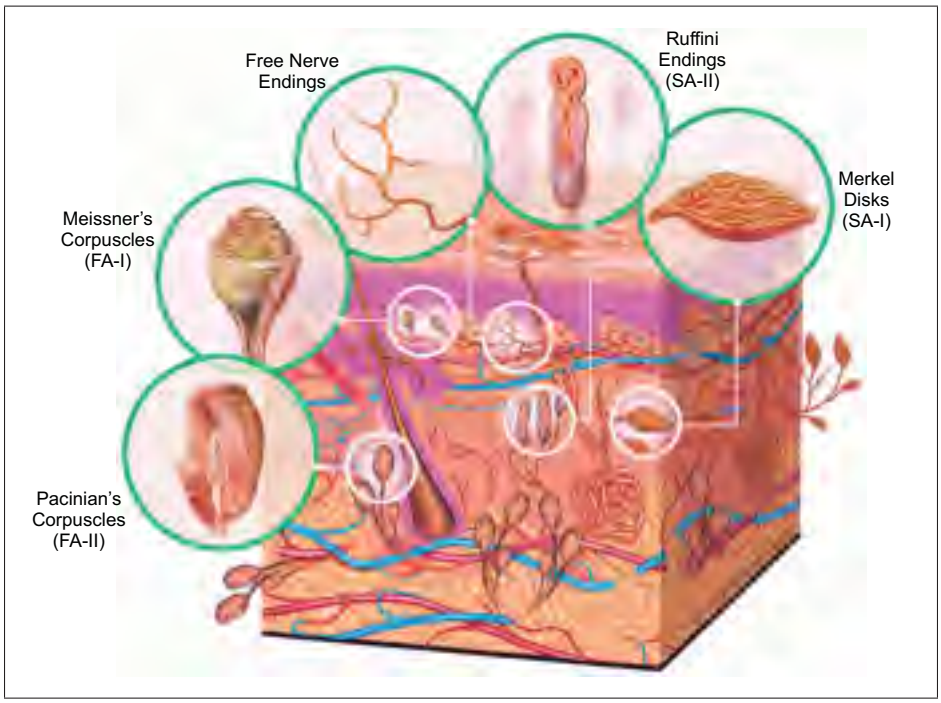

Figure 1.3 Types of cutanesous mechanoreceptos for tactile sense in human skin
Taken from Kleinhans (2015)

a. Meissner's corpuscles are situated within the superficial dermis of the glabrous skin, which is just below the membrane in dermal papillae. Such outer positioning advantages these mechanoreceptors with detection of low-force dynamic events, including initial touch, skin stretch, and low-frequency vibration, as well as motion detection, slip detection and grip control. Due to their dynamic behavior their step function is considered as '$\frac{ds}{dt}$' which normally captures events in a frequency range of 10-60 Hz. Their location near the skin's surface restricts the Meissner's corpuscles to a lower spatial acu-

ity, of 3-4 mm, and a higher population density, of about 43%. They are more specifically defined as Fast Adaptive-I in the classification of cutaneous receptors.

b. Pacinian corpuscles are another type of receptors that respond to dynamic events. Unlike Meissner's corpuscles, they are located deep within dermis layer, which gives them a better spatial acuity of around 10 mm. Due to this formation, they have a lower density, of 13% in the glabrous and hairy skin area. Normally they respond to much higher frequency vibrations, of 50-1000 Hz. Examples of such high-frequency touch events are unlocalized vibration, temporal changes in skin deformation, surface friction, and vibration during the use of power tools. According to their responses to external stimuli, their step function is defined as '$\frac{d^2s}{dt^2}$' and they are classified as Fast Adaptive-II cutaneous receptors.

c. Merkel disks are found in the superficial epidermis of the glabrous skin. They have a lower spacial acuity than Pacinian corpuscles, of just 0.5mm per receptor. However, Merkel disks have a higher population density, making up 25% of the skin's receptors. They record static events, occurring at DC transient to 30 hz so their step function is defined as 's' or '$\frac{ds}{dt}$'. The static events that Merkel disks respond to include sustained pressure, local skin curvature, texture perception and spatial deformation. They are categorized as Slow Adaptive-I cutaneous receptors.

d. Ruffini Endings are a Slow Adaptive-II type of cutaneous receptor. They are also responsible for detecting static force events like directional skin stretch, lateral pressure, finger positioning, stable grasp, shear force and motion detection. Like the Merkel disks, they also respond to stimuli in the rage of DC-15 Hz, and their step function is defined as 's'. These receptors are found deep in the dermis of hairy and glabrous skin. Because of their depth, they have a better acuity, of 7 mm and up, per receptor. They have a low population density, of 19% among all cutaneous receptors.

The combination of kinaesthetic and cutaneous receptors generates a structured view of objects when grasped by the hand. Blending their functionalities enables us to perform sophisticated tasks of dexterous manipulation with ease and adequate safety margins.

1.2 Functionalities of an ideal tactile sensor

Researchers have exploited the instrumentality of these mechanoreceptors by reverse engineering, and have achieved notable results with the assistance of different technologies as published in the studies of Lee and Nicholls (1999), Dahiya *et al.* (2010), Almassri *et al.* (2015), Stassi *et al.* (2014) and Dahiya and Valle (2008). However, mimicking the tactile sensing of the human hand remains a challenge due to constraints regarding data processing, structural density, rate of response, the small size of the components, and the variety of modalities that must be considered. As Dahiya and Valle (2008) state, to emulate the tactile ability of human arm in prosthetics, certain functionalities should be attained by the tactile sensor in order to perform reliably. Fig. 1.4 illustrates the measures, defined by Dargahi and Najarian (2004), that should be considered when designing an artificial tactile sensory apparatus.

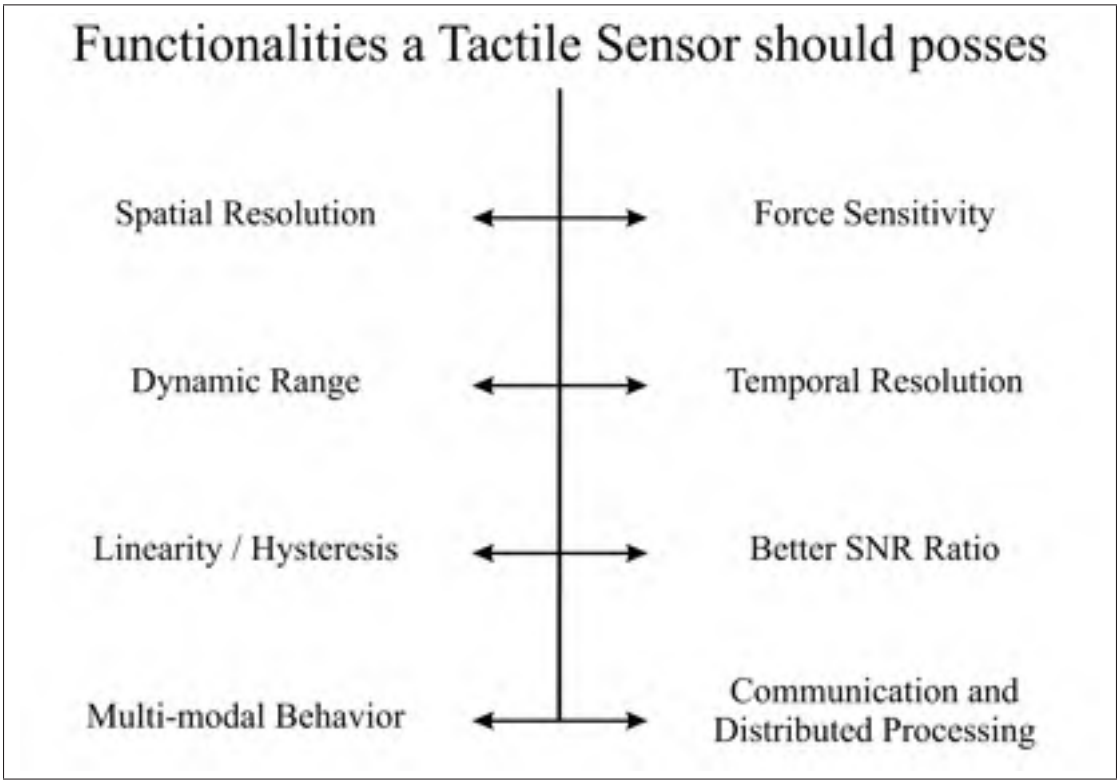

Figure 1.4 Anticipated properties to be possessed by an ideal tactile sensor

a. Spatial resolution

Spatial resolution is the distance between two consecutive contacts on a sensor's surface, where the sensor is able to distinguish them as separate tactile entities. According to Van Boven and Johnson (1994), human skin has varying amount of spatial resolution according to the specific area of the human body. The lips, tongue and fingertips contain a dense concentration of cutaneous receptors, which allow a very good spatial resolution of less than 1 mm. However, it would be difficult to develop robots with such spatial acuity. Dargahi and Najarian (2004) suggests that a spatial resolution of 1-2 mm would be sufficient for the localization of touch events involving small objects. In the ideal scenario, tactile sensors should have extremely small spatial acuity in order to detect small movements or brief contact. However, this spatial resolution can be negotiable up to certain limits, in order to compensate for other parameters, such as better temporal resolution, or multiple sensing elements for multimodal sensing.

b. Vast range of Force sensitivity

A tactile sensor should have a wide range of force sensitivity for detecting both low and high pressure stimuli. A healthy human can detect pressure from items that are lighter than feathers and heavier than gold bars, and can easily detect a wide range of forces during grasping or object manipulation tasks Westling and Johansson (1987). Dargahi and Najarian (2004) suggest that a tactile sensor should be able to accommodate forces ranging from 0.01 N to 10 N to ensure a satisfactory performance. A robotic hand, equipped with the ideal tactile sensors, would be able to recognize anything from a peanut to a heavy dumbbell. This recognition will assist the robot during object-manipulation exercises by providing better grasp reliability. However, as we will see in Chapter 2, current commercially-available tactile sensing systems can only detect either very low forces or very high forces. As of yet, none have achieved the same range of sensitivity as the human hand.

c. Temporal resolution

Temporal resolution describes the processing of touch events and delivering the details to the central nervous system for reaction according to tactile case. Sensing is the initial stage of the control loop. Therefore, sensing and its subsequent data-processing must be completed quickly in order for the body to react to the stimuli within a reasonable time. Human skin has a maximum dynamic resolution of 1000 Hz. Dynamic resolution is provided by the Pacinian corpuscles, whereas static event resolution is delivered by Merkel disks and Ruffini endings, with a maximum resolution of 30 Hz, according to Halata and Baumann (2008). To achieve sensing capabilities in robots that are similar to those of humans, tactile sensors require processing speed resolution frequencies of 30 Hz for the sensing of static events like pressure and force, and 1000 Hz for the sensing of dynamic events like vibration and slippage.

d. Communication and Distributed Processing

In humans, the sense of touch is unique among the senses because of the region it occupies on the human body, as explained by (Lee and Nicholls, 1999). Whereas audio, vision, taste and smell are localized to particular organs in the body, human skin covers the entire body. So, data-processing, and the communication of this data to the nervous system, is more complex for the sense of touch than it is for the other senses. Further, providing the sense of touch to an entire humanoid, or even just a robotic arm, is a challenging task. The first goal to achieve is communication within the entire sensing network, at a speed that abides by the temporal and spatial resolution. And, second is the processing of that data acquitted by the wide spread tactile sensing network. Considering fast acquisition rate(1000Hz) for dynamic event as well as adequate sampling rate(30Hz) for static sensor would demand us to design an efficient data processing system for entire communication network without processing lag, interference and cross-talking.

e. Multimodality

The ability to detect stimuli under different modalities is an essential feature of the ideal tactile sensor Nicholls and Lee (1989). Tactile events can vary widely in terms of forces

and transduction phenomena, so uni-modal sensing is not able to fulfill all sensing requirements. During object manipulation, the forces that may be encountered include normal force, shear force, slippage, vibration, and surface friction. The static and dynamic forces, that are recognized by mechanoreceptors in humans, must be addressed by a tactile sensor in order to have a reliable feedback loop. Surveys by Yousef *et al.* (2011), Lee and Nicholls (1999), Cutkosky *et al.* (2008) and Dahiya and Valle (2008) state that many researchers have constructed a variety of tactile solutions for either pressure or vibration sensing. However, none of them exhibit multimodal sensing capabilities that can mimic the performance of human skin. Moreover, the only commercially available multimodal sensor, Wettels *et al.* (2014), is limited by its small range of sensitivity for static stimuli, and despite having a rate of acquisition that is three times higher than that of human skin, it does not yet have an adequate sensitivity to vibration.

f. Linearity, Hysteresis and SNR ratio

The ideal sensor will perform well despite the limiting factors that are intrinsic to every sensor – linear performance, hysteresis and signal-to-noise ratio (SNR). A linear response to force is desired for a sensor with a wide range of force detection. Some good sensors Maggiali *et al.* (2008) are highly sensitive, in that they can detect forces up to 10^{-3}N, but they tend to saturate at higher-force applications (above 10N).

The ideal multimodal sensor, with a broad range of force sensitivity, will behave linearly when responding to anything from Mili-newtons to several Newtons of force. A non-linear response could adversely affect the speed of the sensor, due to the need for complex modeling and response interpretation.

Similarly, hysteresis can mean that numerous small changes in force end up saturating the sensor after a certain period of time. This could cripple dynamic sensing abilities, where the force ranges are typically minimal due to the nature of the forces. Hysteresis could also amplify the negative effects of non-linearity, as such sensors do not respond properly at certain force levels, according to the forward and reverse curve of saturation.

The ideal sensor must have a relatively high SNR. This is because dynamic events often involve force profiles that appear relatively close to noise, so the sensor must be able to distinguish between real events and base noise. Various types of noise also persist in real world environments, such as vibration, electrical interference, and thermal drift. In any situation, noise immunity is required for reliable and effective sensing.

1.3 Requirement of the tactile sensor

a. Incomplete feedback loop during object manipulation tasks

An overview of recent prosthetic and robotics gives us a clearer idea about the incomplete force feedback loop for manipulation and grasping. Advanced dexterous manipulation has been accomplished with under-actuated mechanisms, in which grip is controlled using current sensors that monitor the motors of the finger actuators. However, there is no one platform available for both localizing contact and detecting force during manipulation and grip control. Most advanced robotic hands and humanoids continue to perform tasks, such as picking up an object, with open-loop control, or even control from camera feedback or current feedback from the motors. A clear solution to this dilemma is a multimodal tactile sensor that will replicate the duties of human skin when integrated with robotic structures.

b. The need for a reliable tactile solution in prosthetics and robotics

A survey conducted by Kyberd *et al.* (2007) shows that tactility is one of the primary features that must be possessed by a good prosthetic hand. Apparently, the challenges faced by robotics researchers from the lack of tactile feedback, such as open-loop control of grasping and unreliable manipulation, persist in prosthetics as well. Toledo *et al.* (2009)'s survey shows us that prosthetic arm and hand mechanisms have evolved from simple hook and parallel grasping structures, to dexterous fingers and under-actuated mechanisms. When we consider the advancement of prosthetics through mechanical design, it is clear that a wide gap of touch sensibility remains open, as there is no reliable tactile solution available to convey the sense of touch through the prostheses of upper-limb am-

putees. A reliable multimodal human skin type tactile sensor is desirable for upgrading prosthetics to a whole new dimension.

c. Unstable manipulation/grasping leads to object damage

Any control loop without corrective feedback results into instability of the system. Open loop grasp control reflects by unreliable grip and inadequate force control. For example, a person would not be able to judge sufficient amount of force required to hold heavy weight or light weight object. Without localization of contact and force feedback, a person would not be able to judge the proper grasp which ends up with object slippage or excessive force grasp results into damage for fragile objects. Considering an incredible amount of progress in mechanical design of artificial hand, lack of ideal tactile feedback restricts them to explore features of under actuated grasp without object moving. Fig. 1.5 shows the results of fragile plastic cup manipulation by an advanced humanoid, i-Cub. In this experiment, the foam cup that was grasped by robot was crushed due to the robot's lack of tactile sensing. Meanwhile, when tactile feedback was used while grasping, the cup remained intact. This experiment demonstrates the necessity of tactile sensors to object safety and reliable grip.

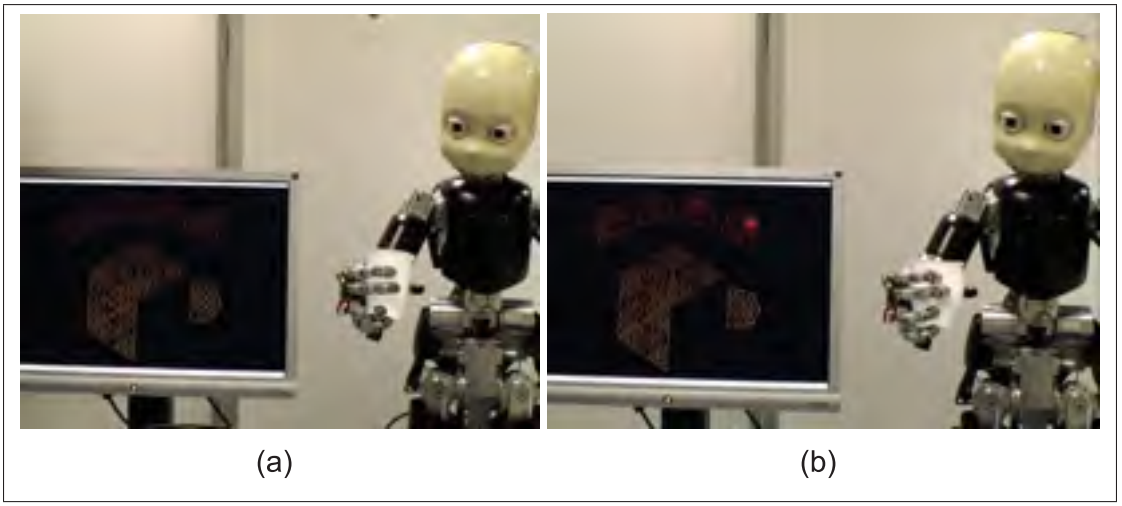

Figure 1.5 i-Cub manipulates a fragile plastic cup (a) with tactile feedback, (b) without tactile feedback

d. The need for continuous visual attention

Without tactile sensing abilities, a person or system has to compensate by involving other senses to successfully accomplish a task. Fig. 1.6 depicts a person attempting to manipulate an object with a prosthetic limb. The prosthetic user must visually monitor the manipulation and grasping tasks in order to accomplish them successfully. So, in the absence of functional mechanoreceptors, it is hard to evaluate the optimal force needed to lift an object. The person must align the prosthetic perfectly with the object, and use continuous visual monitoring in order to complete the feedback loop. It is near-impossible for someone to multi-task when dexterous manipulation must constantly be accompanied by visual attention.

Figure 1.6 Prosthetic user is trying to accomplish manipulation task under continuous visual observation
Taken from Raspopovic *et al.* (2014)

e. Current commercially-available sensors are far from ideal

According to Blank *et al.* (2010), there is currently a large population of upper-limb amputees, whose lives would be greatly improved by smart prosthetic devices with sensing abilities similar to a human hand. In the field of robotics, tactile sensing solutions are also sought by researchers who hope to improve the performance of advance humanoids during tactile tasks. Despite years of research, only a few tactile solutions are commercially

available at present (Wettels *et al.*, 2014)(Pressure Profile Systems)(Weiss and Woern, 2004). A detailed assessment of these sensors shows their many limitations, particularly when one compares them to the features of the ideal tactile sensor as described by Dargahi and Najarian (2004).

1.4 Introduction on static type tactile sensor

Static tactile sensing is a major component for addressing tactile needs (Almassri *et al.*, 2015). Normal pressure, localization of contact, skin stretch, longitudinal pressure (shear force), and spatial deformation are the main types of static tactile events. Plenty of scenarios that involve tactile sensing could be addressed by the simple static sensing of pressure. For example, knowledge of the adequate grip force for holding a coffee cup, or gently grasping a grape without crushing it, is obtained by pressure detection from the mechanoreceptors in the human hand. A detailed study by Dahiya *et al.* (2010) has found that most manipulation and grasping tasks could be accomplished with just the static mechanoreceptors. Although it is important to possess dynamic sensing abilities for detecting initial touch, slippage, and different textures, the basic functionality of pressure on finger phalanges during grasp and manipulation can be thought of as the foundation to tactile sensing, upon which dynamic sensing will later build. Therefore, it is important to consider and implement the static tactile element for imitating human sensory apparatus.

Due to its usefulness in routine tasks like object manipulation and grasping, static tactile sensing has been a favorite research topic in the robotics industry. Advanced robotic grippers have achieved dexterity and finger grasp formations that are comparable to the human hand (Mindtrans, 2015). However, these sophisticated structures still cannot provide reliable object manipulation and optimal grip force due to the lack of complete tactile feedback. Furthermore, a simple robotic jaw, equipped with tactile pressure sensors and a closed-loop manipulation system, could outperform the robotic grippers in terms of successful object manipulation. For this reason, the robotic industry's attention is now focused on developing a tactile sensor for robots to achieve safer grasping during object manipulation.

Prosthetic users also require similar tactile functionalities for their artificial upper-limbs. A survey conducted by Blank *et al.* (2010) shows that the increasing population of upper-limb amputees in the world have stimulated demand for advanced prosthetic devices. Over time, upper-limb prosthetics have evolved from the simple hook to mechanical replicas of the human hand. Current prosthetics (Clement *et al.*, 2011) fulfill almost all the requirements for a comfortable artificial upper-limb – the one feature they are missing is tactile sensing. As a result, most prosthetic hand users depend upon visual feedback for reliable object handling. Even when paying continuous visual attention to the task at hand, however, prosthetics users face challenges when detecting localization of contact, applying the optimal grip force, preventing object damage, etc. Therefore, it is important to develop tactile sensors for upper-limb prosthetics in order to restore the sense of touch to amputees.

There are numerous ways to detect normal stress, as a variety of sensors have been developed based on different transduction techniques (Almassri *et al.*, 2015). A study by Dahiya and Valle (2008) indicates that many researchers were inspired by a variety of pressure sensing techniques when developing new tactile sensors. Since tactile sensing is an in-demand feature for robotics and prosthetics, much research has been undertaken to achieve a better tactile sensing element. A resistive-based approach was applied to the design of a simple pressure sensor, by sandwiching conductive rubber between copper plates Tise (1988). This technology was soon improved upon, with the evolution of different kinds of molding technology for silicone and rubbers.

Another process that has led to better sensors is the use of conductive nano-particles in the filling of material. This has led to a better relative change in resistance, and has given lots of new room for implementing more complex and better resistance-based sensors. In recent years, due to the emergence of novel fabrication techniques, simple but effective pressure measurement techniques have been based on a variety of transduction principles, such as piezoresistive rubber Wang *et al.* (2009), Shimojo *et al.* (2004), conductive ink Choi *et al.* (2005a), EGaIn filled channels Park *et al.* (2010), and Electrical Impedance tomography (EIT) Alirezaei *et al.* (2009), Kato *et al.* (2007). Innovations in micro-fabrication by Micro Electro Mechanical

Structures (MEMS) technology and micro-machining have given us ultra-sensitive sensors Ho *et al.* (2010), Hwang *et al.* (2006) for normal and shear stress measurements. However, the typical drawbacks of these resistive sensors include deviations due to temperature, a low SNR, and hysteresis of the material, all of which limit their potential for development into the ideal sensor.

In contrast to the resistive techniques, opto-electronic technologies have no such restrictions regarding temperature deviation, and they have low levels of electrical noise interference. Opto-electronic sensors are based on the properties of light, such as intensity, reflection, polarization and diffraction. Various researchers have employed the technology for normal stress, shear stress and even dynamic tactile sensing. New devices in opto-electronics, like spectrometers (Dubey and Crowder, 2006), Bragg Gratings (Park *et al.*, 2007), miniature photocells (Mazid and Russell, 2006), fiberoscopes (Yussof *et al.*, 2008), and charge coupled devices (CCDs) (Ito *et al.*, 2011) have contributed to some of the most innovative tactile sensors.

However, despite opto-electronic's variety of methods, and its superiority over resistive transduction, opto-electronics has some drawbacks as well. These relate to the complexity of construction, and the bulky processing circuits that are required. More specifically, opto-electronics requires that the light must be processed at the location where it is received by the sensor, so the sensor necessarily becomes a huge mechanical structure. Two examples of tactile sensors, based on this technology, demonstrate the complexity of processing and the sprawling construction of the resulting sensor: an exoskeleton finger by Park *et al.* (2007), and a tactile sensor, made by Bristol Laboratories Ltd. (Chorley *et al.*, 2009). Finally, optical-based technology is also less-than-ideal due to its cost; when it comes to sensor construction, opto-electronics is more expensive than any other technology.

Opto-electronics and resistance-based technologies are, of course, not the only ones that have yielded better sensors: capacitance-based sensors have also proved popular. Similar to opto-electronics, capacitance-based sensors have relatively lower temperature drift and noise than resistance-based ones. Moreover, the working principle of capacitive technology allows it

to deliver compact sensors with processing circuits that are isolated from the sensing area. However, there is still some bulkiness involved in most of these sensors, and the processing circuits remain complicated.

A few approaches had been made, such as a row-column sandwich by Fearing *et al.* (1987), and by Akasofu and Neuman (1991) with compliant dielectrics. Most of the capacitance-based sensors were designed with a topology of either row-column electrodes in a crossover matrix, or of independent tactile pixels (taxels) with a dielectric layer placed over them. A physics-based analysis of this capacitive technology shows that the measurement of capacitance is given by

$$C = \varepsilon_0 \varepsilon_R \frac{A}{d}. \tag{1.1}$$

Here, A is the shadowed area between the plates, and d is the gap between capacitor's plates. ε_0 is the permittivity of the vacuum and ε_R is the relative permittivity of the dielectric material. A study by Dahiya *et al.* (2010) shows that many researchers have used capacitive technology to develop sensors that measure either the change in gap 'd' or the reduction in area 'A' by the displacement due to stress. Even commercially-available capacitive tactile sensors, such as those sold by Pressure Profile Systems, Inc. (PPS), depend on the displacement between plates due to stress. The implication of this sort of dependency is reflected in the limited force sensitivity range of these sensors, due to limited compliance of the dielectric. Most of these sensors exhibit good sensitivity to the forces above 1 N, but very limited sensitivity to forces below 0.1 N. According to Dargahi and Najarian (2004), a static tactile sensor must be capable of sensing forces as low as 0.02 N. Therefore, we aim to develop a tactile sensor that is sensitive to a wide range of forces.

In contrast to these previous approaches, Mannsfeld *et al.* (2010) has came up with the novel concept of modifying the geometry of the dielectric in order to achieve better compression under relatively small forces (below 1 N). The sensor involved sophisticated lithography techniques during construction, and the chemical process of curing polydimethylsiloxane (PDMS) was used to construct micrometer-sized pillar structures for the dielectric. This dielectric al-

lowed the sensor to detect the pressure of $10^{-3}\frac{N}{cm^2}$. In recent years, Wang *et al.* (2014), Cheng *et al.* (2009) and Surapaneni *et al.* (2013) have each designed capacitive tactile sensors with the help of MEMS technology. All of these MEMS-designed force sensors exhibit very good sensitivity to pressures below $1\frac{N}{cm^2}$. However, when it comes to higher pressure (above $1\frac{N}{cm^2}$), they experience saturation as a result of the complete compression of the micro-designed fabricated dielectric layer. It is possible that in future, the consideration of the geometrical aspects of the dielectric will lead to tactile sensors with the ability to measure minuscule forces. For instance, one could construct a dual-staged dielectric, by superposing the micro features of the dielectrics described above, over a layer of relatively larger features. This might enable a sensor to be highly sensitive to both low and high pressure.

Integrated circuits (ICs) are a recent trend in touch screen apparatuses, but they are also relevant to capacitance-based tactile sensors. Within the electronics industry, developments in resistive touch and capacitive touch technologies have heralded a revolution in touchscreen devices such as cellphones and tablets. Their function is to deliver digital information, according to the resistance/capacitance between the skin of the user's finger and the electrodes that are laid over a transparent and conductive material, such as Indium Titanium Oxide (ITO) film. The touchscreen system thus functions similarly to a capacitance-based tactile sensor.

ITO film is expensive and rigid, but fortunately there are some alternatives. We have decided to form the capacitor for our sensor by using layers of conductive wire mesh instead of ITO, and by using a compliant material with a relatively high permittivity for the dielectric. The conductive wire matrix can be connected to a touch screen controller to give us digital details of the tactile event. This setup could drastically reduce the size of the sensor, due to Very Large Scale Integration (VLSI) of the chip. This system will also avoid the need for a bulky processing circuit, which is one of the main problems with previous capacitance-based sensors.

In recent years, Maggiali *et al.* (2008), Cheng *et al.* (2009) and Hu *et al.* (2014) have all designed tactile sensors based on touchscreen IC technology. Maggiali *et al.* (2008) designed a sensor by laying sensing taxels on flexible printed circuit board (PCB), and placing a capaci-

tance sensing IC on the opposite face of the taxels on the PCB. This study also used PU foam as the dielectric and sprayed a carbon layer as the ground plane to form a capacitor. The design is compact and has the ability to extend by interconnection. However, this sensor still exhibits some hysteresis due to the damping of the PU foam, and it has a limited range of sensitivity.

A commercially-available tactile sensor, namely the RoboTouch by PPS, achieves capacitance sensing with an application specific integrated circuit (ASIC) as the sensing element. PPS claims to have good sensitivity for a wide range of forces, but still we can see from sensor's performance profile that it is limited to 0.1 N as its minimum force detection. This is far above the minimal force detection level of 0.01 N that was suggested for an ideal tactile element by Dargahi and Najarian (2004). Further analysis shows that the RoboTouch sensor is also limited due to the properties of the flexible elastomer that acts as a dielectric, as it displays limited compression when faced with low pressure events.

We aim to design a static force sensor based on the capacitive transduction principle. Based on our overview, we have three main goals for our sensor: it should be compact in size, relatively low-cost, and able to detect very low pressure as well as high pressure events. To these ends, we will pursue several design-related considerations. First, to ensure compactness, we will take a micro-design approach to the construction of the dielectric, and integrate an ASIC chip for capacitive sensing. Second, we intend to keep the cost of the sensor low by maintaining efficient communication within the sensor, similar to what was done in (Maggiali *et al.*, 2008). Finally, we will use a MEMS design for the dielectric and the sensing elements, so that the sensor will be able to detect very low pressure events.

1.5 Introduction on dynamic tactile sensor

Tactility is a feature long awaited by the robotics and prosthetics fields. The provision of exteroceptive cutaneous feedback could help robots to achieve better grasping and manipulation capabilities when interacting with their environment, as described in Cutkosky *et al.* (2008). Tactile interaction will provide context and coordinate detail about contact with objects. Em-

ploying a database of tactile events could help robots execute tasks that require a sense of stable grasp, localization of touch, adequate grasp force, object slippage, and orientation of the object during manipulation. However, the current state of these technologies remains vastly inferior to the capabilities of the human sensory apparatus. Moreover, a survey on the sensors for robotic hands by Almassri *et al.* (2015) found that most of the research is focused on sensory perception under static conditions, and does not include dynamic information. Although many studies have yielded impressive results for measuring tactile pressure events, they still cannot perform at the level of the human sensory apparatus. The core reason for this is the variable nature of tactile stimuli. According to Halata and Baumann (2008), current artificial tactile sensing methods are only just becoming capable of sensing the details of static pressure, whereas human skin can detect far more sophisticated events than the simple application of pressure.

A review of previous research shows that tactile sensory perception generally occurs under one of two conditions: static or dynamic. These conditions encompass a variety of tactile events, such as the static events of normal pressure or shear force, and the dynamic events of vibration, slip detection, surface recognition, and skin stretch. Dynamic events can also involve other properties like temperature, humidity and pain. Real-time human hand manipulation tasks depend not only on the level of pressure, but also on the various modalities of dynamic sensing, so the ideal tactile sensor must be capable of multimodal sensing. As current pressure sensing techniques are capable only of static sensing, the ideal tactile sensor will combine these abilities with dynamic sensing as well.

For healthy humans, many events are managed by dynamic sensing, through mechanoreceptors in the human hand that engage during object manipulation and grasp control (Heyneman and Cutkosky, 2014). For example, the act of holding a water bottle is not just a static force event. Due to the presence of less force/surface friction, corrective force application is required to prevent the object from slipping out of one's grasp. In these types of situations, dynamic sensing takes on an essential role, to complete the feedback loop that is required for successful object manipulation. According to Halata and Baumann (2008), in healthy human

skin this process relies on fast adaptive (FA) receptors such as Meissner's corpuscles (FA-I) and Pacinian corpuscles (FA-II), which are the sensory receptors that engage during dynamic events. These events include initial touch, skin stretch, vibration, motion and slip detection, grip control and surface friction, all of which are detected by the FA mechanoreceptors. Vallbo *et al.* (1984) and Provancher (2003) describe the afferent nerve signals that are used during tactile events. FA mechanoreceptors only respond to changes in force resulting from a dynamic event. If we look at the concentration of FA mechanoreceptors in humans, 56% of the population density of mechanoreceptors is occupied by FA mechanoreceptors, as detailed by Halata and Baumann (2008). We can therefore conclude that the complex nature of tactile manipulation should be considered a blend of static and dynamic sensing. It would be unfair to neglect aspects of dynamic sensing in favor of mere pressure-related tactile sensing capabilities, when both static and dynamic sensing capabilities are shown to be equally important.

Although many past researchers have attempted to create a dynamic tactile sensor, from an architectural point of view, none have been perfectly successful, particularly in terms of processing layout and compactness. Many technologies have been employed to record dynamic responses, such as Piezoelectricity by (Yamada *et al.*, 2002), (Goeger *et al.*, 2009), the capacitance effect Schmidt *et al.* (2006b), the microphone effect(Tanaka *et al.*, 2011), (Mayol-Cuevas *et al.*, 1998), opt-electronics (Romano *et al.*, 2009), (Dubey and Crowder, 2006), (Mazid and Russell, 2006) and a MEMS accelerometer (Tremblay and Cutkosky, 1993). Preliminary experiments by Cutkosky and Hyde (1993) involved fusing accelerometers into foam fingers and measuring the movements that resulted from the slippage of a grasped object. In another type of dynamic sensor piezoelectric films were used in rubber skin for rigid fingers Howe and Cutkosky (1993). This sensor was used to recognize surfaces based on signals and its deconvolution filters. More recently, Wettels *et al.* (2014) have developed the *Biomimatic Tactile Sensor* for prosthetics and robotic hands. Their design uses a fluid pressure sensor to propagate vibration that is generated on the rubber surface of the finger. Although it possesses modalities for static, dynamic, and temperature sensing, this sensor has some drawbacks regarding its mechanical integration with the robotic hand. To accommodate the sensor, an entire phalanger has to be

replaced by the sensor assembly. Another multimodal tactile sensor is presented by Choi *et al.* (2005b), in which dynamic sensing is based on PolyVinylideneDiFluoride (PVDF) films, and static sensing is achieved with pressure variable resistor ink. Although this sensor is compact in size and thin enough to perform as a skin, the use of two different working principles for static and dynamic sensing makes it difficult to integrate the separate processing layouts for signal processing. From this overview of dynamic tactile technologies, we find that most of the previous sensing designs are dependent on having separate structural and electrical layouts. Compactness and efficient space utilization are also difficult to achieve due to the extra elements.

By contrast, the multimodal sensor presented in this thesis has both a compact size and an adequate bandwidth for dynamic touch activities. This is because the same capacitive sensing principle is employed for both static and dynamic sensing. As shown in Fig. 4.3, our sensor uses the same copper surface for each layout in order to maximize the dynamic effects, without restricting the static sensing area. In fact, the only difference between the static and dynamic sensing processes is with the electrical processing circuit itself. This is because dynamic events often involve a high frequency content. Another aspect of our sensor that maximizes dynamic sensitivity is the use of a capacitance edge effect in our design. Such a provision assists with ensuring a uniform dynamic sensitivity over the entire surface of the sensor, as well as an increased response of capacitive behavior. In sum, the sensor presented here is a capacitance-based multimodal sensor, which is able to notify the user of both pressure distribution, and dynamic events, during object manipulation tasks.

1.6 Conclusion

In sum, the human sense of touch is complex in nature provided by a wide spread and multimodal in sensitivity. For the design of a good tactile sensor, a person should imitate most of the modalities of each mechanoreceptors described in this chapter. Moreover, instead of focusing only on pressure sensing tactile sensor, inclusion of dynamic modality could assist for

specific tactile events of vibration and slip which are also essential in the real world grasping and manipulation.

CHAPTER 2

SURVEY ON PREVIOUS TACTILE SENSING SOLUTIONS

Tactile sensors have proven their value when it comes to completing the feedback loop during object manipulation. For this reason, numerous studies have attempted to develop a tactile element that will act in a similar way to the human sensory apparatus. Although a variety of transduction techniques have been applied, and a few commercially-available tactile sensors seem promising, as explained in chapter 1, overall the robotics community is still far from achieving the ideal tactile sensor. This chapter outlines few of the popular commercial tactile sensors in the section 2.1. Moreover, following section 2.2 consists information about non-commercial solutions and relevant experiments which are bifurcated into the section 2.2.1 for static and section 2.2.2 for dynamic tactile sensing technologies.

2.1 Survey on commercially available tactile sensors

2.1.1 'RoboTouch' by Pressure Profile Systems

Robotouch, by Pressure Profile Systems is one of the most popular sensors on the market, because it holds up well to higher pressure and has better immunity to noise and hysteresis. Its manufacturer, PPS, has used the capacitance-based sensing principle, which brings the advantages of compact construction, very low drift on temperature, and relatively good noise performance. PPS has also integrated capacitance-to-digital converter ICs within the sensor, allowing it to avoid the problems caused by bulky capacitance-processing circuits. According to the specification sheet, the RoboTouch sensor can withstand forces of up to 100 psi (68.95 $\frac{N}{cm^2}$), despite being just 0.5mm thick. These robust and compact properties make the RoboTouch highly advantageous for integration with robotic hands. Fig. 2.1 depicts the RoboTouch tactile sensors attached to the fingers of a Barette hand.

However, the RoboTouch has several drawbacks: it lacks sensitivity to low pressure, it is unimodal, and it is relatively expensive. The sensor exhibits excellent sensitivity to forces above

Figure 2.1 RoboTouch tactile sensors by PPS on Barette hand

$1\frac{N}{cm^2}$, but no sensitivity to tactile events below $0.1\frac{N}{cm^2}$. The RoboTouch is suitable only for static sensing, but from chapter 1, we know that the modality of dynamic sensing is crucial during grasp control and object manipulation. The main reason for these limitations is that dynamic events typically involve a low-intensity stimulus that must be detected extremely quickly. According to Dennerlein *et al.* (1997) and Fagiani *et al.* (2011), the vibrotactile information for dynamic events can occur at a stimulus frequency of 500 Hz, whereas the bandwidth of acquisition for the RoboTouch is only 100Hz.

2.1.2 Weiss Tactile Sensors

Weiss Robotics has developed piezo-resistance-based tactile sensors that are fabricated with a carbon-enriched elastomer of Poly Tetra Fluoro Ethylene (PTFE). The sensor illustrated in Fig. 2.2 functions due to the mutual resistance between single-sided electrodes. This resistance is measured by a DSACON32 controller, as shown in Fig. 2.2(a). Weiss sensors have also been integrated with robotic hands, as shown by the Allegro hand with Weiss sensors that is depicted in Fig. 2.2(b). Here, the processing circuit is situated under the palm, which allows the

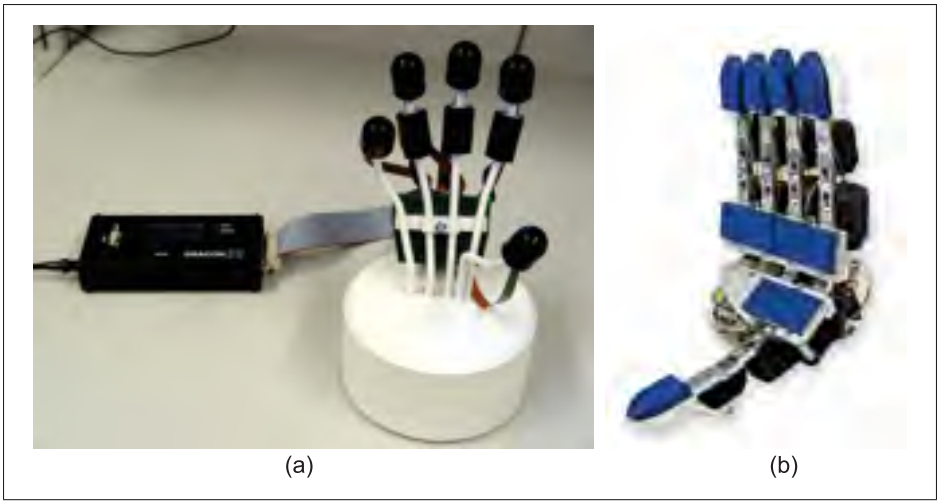

Figure 2.2 Weiss sensors on allegro hand
Taken from Weiss and Woern (2004)

entire assembly to be neat and compact. But while the single-sided tactile electrodes, placed beneath the PTFE layer, provide for easy fabrication and processing of the piezo-resistance, such mutual resistance leads to the indirect measurement of forces and lower sensitivity. This type of sensor is thus less sensitive than sensors built with double-sided electrodes and a piezo-resistive layer between them.

According to the results of Weiß and Wörn (2005), PTFE exhibits a good range of sensitivity up to 2000 Pa ($200\frac{N}{cm^2}$). It also has low creep with temperature and time, compared to silicone rubber and Ethyl Vinyl Acetate (EVA) foam. However, the PTFE exhibits substantially greater changes in its mechanical and electrical properties, due to drift, than does any capacitance-based sensor. Drift thus results in a non-uniform response and hysteresis. Finally, the sensor shows almost no sensitivity to forces below 2 N. Therefore, despite possessing the virtues of ease of construction and good sensitivity to higher static forces, the lack of multimodality, creep in response, and inability to sense forces below 1N prevent this sensor from being considered ideal.

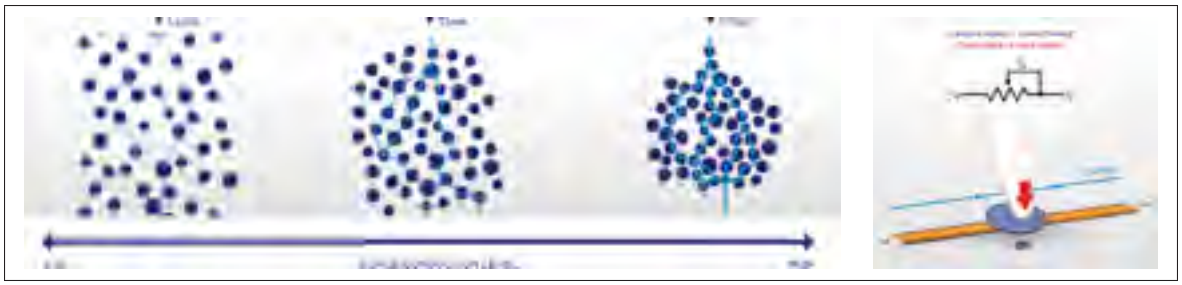

Figure 2.3 (a) Percolation effect in material under stress, (b) Model of the sensor based on QTC

2.1.3 Quantum Tunneling composite (QTC) by Peratech Ltd.

Some researchers (Wang *et al.*, 2009; Huang *et al.*, 2008) have used the modern technique of doping fillers into silicone, in order to improve the silicone's electrical properties for use in sensor construction. As several types of fillers have recently been developed, such as nano-powders of carbon black, and metal particles, some good sensors have resulted from the tunnelling effect of doping of these fillers into silicone rubber and polymers. Although the doping of such conductive composites improves the piezo-resistive properties, the relative change in resistance is still too low for the applied range of forces. To overcome this hurdle, Peratech has developed metal particles with spiked surfaces, which increase the probability that the percolation effect will occur under stress. Such geometrically-modified particles, when doped in polymer, result in a better relative change in resistance at small forces (below 10 N). However, the fillers soon cause the overall mechanical properties of the polymer to degrade (Bloor *et al.*, 2005).

A sensor constructed with QTC material, by Zhang *et al.* (2013), exhibits low hysteresis and a better range of force sensitivity; however, the minimal force sensitivity remains missing, as does dynamic sensing. Furthermore, the percolation effect is not always uniform. The charge conduction path is randomly formed with particle distributions, shown in Fig. 2.3, a topology that leads to a non-uniform response for similar forces. Also, as we saw previously with the Weiss sensors, sensors based on resistive technology always have some level of drift in their

responses. It is therefore quite challenging, relative to the capacitance-based PPS sensors, to achieve accurate measurements and repeatability in the sensor's response.

2.1.4 'BioTac' multimodal tactile sensor by SynTouch

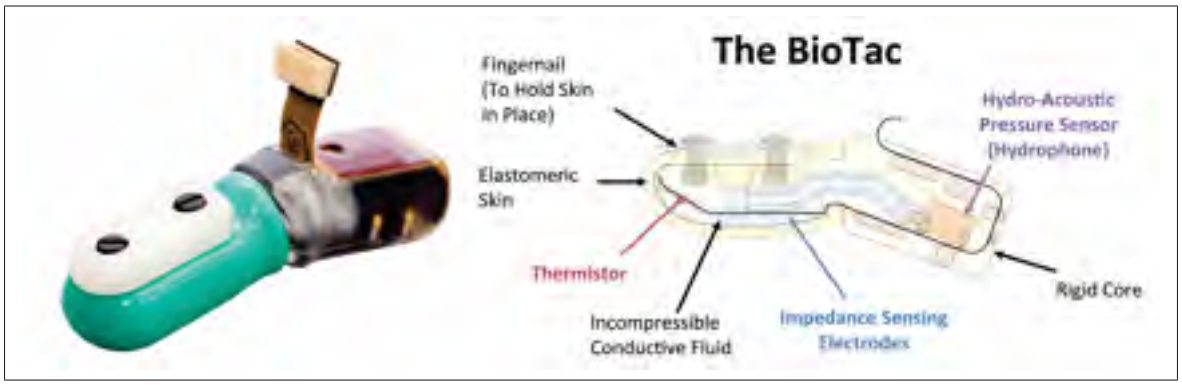

Figure 2.4 Syntouch multimodal sensors namely biotac

Today, the only commercially-available multimodal sensor is the BioTac, as described in Lin *et al.* (2009) and illustrated in Fig. 2.4. The BioTac sensor is capable of detecting pressure, vibration and temperature, all of which are relevant to the modalities under which the human sensory apparatus operates. The sensor measures pressure by way of impedance measurement between the ground and the sensing electrode, with a semi-conductive fluid between the two layers. The same semi-conductive fluid is used for dynamic sensing, which is achieved with a hydrophone pressure sensor that detects the vibrations conveyed by the fluid.

Also, some designated thermistors are placed strategically to measure the temperature stimulus at the finger's surface. This multimodality brings with it the first challenge for construction, because the fabrication and tuning of the sensor is quite complex, and the accommodation of the all processing circuits contributes to the bulkiness of the sensor. In fact, the sensor described here has biggest the drawback in the sense of bulkiness, because to integrate this sensor with a robotic hand, one has to redesign entire distal phalanger of the hand.

The response of the sensor, as defined by Wettels *et al.* (2007), shows that it has a force measurement range from 1N to 20N. However, the sensor response for the forces below 1N seems to be saturated. The dynamic sensing is also characterized by low sensitivity. The viscoelasticity of the fluid induces damping, and the vibrations are not detectable by the hydrophone, as displayed in Fig. 2.4. Although this sensor has a good spatial resolution of 1 mm, and acquisition frequency of 2 KHz for dynamic sensing, the low sensitivity to pressure below 1 N, inability to detect vibrations, and need for spatial integration, mean that this is not the ideal multimodal tactile sensor.

2.1.5 Barometric MEMS IC base tactile sensor by 'Takktile Llc.'

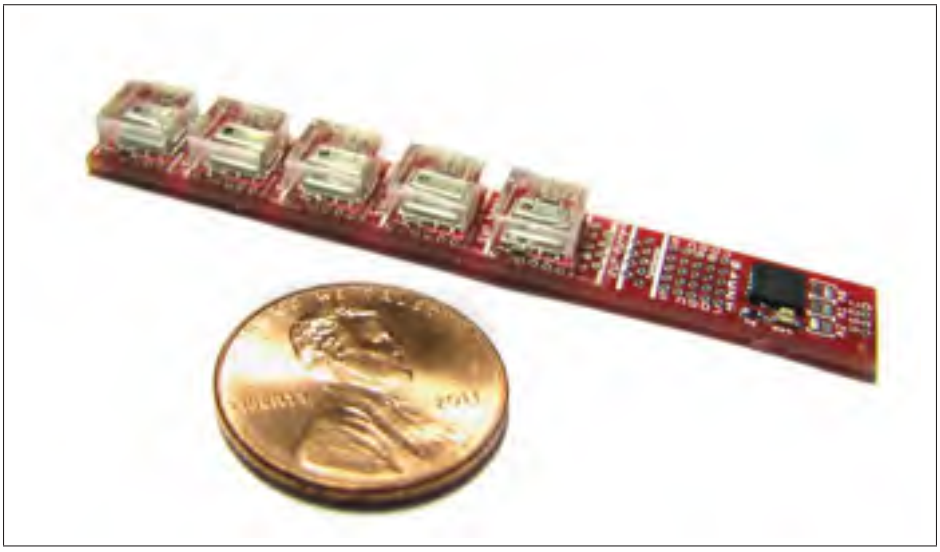

Figure 2.5 Takktile sensors by right hand robotics
Taken from Tenzer *et al.* (2014)

TakkTile LLC has developed a novel tactile sensing approach using barometric pressure-sensing ICs, which are typically used for the weather stations and global positioning system (GPS). These barometric ICs are designed with MEMS technology, which delivers great compactness of the sensor's construction. The sensor fabrication processing method is also advantageous due to its low cost. Tenzer *et al.* (2014) has designed a matrix of such ICs that is cast under liquid polymer. This provides better sensitivity by direct mechanical contact to the MEMS

pressure sensor, and also gives extra protection to the ICs during extreme force situations, which makes them more robust and durable for object manipulation tasks.

A single IC of the TakkTile sensor can detect a wide range of forces (from 0.01 N to 6 N). The main drawback of the sensor is the IC's temperature drift. According to Tenzer *et al.* (2014) the sensor could creep up to 25% of its value on normal room temperature. Another disadvantage of this sensor is its lower spatial resolution. The sensor depends on the ICs for its sensing capabilities, but the most compact matrix layout has a spatial resolution of around 8 mm, which is far greater than the 1-2 mm that was recommended by Dargahi and Najarian (2004).

2.2 Review on non-commercial tactile sensing contributions

Apart from the commercially available sensors, numerous other approaches have been taken to imitate the human tactile sensory apparatus. Although many of these were not completed, and so did not end up as a finished product available in the market, they have still made contributions that have lit the path for novel sensor designs.

2.2.1 Review on static sensing approaches

- Capacitance measurement by Maggiali *et al.* (2008)

  In the past few years, the emergence of touch controllers has spurred a revolution in the touchscreen device industry. Normally, these controllers measure the change in parameters, such as resistance or capacitance, that are induced on the transparent ITO electrodes screen by the touch of a human finger. Fig. 2.6(a) shows the formation of the capacitance-based touch screen, where a high frequency (250KHz for AD7147) pre-charging wave is casted on the driven lines and is measured on the receive lines by a certain level of charging. The time that is taken for the charging is measures by the counter, which is started in parallel with the pre-charging wave. Therefore, the counts of the counter are proportional to the time it takes to achieve a certain level of charge on the sensing electrodes. Unlike

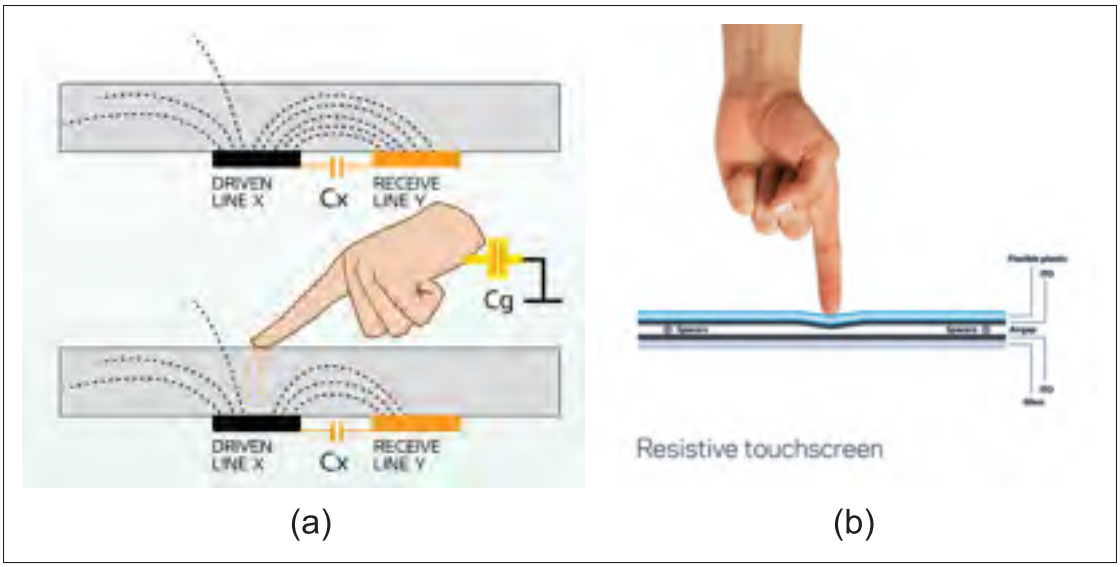

Figure 2.6 Touch screen technologies based on (a) capacitive measurement and (b) resistive measurement

the capacitance-based touch screen, the resistive touch screen has a simple formation. As illustrated in Fig. 2.6(b), ITO electrodes are sandwiched on both faces of transparent compliant material, and the resistance is measured by a controller between the two matrices of ITO layers.

Figure 2.7 Capacitive tactile sensor formed by (a) AD7147 'captouch' controller and (b) formation of the capacitor
Taken from (Maggiali *et al.*, 2008)

With the assistance of touchscreen controllers, many researchers have formed various tactile sensors based on capacitive or resistive change with pressure. Maggiali *et al.* (2008) used an AD7147 chip from Analog Devices to measure change in capacitance, as shown in Fig. 2.7(a). They used silicone rubber foam as a dielectric, coating one face of it with conductive silicone as shown in Fig. 2.7b. The use of these sort of capacitance-processing ICs gives a great advantage in bypassing the bulky and complex capacitance-processing circuit and enables fine tuning of the sensor by digital controls. Moreover, such ICs have digital communication units on board, so by interconnection one can cover a huge area for sensing and distributed processing. Due to such processing advantages, Pressure Profile Systems have also designed their commercial tactile sensor with capacitance-processing controllers made by Cypress Semiconductors. However, despite all their flexibilities, these capacitive sensors still have a small range of force measurement (1-20 N), and lack sensitivity to forces below 0.1N.

- Highly sensitive capacitance based tactile sensor by Mannsfeld *et al.* (2010)

  Another impressive capacitive sensor was formed by Mannsfeld *et al.* (2010). This sensor features with improved geometric aspects of the dielectric by MEMS design. Pressure Profile Systems, Maggiali *et al.* (2008) and Ulmen and Cutkosky (2010) used silicone foam or polymers as the dielectric. Under normal stress, these materials have the tendency to spread into surrounding space, because they are almost completely non-compressible. Therefore, during pressure application, these dielectric materials respond with negligible displacement for small forces (below 1 N) which means they essentially have no sensitivity to these forces.

  Aside from these developments, Mannsfeld *et al.* (2010) has attempted to construct a novel dielectric, using soft lithography processes to develop array of micrometer-sized pillars of PDMS. This micro-structured dielectric can easily be compressed with a very small pressure and circumvent the problem of limited sensitivity to the small forces. Such an effect greatly enhances the sensor's response by way of sensitivity and relaxation time. A sensor based on this innovative dielectric shows force sensitivity up to $10^{-3}N$.

2.2.2 Review on Dynamic sensing approaches

As we argued in chapter 1, dynamic sensing is an essential feature to be considered while designing tactile sensors. Thus far, a few attempts have been made to construct a dynamic tactile sensing apparatus. There are two main approaches that tend to be used for dynamic sensing: piezo-electric film-based sensors, and MEMS-based sensors. While these are by far the most common, some researchers have developed other approaches as well, such as capacitor microphone (Schmidt *et al.*, 2006a), optoelectronic (Dubey and Crowder, 2006),(Mazid and Russell, 2006) and piezo-resistive (Fishel *et al.*, 2008), (Vatani *et al.*, 2013), (Teshigawara *et al.*, 2010) transduction principled sensors.

- Dynamic sensor designs based on Piezoelectric films

  The piezoelectric transduction technique has proven to be a popular one, because of the nature of its response upon force application. Handbook of robotics by Cutkosky *et al.* (2008) shows that PVDF films are favored for the construction of dynamic tactile elements due to their better piezoelectric properties. A detailed study on PVDF by Vinogradov and Holloway (1999) shows that dipoles are formed due to hydrogen and fluoride atoms, which release extra charges under stress. This release results in a voltage gradient on the faces of the PVDF, according to the polling effect. With the use of a charge amplifier, Howe and Cutkosky (1993) and Yamada *et al.* (2002) have implemented dynamic sensors for detecting incipient slip and friction properties of a surface. Both approaches show that one can design a thin and compact dynamic sensing layer, that is similar to human skin, with PVDF. This has driven more researchers to design better dynamic sensors. Choi *et al.* (2005b) has constructed a multimodal tactile sensor, where PVDF was used for the dynamic modality. The static sensing capabilities of the sensor were constructed with pressure-variable ink electrodes that are printed over polyester films. Such a sensor shows some promising results, and it is similar to Syntouch's 'BioTac' in terms of multimodality. However, both sensors share the common challenge of integration, because the multiple sensing principles require separate processing circuits. The complex integration

leads to bulkiness of the sensor, rendering it unable to imitate the human sensory apparatus to a satisfactory degree, and thus unsuitable for the purpose of creating a sensitive robotic skin.

- Dynamic sensor designs based on MEMS

  MEMS have generated new interest in sensor design. Following advancements in manufacturing technology, including lithography and metal deposition techniques, a range of MEMS devices have been introduced. Howe and Cutkosky (1989) used an accelerometer to measure vibrations, in the hopes of applying this technology to slippage detection and texture perception. That approach was improved upon with the use of two accelerometers, by Tremblay and Cutkosky (1993) and Cutkosky and Hyde (1993), which proved useful for filtering out spurious vibrations.

In other developments, Ho *et al.* (2011) designed a micro-scaled force-torque sensor that was fused inside a polyurethane (PU) artificial finger, to detect incipient slip during object manipulation. Others (Su *et al.*, 2010; Ho *et al.*, 2010; Lee *et al.*, 2008; Thanh-Vinh *et al.*, 2014) have focused on the use of MEMS in the design of static sensors. All of these micro-fabricated sensors are incredibly sensitive to forces below 1 N. However, each of them saturates at higher forces due to their small force-moment limitations, and the fabrication of these MEMS devices requires special lithography labs and sophisticated, expensive manufacturing equipment. In addition, the use of the same processing circuit constrains the potential for multiple designs on the same area, limiting these sensors to uni-modality. This constraint urges us towards the development of a tactile sensor with a singular transduction principle for static and dynamic sensing, that will be simultaneously compact, highly sensitive, and easy to manufacture.

2.3 Conclusion

In brief, the review of literature on tactile sensing gives us ideas about behavior of tactile events and the developed alternatives of the tactile sensing. Such study has paved the path for the future innovations of this thesis by delivering benchmarks of performance and exploration

of the technologies. Indeed, review of literature is handy for future experiments and designs of the novel tactile sensor.

CHAPTER 3

STATIC TACTILE SENSOR

3.1 Introduction

Pressure stress measuring tactile sensor has been the most explored region in the research of a tactile sensor. Chapter 1's static sensor introduction section elaborates the importance of the static type sensor. Along with that chapter 2 explains the available alternatives for the static tactile sensors which are yet incompetent as an ideal sensor according to the sensor requirements explained in the section 3.2. We took this opportunity to explore more into non-commercial researches for capacitive tactile sensors and we found a strong need for the better dielectric instead of conventional alternatives shown in section 2.2. Hence, we have tried to develop a novel soft dielectric with consolidating modern techniques of micro-fabrication and doping of nano-materials as represented in section 3.3 to enhance the capacitive response as illustrated in section 3.5.1. Next stage is to build the static tactile sensor with the newly developed dielectric and capacitance measuring ASICs. Section 3.4 shows the construction of dielectric layer with the sensor assembling for the experimentation. And lastly, section 3.5 will concentrate on the variety of trends on force, stress and SNR to evaluate sensor performance.

3.2 Sensor requirements for static tactile sensing

Growing appeal from prosthetics and robotics sectors and continuous progression of new sensing techniques have inspired many researchers for implementing an ideal tactile sensor. Most of the researchers have bidden for a basic tactile sensor engulfed to static pressure sensing plot. According to Dargahi and Najarian (2004), Dahiya and Valle (2008), Yousef *et al.* (2011) and Nicholls and Lee (1989) , a good pressure tactile sensor should include properties as follows.

- Wide range of force detection

Most of the pressure tactile sensors are designed to measure forces in the range of 1-10 $\frac{N}{cm^2}$ whereas grasping force for each object varies according to size and weight of the object. A good tactile sensor should be able to detect small pressure during contact as well as large pressure during heavy object lifting also. Many static tactile sensors have displayed very good response for either very small pressure or very large pressure on same area. But still there is a wide gap open for a better static type tactile sensor which can detect small as well as very large pressure stimuli on same area. Commercially available tactile pressure sensors like *Pressure Profile System(PPS)* based on capacitance and *Peratech Technologies* based on tunneling effect claim to detect higher forces however minimal pressure sensibility is still lacking in their products. Another multimodal tactile sensor sold by *SynTouch* has same limitation for lower pressure detection. On the other hand, continuous growth of Nano technologies brings up MEMS and micro design components. Sensors based on such technologies are extremely sensitive for smaller stimuli. Mannsfeld *et al.* (2010) has done some work to detect very tiny pressure force element by MEMS design in dielectric. However, they saturate at large force due to mechanical deformation of that MEMS component. A solution to this paradigm is to blend both qualities of heavy pressure as well as very small pressure in to one and we can realize it by superimposing MEMS features over normal high force pressure tactile sensor.

- Better spatial resolution

  Halata and Baumann (2008) points out an important function of SA type mechanoreceptor is to localize the touch over human skin. Imitating that functionality, a normal static tactile sensor should consist better spatial resolution over tactile surface. There are many technologies such as row-column sandwich approach for capacitive and resistive technologies, bi-cubic filtering, MEMS design and tomography design which leads us to better spatial resolution. However, each approach is constrained by some implications such as ghost point effect in row-column sandwich & EIT; challenges of fabrication and force saturation in MEMS. Lin *et al.* (2009)'s 'BioTac' sensor depends on thermal detectors for localization of contact which leads to relatively small spatial resolution. Pressure Profile Systems

is using software based bi-cubic filtering technique where they are averaging force on two points and get us mid point but still it's not accurate assumption for spatial resolution. However, one can choose smaller sensing elements and bi-cubic filtering could get us relatively better accuracy and spatial resolution as illustrated in Fig. 3.1.

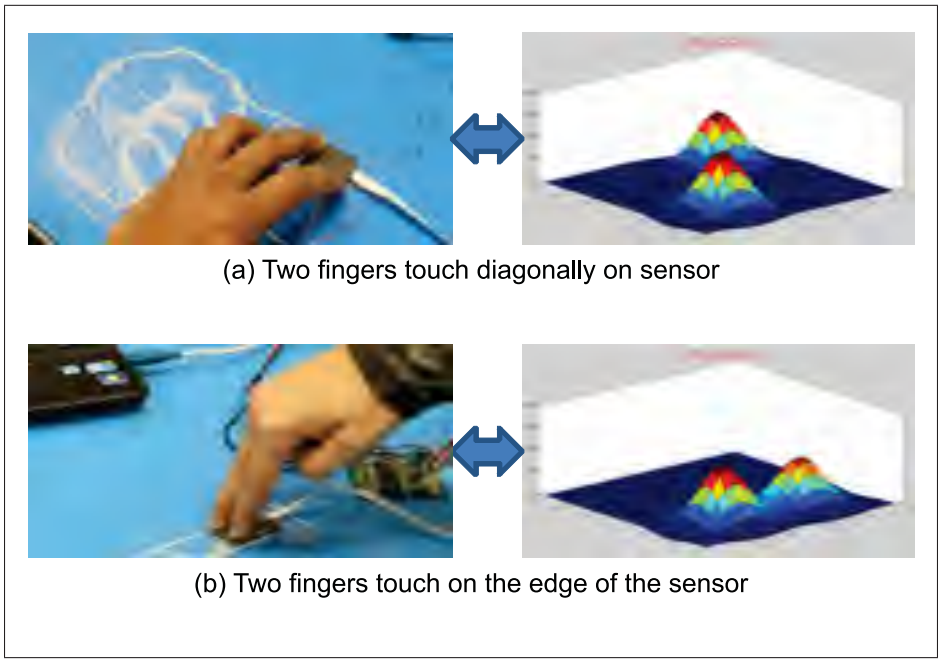

Figure 3.1 Tactile sensor visualization with bi-cubic mesh due to touch (a) diagonally and (b) on the edge

- Better SNR, low hysteresis and low thermal drift

  Most of the technologies involved with tactile sensor development suffers from some of these discrepancies. resistive and capacitive techniques have some of the thermal drift and hysteresis problem which is mostly due to material's mechanical properties. Schmitz *et al.* (2011) shows capacitive based novel tactile sensor however response of their sensor depends on damping ration of the dielectric foam slab's mechanical properties. Optics based tactile sensors doesn't have thermal drift but still some amount of hysteresis and complexity of fabrication is big challenge in them. Considering exoskeleton finger made by Park *et al.* (2007) and Chorley *et al.* (2009) are good examples for better optical based

tactile sensors but considering sophisticated electronics and compactness hold them back in the race to be ideal tactile sensor. Tunneling effect based sensors are popular due to their ease in fabrication but thermal drift cause difficulties in judging its behavior as conductivity of carbon doped rubber changes with time and similarly mechanical properties of rubber is directly affects the hysteresis of the sensor.

Some times small force components are not able to get noticed because noise in the sensor is relatively higher and hysteresis of the sensor doesn't allow it to trigger the notable force level of the sensor. In such circumstances, one would desire a sensor built on relatively less hysteresis and very good SNR of similarly like optoelectronic but also complexity of fabrication and processing has to be justified also.

- Compact and ease of fabrication

  Human skin is the basic organ for the tactile sensing over entire body. The structural property of tactile sensor should exhibit human skin type functionalities in order to perform as artificial skin over mechanical skeleton of robotic/prosthetic hand. compactness and ease of integration should be the main facts a tactile sensor should adopt. Some of the innovative tactile sensor have very complex structure where they can't perform as human skin on structure but to accommodate them, one has to replace entire distal phalanger. Row column based capacitive and resistive based sensors have better construction flexibilities as layered formation. Peratech and Pressure Profile Systems are examples of those kind of skin type thin tactile sensors in the current market. Innovations in liquid silicone casting techniques and micro-machining of the molds could assist us in developing minimal thickness of sensor. Inclusion of techniques like spin coating and MEMS design could compose real thin material for design of our project.

3.3 Redesigning dielectric with microstructures and nanoparticles filling

Most capacitance-based tactile sensors use the relative change in the distance, d, between two conductive plates to measure the applied pressure p_a,

$$p_a \propto C = \varepsilon_r \varepsilon_0 \frac{A}{d}, \tag{3.1}$$

where C is the capacitance value, ε_r is the relative static permittivity, ε_0 is the vacuum permittivity ($\varepsilon_0 \approx 8.854 \times 10^{-12}$ F/m), and A is the overlap area of the plates. One element that limits the sensitivity of these sensors is the mechanical response of the non-conductive material, used between the electrodes and the ground plane, that serves as a dielectric and as a spring-like element. Many researchers have used a plain layer of soft polymer, such as silicone Leineweber *et al.* (2000), to create a soft dielectric that will deform under applied stress. However, silicone, like most polymers, is incompressible. This means that for a wide range of applied pressure, its total volume will remain unchanged, and in reaction to a compressive force on a specific area, some region of the dielectric will have to expand. This behavior leads to poor compliance of the soft material and to a very slow recovery time once pressure is released, two shortcomings that result in hysteresis and a low level of sensor sensitivity. To circumvent these drawbacks, some researchers have instead used silicone foam (Schmitz *et al.*, 2010) or urethane foam (Hoshi and Shinoda, 2006) to form the dielectric for their capacitance-based tactile sensors. However, although the volume of foam can change under pressure, leading to a more sensitive pressure sensor, ordinary foam is still subject to hysteresis. Ulmen et al. Ulmen and Cutkosky (2010) circumvent this limitation by using a closed cell PU foam. The ratio of the stiffness-to-damping in a foam with a closed cell structure is higher, due to the trapped air that acts as a spring-like element. The nonlinearity of the response is thus drastically reduced. However, because of this structure, the stiffness of this type of foam is still relatively high and its permittivity is relatively low. Closed cell foam thus leads to a sensor with a middling level of sensitivity.

In order to drastically increase the sensitivity and decrease hysteresis, Mannsfeld *et al.* (2010) made a significant breakthrough by creating a micro-stuctured dielectric out of PDMS. Using soft lithography, they constructed micro-features in a PDMS layer, thus producing a material with room for silicone to expand locally. Consequently, they have lowered the apparent stiffness of the dielectric and reduced hysteresis. From our point of view, the sole drawback of their approach lies with how the sensor is manufactured. Soft lithography is a time-consuming process typically used for making micro-electromechanical systems (MEMS) that requires a significant amount of specialized equipment. Although this production method would be perfectly suitable for a high production volume, the current market for tactile sensors remains small.

The dielectric of the sensor we are proposing is also micro-structured, but the size of the features is of a larger magnitude. Working at a larger scale allows us to use a simpler manufacturing process, that requires almost no specialized equipment. Also, despite the trade-off made regarding the size of the features, the lowest pressure that can be recorded by our sensor is in the same range as what was reported in Mannsfeld *et al.* (2010). This is achieved by exploiting the geometry of the features, and, more importantly, by increasing the permittivity of our dielectric by embedding nanoparticles of ferroelectric ceramics within a very soft silicone. The following section presents the design of the dielectric and describes the process we used to manufacture it.

3.3.1 Building a Double-staged Microstructure

To be comparable to the apparatus of a human hand, a tactile sensor should be capable of measuring forces up to 10 N on a surface of 1 cm^2 (100 Kpa) (Dargahi and Najarian, 2004; Dellon *et al.*, 1995; Ehrsson *et al.*, 2001). To achieve fine manipulation it is also important that the sensor remains highly sensitive in the range under 1 N (Westling and Johansson, 1987) on the same area. From a technical point of view, these two constraints are very difficult to satisfy simultaneously, as they require the sensor to sense a considerable range of forces while also being very sensitive to low forces. We aim to accomplish this by micro-structuring our

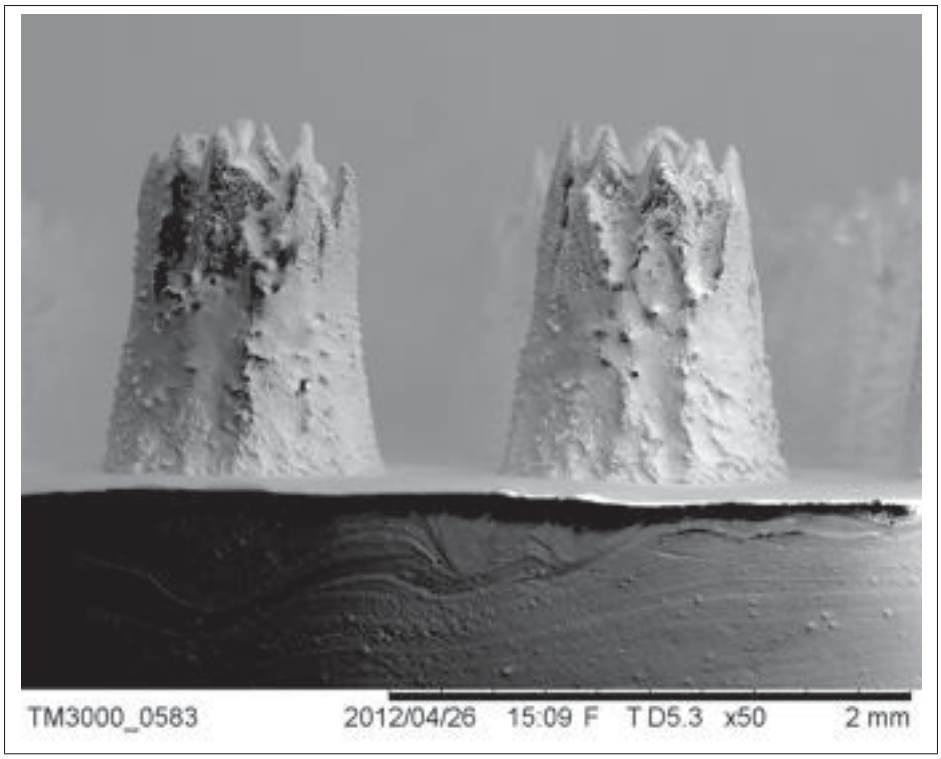

Figure 3.2 Side view of the feature's double-stage geometry, taken with an SEM microscope

dielectric with two layers of different-sized features. The first stage is composed of conic features with a base diameter of 900 μm. Their apex is at 5 mm and their height is truncated at 800 μm. Due to their size and their density over the surface (64 per cm^2), these features account for a significant variation of the distance d between the two conductive plates of our capacitive sensor over most (10-100 Kpa) of the range of the possible applied pressure. In order to increase the sensor's sensitivity to low pressure, on top of each of these truncated conic features we have placed 10 smaller cones of 80 μm base diameter and 100 μm apex. These smaller geometric extrusions are very easy to deform, and so they increase the variation of the distance d of eq. (3.1) for very low applied-stress values. However, their effect is almost null for higher stresses as they rapidly reach their maximum compressibility. Fig. 3.2 shows a side view of the superposed features, taken with a Hitachi TM3000 scanning electron microscope (SEM).

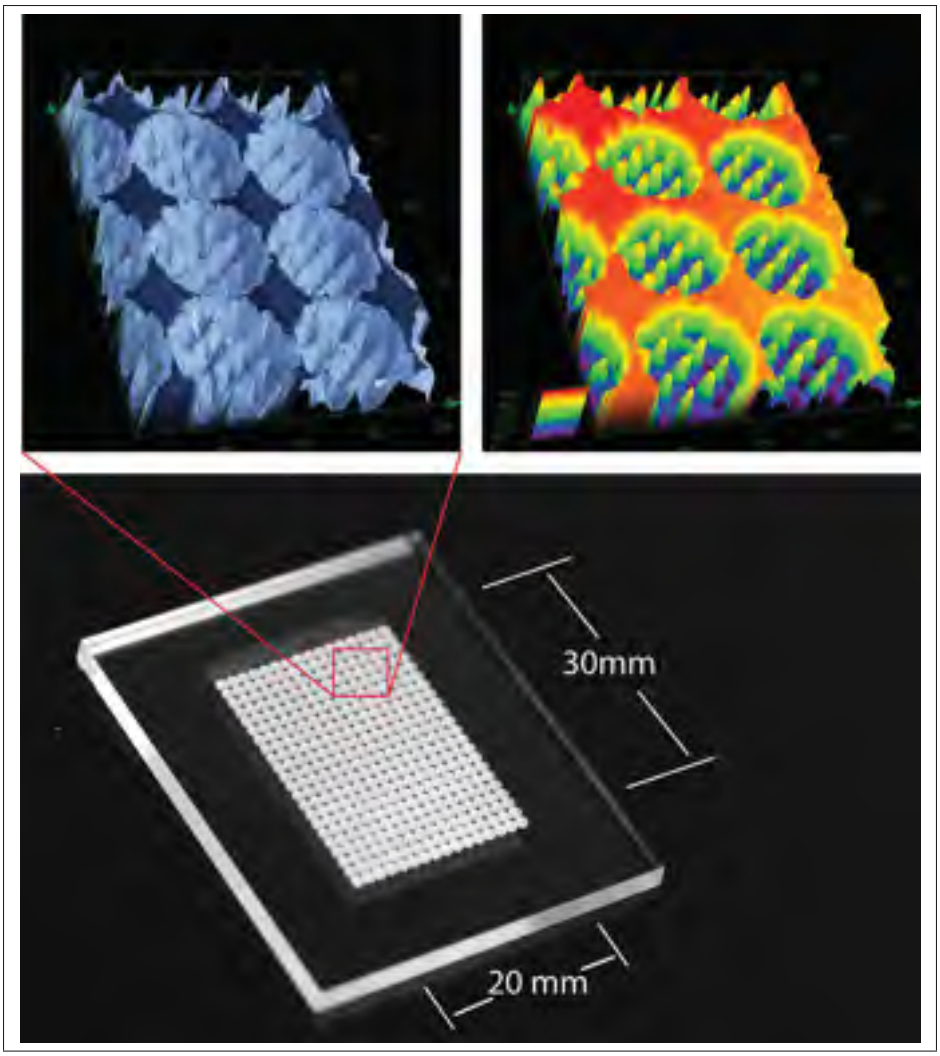

Figure 3.3 Mold for the microstructured features

Our micro-structured dielectric is made of a soft platinum-cure silicone rubber, Ecoflex (Shore 00-30 hardness) from Smooth-On, Inc., that is cast in an acrylic mold. The mold is engraved using a conventional CO_2 laser (Epilog Helix 40 watts). The maximum effective resolution of our laser cutter in the acrylic is 600dpi. Indeed, due to the spot size of the laser, as well as the heat diffusion in the mold material, it is not possible to engrave any features smaller than the size associated with this resolution. The base diameter of our smallest features is closely related to this limitation. By controlling the speed of the machine and the power of the laser, we can control the height of the features as well as the cone angle. Following multiple experiments, we found that raster engraving the acrylic in a single pass with a laser power of

90% and speed of 25% gave us the desired depth of the mold (900 μm) and the best result in terms of sharpness. Fig. 3.3 depicts the resulting mold, as well as close-up 3D view taken with an optodigital microscope (Olympus DSX100).

3.3.2 Increasing the Permittivity of the Dielectric

By microstructuring our dielectric material, we aim to lower the stiffness of the material and reduce the hysteresis that arises from the incompressibility of silicones. To further increase the pressure sensitivity of our capacitive-based tactile sensor, we also hope to raise the static relative permittivity of the dielectric material.

There are two incentives for increasing the dielectric constant of our material, both of which lead to a better SNR. The first reason is that, for a given applied pressure, increasing the dielectric constant will increase the magnitude of the capacitance change, ΔC, for a given force. This is true even if the relative change in capacitance, $\Delta C/C_0$, is the same. Most commercially available capacitance to the digital converters (CDCs) function based on the time measurement of a response of the capacitor to an excitation signal (Gasulla *et al.*, 2005). The time is measured with a counter that is limited in resolution. Therefore, up to a certain range, the bigger the variation (in Farads) of the capacitance, the higher the amount of count will be, thus increasing the SNR.

Our second incentive is closely related to the fact that our dielectric is microstructured. Most of the capacitance-based tactile sensors that were proposed in the literature (Leineweber *et al.*, 2000), (Schmitz *et al.*, 2010) ,(Ulmen and Cutkosky, 2010), (Hoshi and Shinoda, 2006) and (Castelli, 2002) consider pressure measurement to be a direct function of the change in the distance, d, between the two plates of the capacitor, i.e.,

$$p_a \propto \varepsilon_r \varepsilon_0 \frac{A}{d(p_a)} \,. \tag{3.2}$$

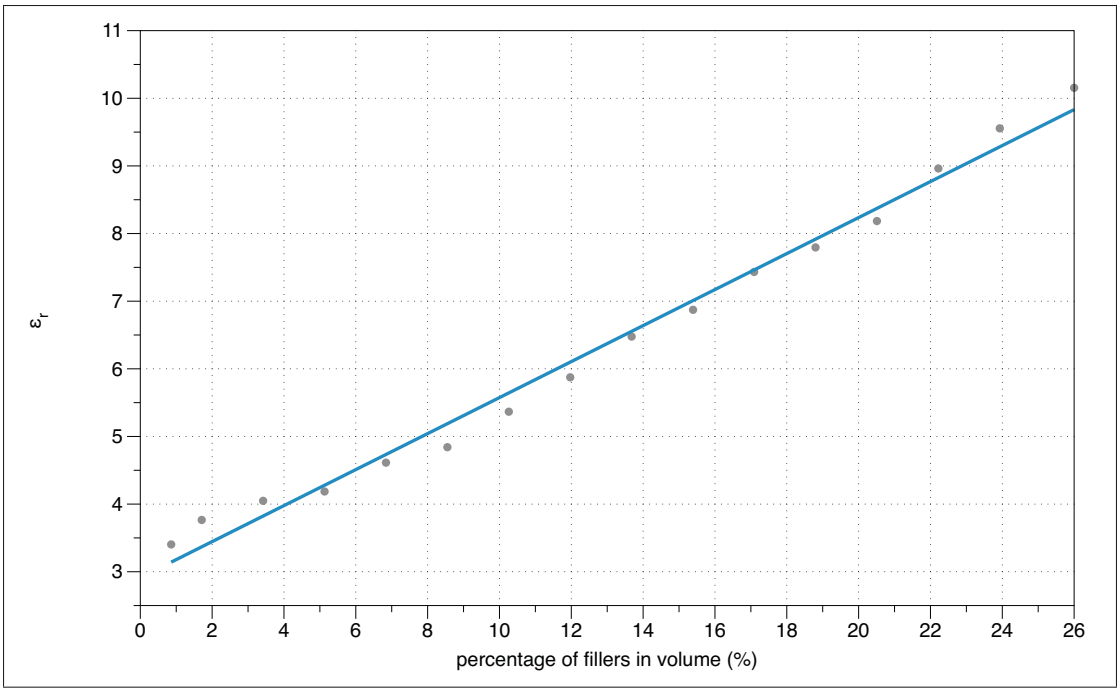

Figure 3.4 Permittivity of the composite for different volume fractions of $BaTiO_3$

This assumes that there is no interaction between the compression of the dielectric, and the static relative permittivity of the material. For tactile sensors in which the dielectric is formed by a plain silicone sheet (Leineweber *et al.*, 2000) or closed cell foam (Ulmen and Cutkosky, 2010), this is a valid approximation. However, due to the microstructure of our dielectric, in our case the static relative permittivity will vary as the proportion of air to silicone in a given volume changes with the applied pressure. The pressure measurement then becomes:

$$p_a \propto \varepsilon_r(p_a)\varepsilon_0\frac{A}{d(p_a)}\,. \tag{3.3}$$

This characteristic increases the non-linearity of the response as well as the capacitance variation for a given load, thus raising the sensitivity of the sensor. In order to maximize this effect, the material used in the sensor should be of a very high relative permittivity, as it will increase the variation between the overall dielectric constant under no load and under maximum load. The dielectric constant of most low Shore hardness polymers is below 5. The

silicone used in this work is no exception, as its static relative permittivity is 3.2. In order to increase this property, we have embedded high-permittivity nanoparticles of ferroelectric ceramic into our silicone. Other researchers have also added this type of filler in order to increase the dielectric properties of a material. Nanoparticles of ferroelectric ceramic have previously been embedded in epoxy (Rao *et al.*, 2001), PU (Pyun *et al.*, 2002), polyamide (Dang *et al.*, 2008), PDMS (Khastgir and Adachi, 2000) and other silicones (Liu and Shaw, 2001) for this purpose. The important aspect of our research is that we are exploring how this technology can be applied for the purpose of tactile sensing.

The best filler candidate for increasing the dielectric constant of our silicone would seem to be calcium copper titanate (Chung *et al.*, 2004) (CCTO, $CaCu_3Ti_4O_{12}$) due to its incredibly high dielectric constant ($\varepsilon_r > 250000$) (Guillemet-Fritsch *et al.*, 2006). However, to use this material would be to contradict our claim regarding the simplicity of our approach, since, to the best of our knowledge, nanoparticles of CCTO are not yet available on the market and thus must be synthesized in a chemical lab.

Two alternatives are barium titanate ($BaTiO_3$) and lead magnesium niobate-lead titanate (PMN-PT, $Pb(Mg_{1/3}Nb_{2/3})O_3$-$PbTiO_3$), nanopowders that have also a high dielectric constant. These two ferroelectric ceramics are commonly used in the manufacturing of capacitors with high capacitance values (Yoneda *et al.*, 2000), and they are low in cost and widely available.

We used two types of nano-particles to increase the permittivity of our micro-structured dielectric. The first is $BaTiO_3$, of 200nm in size and tetragonal shape, sold by US Research Nanomaterials, Inc. The second type is PMN-PT, spherical microparticles of 3μm in size, sold by TRS Ceramic, Inc. under the name PMN-38. According to their manufacturers, these materials have a dielectric constant at room temperatures of, respectively, 4000 and 19000.

Fig. 3.4 shows the values of the dielectric constants we obtained for different volume fractions of $BaTiO_3$ and PMN-PT that were embedded in our silicone matrix. These values were calculated according to eq.(3.1) using the capacitance measured at 100hz with an LCR meter (B&K Precision 878B) of different dielectric samples of a known area and thickness (4 cm^2 and

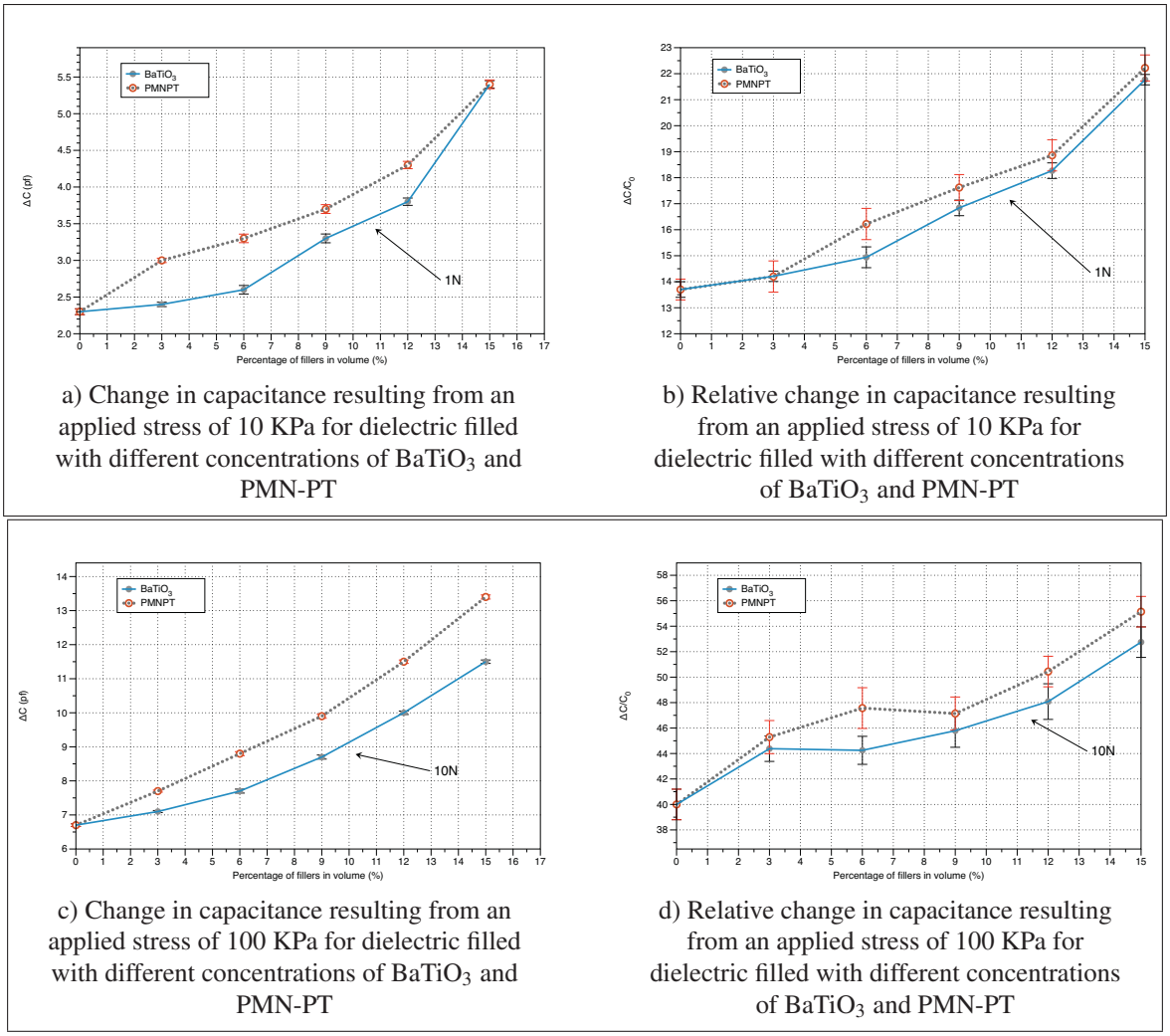

a) Change in capacitance resulting from an applied stress of 10 KPa for dielectric filled with different concentrations of $BaTiO_3$ and PMN-PT

b) Relative change in capacitance resulting from an applied stress of 10 KPa for dielectric filled with different concentrations of $BaTiO_3$ and PMN-PT

c) Change in capacitance resulting from an applied stress of 100 KPa for dielectric filled with different concentrations of $BaTiO_3$ and PMN-PT

d) Relative change in capacitance resulting from an applied stress of 100 KPa for dielectric filled with different concentrations of $BaTiO_3$ and PMN-PT

Figure 3.5 Electromechanical characterization of different dielectrics

2 mm, respectively). Fig. 3.4 suggests a near-linear relationship between the volume fraction of filler and the dielectric constant of the composite. These values are also similar to what was reported (Khastgir and Adachi, 1999, 2000; Shen *et al.*, 2004; Randall *et al.*, 1992; Cherney, 2005) for similar particles in a comparable cross-linked matrix of silicone.

Considering the high permittivity of the ceramic particles that were used, the value of the dielectric constant we obtained for our composite may seem low in contrast. However, the resulting dielectric constant of a composite is not a simple function of the ratio of polymer matrix to the filler. This is due to the fact that a single crystal of the ceramic particles does not have the

same permittivity along all three axes (Cherney, 2005; Carpi *et al.*, 2008; Khastgir and Adachi, 2000). For example, a single crystal of $BaTiO_3$ has a permittivity of 4000 along the a axis, 100 along the b axis, and 100 along the c axis. Since these particles are randomly aligned in the polymer matrix, the overall resulting permittivity is low.

To align the particles, and therefore obtain a higher dielectric constant, some authors have proposed cross-linking the polymer matrix under an electric field. Randall *et al.* (1992) have shown that applying an electric field during curing effectively aligns the particle in the field. However, the dielectric constant they report for their composite, like the one reported in a similar study (Khastgir and Adachi, 1999), does not exceed the value presented in Fig. 3.4. Indeed, none of our experiments using a silicone composite, polled at 2.5 kV/mm during curing, showed any significant improvement of the dielectric constant. Moreover, curing the silicone-ceramic mixture under a field is known to form pearl chains (Tomer and Randall, 2008) that increase the compressive modulus of the material, thus lowering the overall sensitivity of the sensor.

Some authors (Qi *et al.*, 2006; Cherney, 2005) have also proposed the addition of metallic particles to the composite, such as Ag, in order to further raise the dielectric constant. Although this technique does slightly increase the dielectric constant, it has a downside, as preliminary experiments conducted in our lab show that the compressive modulus and the hysteresis of the resulting material are considerably higher as well.

This is in light of the fact that in our application the response of our sensor is dependent on both the electrical and the mechanical properties of the dielectric. This means that the relative permittivity of the dielectric alone is not sufficient to characterize the performance of our sensor; we must also take the compliance of the dielectric material into account. If we consider only the electrical properties of the composite, PMN-PT seems to be the best choice, as it is supported by the data shown in Fig. 3.5.

However, as we must also address the mechanical side of the problem, we conducted various tests to characterize the relation between the applied stress and the variation in capacitance.

More specifically, these tests were performed on a single taxel, 30 mm^2 in size, of the microstructured dielectric we created using the mold presented in Fig. 3.3. Fig. 3.5 shows the capacitance variation, ΔC, for different volume fractions of the two nanoparticles, and for two different stresses (10 KPa and 100 KPa). It also shows the relative change of capacitance, $\Delta C/C_0$, for the same characteristics. These data were taken with a Mark-10 force tests stand (ES20) equipped with a Mark-10 M4-10 force gauge and a Mitutoyo 543-693 displacement gauge. The capacitance data were recorded with the LCR meter, as mentioned previously.

Despite the clear advantage of higher dielectric constant of PMN-PT comapred to $BaTiO_3$, Fig. 3.5 shows that the capacitance variation and the relative change in capacitance are nearly identical for the two different composites at applied stress levels of 10 KPa and 100 KPa. Furthermore, some hysteresis was observed for the sensor when using the PMN-PT-filled dielectric. Our decision was also swayed by the fact that PMN-PT costs almost twice as much as $BaTiO_3$. Therefore, although PMN-PT has a slight advantage, we decided to use $BaTiO_3$ for the filler.

3.4 Sensor Fabrication

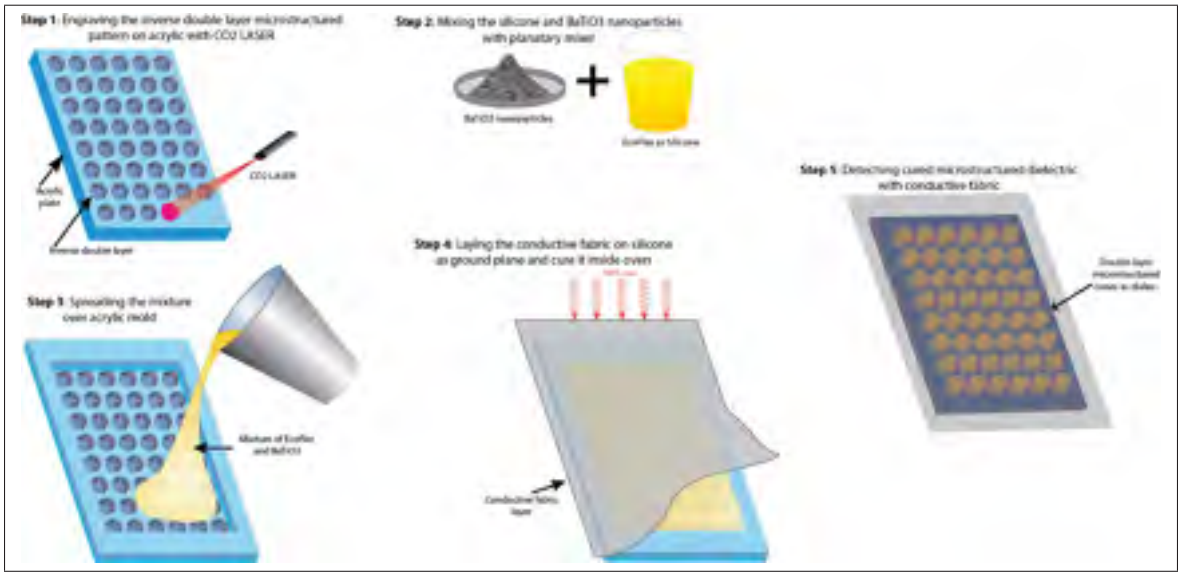

Figure 3.6 Process of fabricating the dielectric

The process of fabricating our tactile sensor consists of two steps: constructing the double-layered micro-structured dielectric, and then integrating it with the entire sensor assembly to form a single unit.

3.4.1 Construction of the Dielectric

The dielectric is fabricated according to the procedure illustrated in Fig. 3.6. The first step is making a mold for the double-layered dielectric. Rather than using a sophisticated and expensive method, such as MEMS, to manufacture the microstructures, we instead accomplish simplified manufacturing using machines that are available in most fabrication labs. The acrylic mold is fabricated by raster engraving the desired pattern at 600DPI using a CO_2 Laser Cutter (Epilog Helix 40 Watts). The resulting mold, shown in Fig. 3.3, is then cleaned with alcohol and dried under a pressurized-air jet. The dielectric itself consists of a silicone and nanoparticle composite. Nanoparticles of $BaTiO_3$ (US Research Nanomaterials, Inc., 200nm tetragonal) are added to a very low hardness platinum cured silicone (EcoFlex Shore 00-30 from Smooth-On, Inc.) in a volume fraction of 25%. Since nanoparticles tend to form agglomerates (Baldyga *et al.*, 2008) which can affect the homogeneity of the mechanical and electrical properties of the sensor, we mix the composite for three minutes in a planetary mixer (Thinky ARE-310), and we use a vacuum degassing chamber to remove trapped air bubbles. Although our mixing technique does not fully prevent the agglomeration of particles, it does provide a sufficient level of uniformity, as shown in Fig. 3.7.

The homogenized mixture is poured into the mold, and a piece of highly conductive fabric is laid over it. This conductive fabric (cobaltex, from Less-emf.com) is made of nickel and copper fibers and is 0.1mm thick. Within the sensor, it will be connected to the ground of the circuit, and will also act as one of the capacitor's plates. An acrylic sheet is laid over the fabric in order to ensure that the silicone is evenly spread over the microstructured area. The entire arrangement—consisting of the mold, the silicone-nanoparticle composite inside it, the conductive fabric, and the acrylic sheet on top—is then placed in an oven at 90 °C to cure the silicone mixture. The main reason for curing at such a high temperature is to ensure

that the nanoparticles are evenly distributed in the resulting dielectric. If left to cure at room temperature, it would take 48 hours to reach 90% of the ultimate cure, during which time the nanoparticles might separate from the silicone and accumulate at the bottom of the mold. We sped up the process by curing at 90 °C, which, according to the manufacturer's specifications, allows the silicone to reach the same level of cure in just four hours. After curing the silicone, we carefully removed the dielectric from the mold and left it to cool until it reached room temperature.

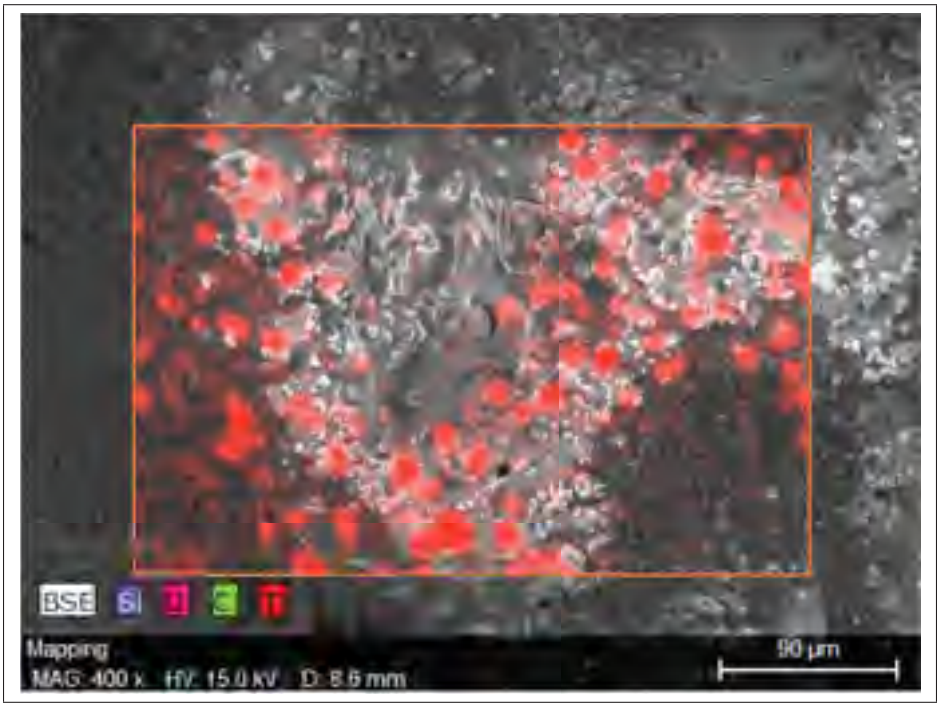

Figure 3.7 Agglomeration of $BaTiO_3$ particles in the silicone.
Image taken with an SEM microscope (Hitachi TM900)

3.4.2 Assembling the Sensor

In this stage of the sensor fabrication, the dielectric, with the conductive fabric on one side, is laid over a rigid PCB. The PCB features taxels, sized 6mm by 6mm, in the pattern of a 3 by 4 matrix, as illustrated in Fig. 3.8. On the other side of the PCB, the taxels are connected

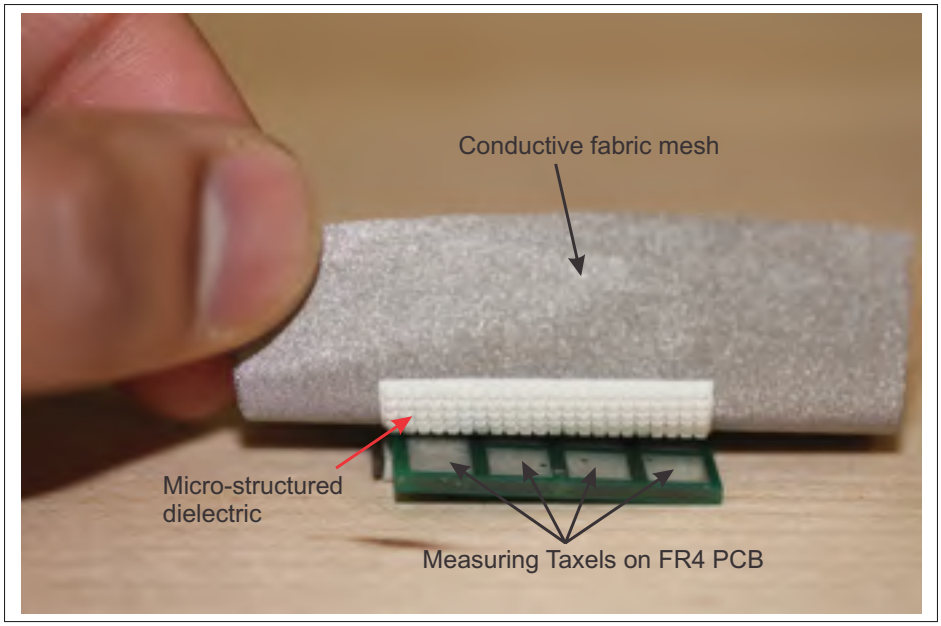

Figure 3.8 Assembling the sensor by placing the microstructured dielectric skin on the sensor PCB

to a PSoC3 micro-controller unit (MCU) made by Cypress Semiconductors, which includes a CDC converter as a functioning block inside the chip. There are numerous advantages to using such an MCU: it enhances the sensor's tuning ability and provides greater design flexibility, while being compact and low-cost. Other researchers (Schmitz *et al.*, 2011; Peng and Lu, 2015) have also produced novel tactile sensors designed with the help of similar capacitance-measurement ICs. In our sensor, the capacitance at each taxel is measured by the Cypress MCU, which delivers the 16-bit number to us as counts. We communicate the sensor's 16-bit data, via an RS-485 interface, to the computer for visualization. For the computer, we used Qt to design a graphic user interface (GUI) that converts the taxel data into a raw-column format. The resulting data matrix is equivalent to the layout of the taxels, as shown in Fig. 3.9. In the visualization, bi-cubic filtering is applied to each neighboring taxel, to generate a smooth mesh of data that reproduces the tactile points.

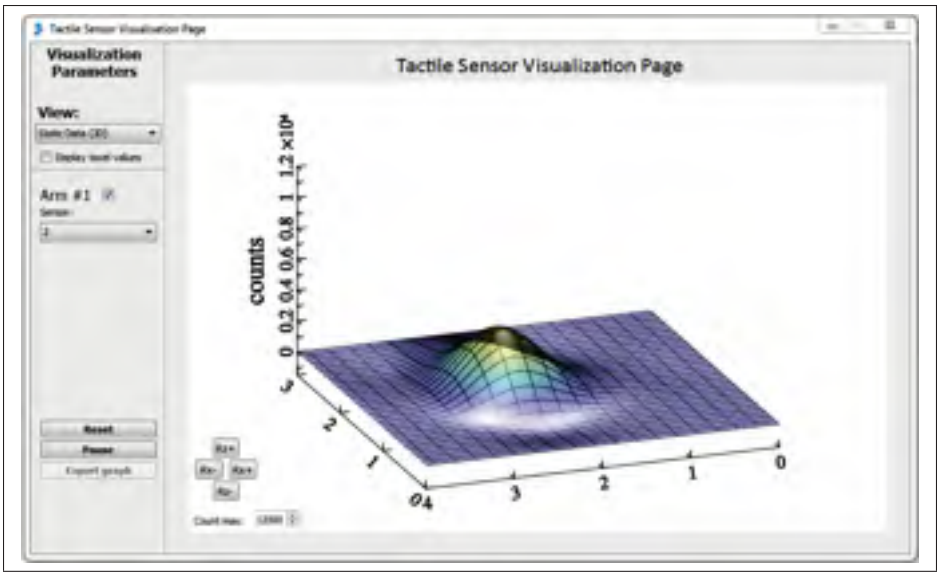

Figure 3.9 GUI for the tactile sensor, created with Qt software

3.5 Results

Our goal was to build an innovative dielectric to allow the sensor to have high sensitivity to low forces, and a wide range of force detection capabilities. In this section we validate our design assumptions by characterizing the sensor's response to pressure.

3.5.1 Response of the Dielectric to Displacements Induced by Force

As we highlighted in Section 3.3, the combination of the silicone micro-structure and the nanoparticle filling creates a material with a permittivity that varies as a function of stress, which further amplifies our response. To validate our assumptions, we recorded the dielectric's capacitive response on the force bench which was previously used to characterize the different dielectric materials (see Section 3.3.2). The novel dielectric is placed between 2.25 cm^2 copper plates, and forces of 0N to 50N are applied on the surface area. Fig. 3.10 shows the measured relative change in capacitance, due to relative changes in the displacement resulting from the force. According to eq. (3.1), we anticipate that for a fixed-area capacitor, the behavior of the relative change in the capacitance will be in proportion to the displacement. This effect is shown by the green curve in Fig. 3.10.

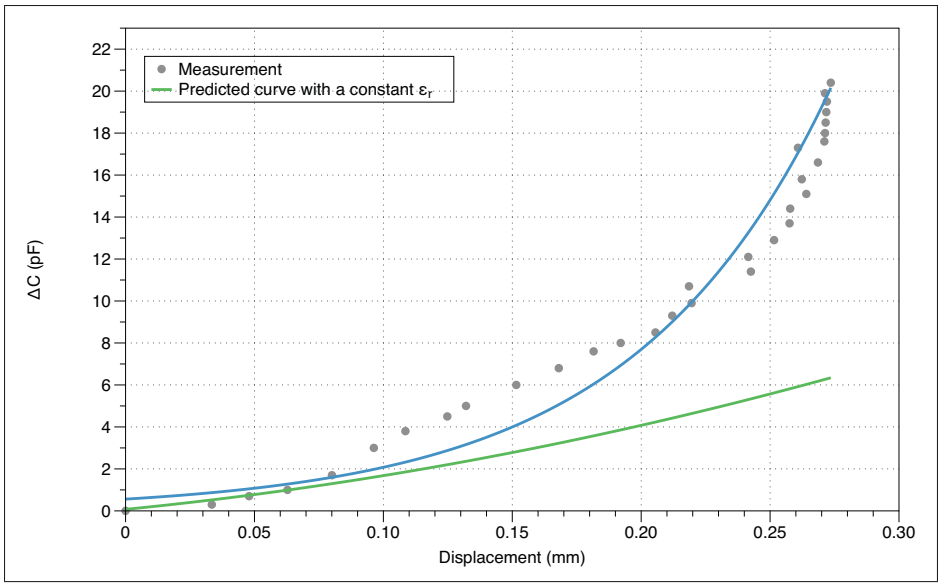

Figure 3.10 Change in capacitance due to displacement

However, when we actually measured the values of ΔC, we found that it exhibits the enhanced response with the displacement. Further analysis of the data confirms our expectations, as it shows that the relative permittivity of the micro-structured dielectric changes with displacement. Fig. 3.11 depicts this effect.

This non-uniformity in the relative permittivity of the dielectric contributes to the large change in capacitance, which is more than double that of a conventional fixed relative permittivity capacitive sensor.

3.5.2 Response of the Sensor to Pressure

We applied a range of forces to a single taxel, to measure the relation between pressure and the CDC counts of the sensor. Fig. 3.12 shows the setup of the experiment. We used a Mark-10 force gauge (ES20) bench with a resolution of 0.02N, and a displacement meter (Mitutoyo 543-693) with accuracy of $1\mu m$. The sensor was mounted on a stable base and connected to our computer for data recording and visualization. Predefined standards (Dargahi and Najarian, 2004) state that a tactile apparatus should have a force detection range of 0.01-10N. Accordingly, we exerted forces on the sensor taxel ranging from 0.02N to 15N.

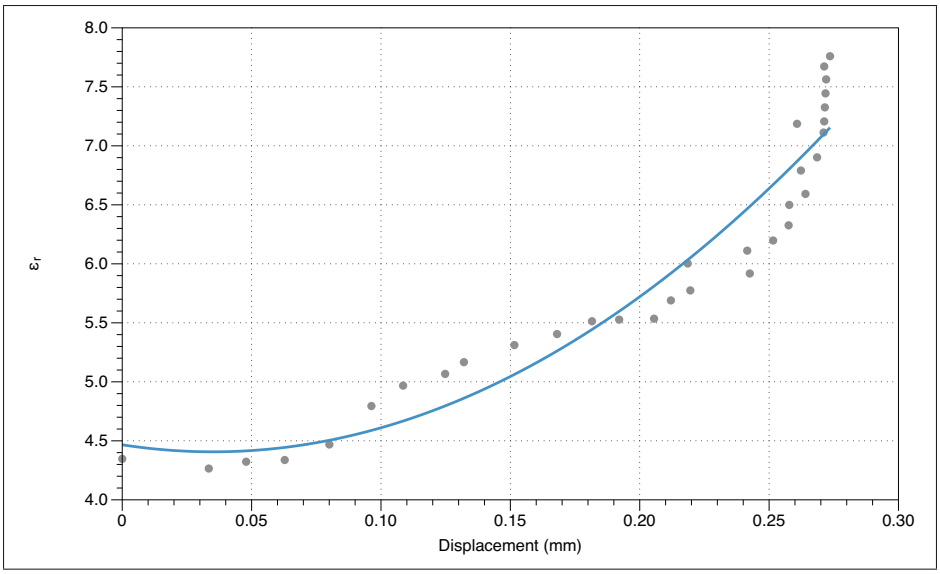

Figure 3.11 Change in the relative permittivity of the dielectric with displacement

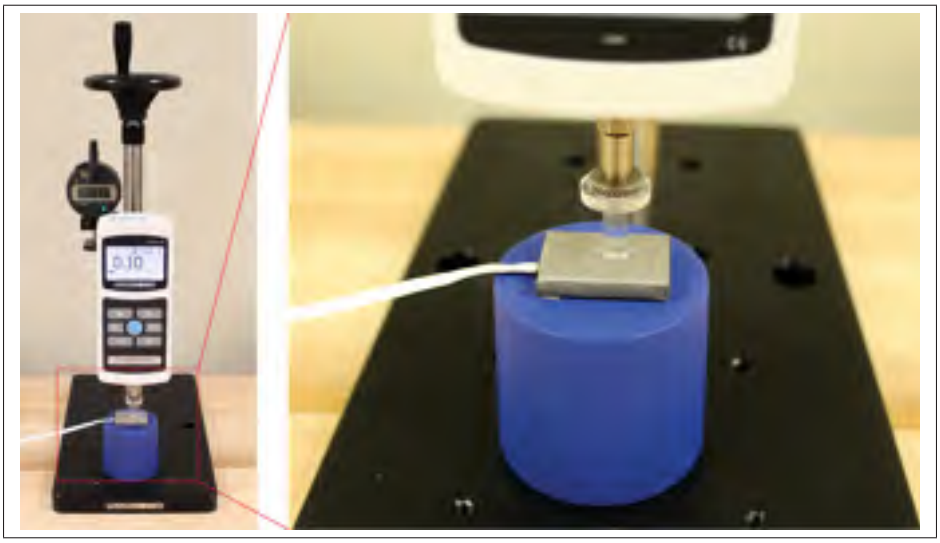

Figure 3.12 Setup of the experiment for validating the sensor

The response of the sensor to an applied force is given in Fig. 3.13. We see the effect of the dual-staged sensor when we observe the different slopes. The CDC count for forces below 1 N exhibits rapid variation, but becomes less varied at higher force levels. We further analyzed the data by adding displacement measurements, which allowed us to find the stiffness displacement

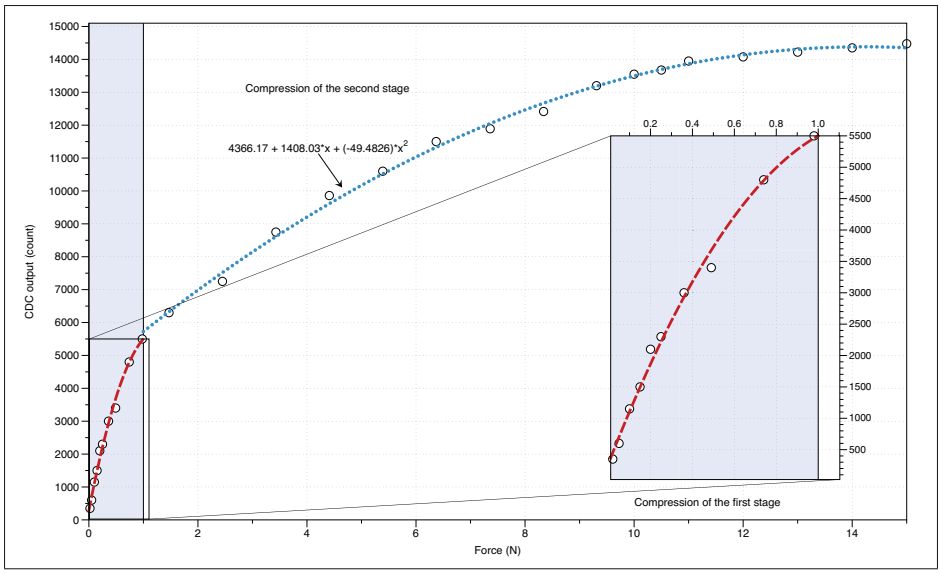

Figure 3.13 Force-to-capacitance count plot for the microstructured dielectric

relationship shown in Fig. 3.14. This graph depicts two main trends in the stiffness profile, which accords with our expectations; before beginning the experiment, we hypothesized that these trends in slope would occur due to the compression of the double-layered microstructured dielectric.

3.5.3 Demonstrating the High Sensitivity of the Sensor

The sensor presented here was designed to be sensitive to extremely light pressure as well as to a wide range of pressure, so that it can measure the forces that are relevant to performing grasping and object manipulation tasks. As we discussed in the introduction, most of the capacitance-based sensors that can measure a considerable amount of pressure exhibit limited sensitivity to low pressure (forces below 0.1 N/cm^2). In the real world, many tasks require sensory perception of a very light touch, such as handling a fragile object, or grasping a mechanically unstable object like a ball on a table. We hope that our sensor design will move us closer towards this goal.

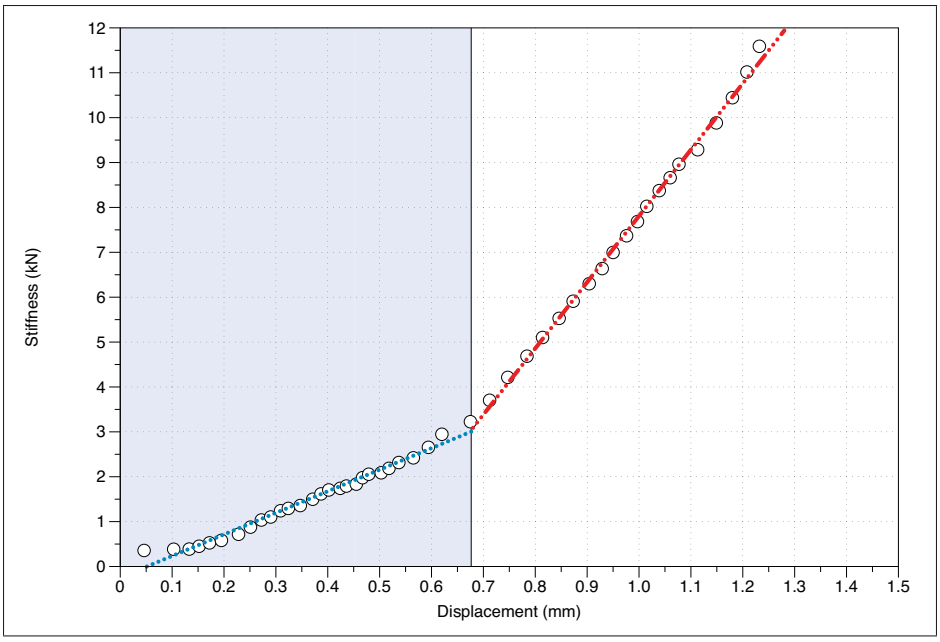

Figure 3.14 Stiffness profile of the sensor

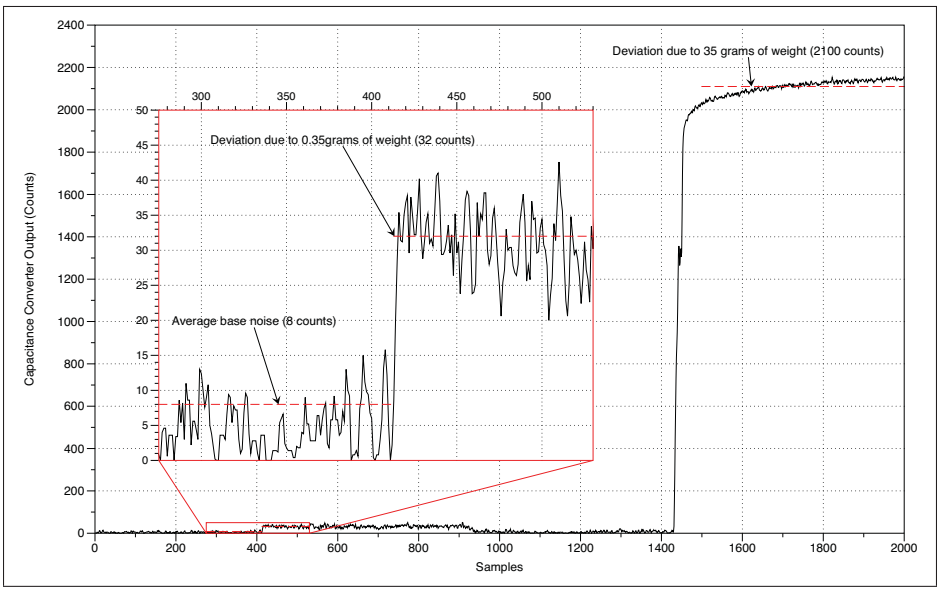

Figure 3.15 Graph showing SNR for the minimal force on the taxel

The minimal force that our sensor can detect is lower than that of the test bench used in the previous subsection. Therefore, here we place very light-weight objects on our sensor to observe its response. Fig. 3.15 shows the sensor's response to a very light pressure (0.35 grams

on a single taxel). Despite this low pressure, we recorded a signal that was four times higher than the mean noise level of eight counts. To put this result in perspective, the same figure also shows the sensor's response to a weight that is 100 times higher than before (35 grams on a single taxel). Although this weight is still very light, here we obtain a sizable 2100 counts.

We used the same weight (35 grams) to test the drift in the sensor's response. After letting the weight sit for eight hours, we observed drift in the range of 20 counts. This represents a drift of less than 1%, a near-negligible amount in the context of our applications.

3.6 Conclusion

In summary, this chapter introduce a novel double layer soft dielectric which is developed after detailed study over variety of dielectrics and their limitations. We have blended the technologies of doping, MEMS design and low-cost fabrication to achieve the highly sensitive double layer micro-structured dielectric. Moreover, this chapter exhibits development of the static tactile sensing unit by using the touch screen ASIC controller and micro-structured dielectric skin layer. Resulting device shows the sensing performance which is not only sensitive to the millinewton forces but responds to the high forces also by delivering wide range of sensitivity. Such vast range and sensitivity to minuscule forces would assist us during graping and manipulation of fragile objects withouts any damage.

CHAPTER 4

DYNAMIC TACTILE SENSOR

4.1 Introduction

Dynamic tactile sensing is equally important and widely occurring scenario just like static tactile sensing in the human skin. However, most of the researchers have overlooked that part of sensing due to a variety of reasons as we faced in the section 1.5 in chapter 1. Fewer number of researchers have worked on the dynamic sensing part as mentioned in the review of literature in the chapter 2. From their work, we have classified certain aspects which have to be considered during the dynamic sensor designing which is explained in the section 4.2. Keeping all the design factors in the mind, we will implement the preliminary dynamic tactile sensor as in section 4.3. Following that, the design will be implemented inside the programmable system on chip (PSoC) for ease of processing and integration with the static tactile sensing will be narrated in section 4.4. Accomplished sensor must be optimized for its performance according to the task requirement and performance. For such purpose the isolation region between static taxel which is used as the dynamic taxel is redistributed geometrically to deliver uniform sensitivity over sensor area will be presented in section 4.5. For the optimization, we used geometrical aspect of dynamic taxel by distributing it evenly on whole area. However, such redesigning has boosted the capacitance's special behavior known as edge effect and resulted into more sensitive dynamic sensor than normal ones as shown in section 4.6. Furthermore, the final product's experimental validation, performance trends and comparison with the human sensory threshold is shown in section 4.7.

4.2 Sensor requirements for dynamic sensing

- Dynamic sensing is essential for recognizing tactile events with sufficient bandwidth. Halata and Baumann (2008) shows that FA-I and FA-II type receptors in human skin meet all the requirements of a dynamic sensor. Vallbo *et al.* (1984) and Provancher (2003) de-

scribe how FA type mechanoreceptors respond through the nerves, as shown in Fig. 4.1. They state that SA type receptors only generate impulses when there is a steady application of pressure, i.e. they only respond when under static conditions. By contrast, FA type receptors only react to a change in force, meaning they only respond when under dynamic conditions. Even if the strong pressure is applied to the skin at some level over a period of time then there will be no response from the FA type receptors. In the real world, many events require static and dynamic sensing to take place simultaneously. For example, a mobile phone grasped by a person is a pressure-sensing static event, while the vibration that alerts one to an incoming call is a dynamic event. Although static type SA-II receptors also deliver some response during changes in force, their lower frequency of acquisition is insufficient for capturing dynamic events. Halata and Baumann (2008) and Westling and Johansson (1987) claim that the response frequency for SA type receptors is approximately around 30 Hz, whereas FA type receptors have response rates of up to 1000 Hz with maximum information delivered at 250 Hz. Also, the previous dynamic sensors using accelerometers by Fagiani *et al.* (2011) and PVDF films by Cotton *et al.* (2007) indicate that slip and friction details are mostly below 500 Hz. We desire a dynamic sensor with an sufficient acquisition frequency to capture all of the dynamic activities upto 500 Hz.

- At any point, one may seem to be able to obtain data for the dynamic events by analyzing the time derivative of the static data. Unfortunately, this method does not actually allow one to achieve true dynamic sensing capabilities, for these two reasons below.

    a. The dynamic sensor's acquisition rate must be fast enough to capture the harmonics induced as a result of dynamic activity. The main reason for this is that the design of the static tactile sensor is dependent on the CDC in our case. Normally, these sort of devices use charge-discharge time calculations for measurement of the capacitance. According to this process, each capacitance measurement circuit requires a certain length of time for the charging and discharging cycle to occur which results into refresh rate below 20 Hz generally for all CDC based devices. In order to use the same

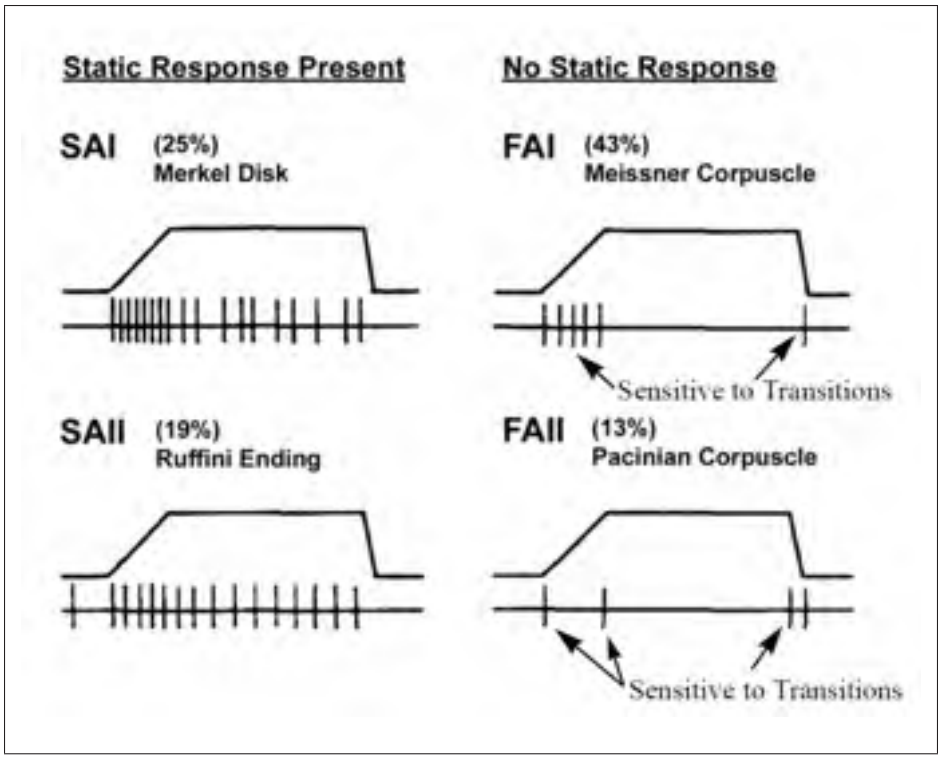

Figure 4.1 Response of the mechanoreceptors in human skin upon application of pressure

topology for dynamic sensing, two problems must be addressed. First, we must rectify the fact that it will be substantially slower than our requirement of 500 Hz desired bandwidth. Second, we must find a solution to the time differentiation problem. Time differentiation here means that the sensor will pick up most of the noise from the charging-discharging cycles, which is very close to the dynamic signals. This could potentially lead us to the third problem: an aliasing effect, wherein an inadequate sampling rate causes the sensor to falsely recognize a low frequency dynamic signal that does not represent the true events.

b. The typical pressure sensor will always have some limits due to factors like hysteresis and the SNR, but a dynamic sensor must possess a higher SNR and lower hysteresis. Unlike static events, dynamic events involve a very small force deviation with a very fast rate of change. Compared to static forces such as pressure, most of the dynamic activities have very low force intensity. Even if we could make a very fast pressure

sensor, other problems would still exist. The dynamic signals might appear in the same range of the base noise due to its very low intensity. Therefore, similar properties of dynamic signals which are very close to noise could be suppressed by filter, or hysteresis in the loop would prevent the signals from being recorded. At this instance, if one records static force and depend on the time derivative than it could result in no dynamic activity or false detection due to aliasing effect also.

- If the tactile sensor is to function as a skin-type structure that is fully integrated with a robotic hand, it must be thin and compact. Most of the researchers have experimented with dynamic sensing by using separate transducing phenomenon and processing circuits, by such methods as PVDF films (Yamada *et al.*, 2002), the Accelerometer (Cutkosky and Hyde, 1993) and the piezo-resistive sensor (Teshigawara *et al.*, 2010). Even, recently introduced multimodal sensors such as Choi *et al.* (2005b) and Wettels *et al.* (2014) consist discrete sensing phenomenon as well as processing paths for static and dynamic tactile events. Such variety in processing burdens the sensor's bulkiness and complexity in construction. In this situation, an optimal solution is to design a multimodal sensor with a single transducing phenomenon for both static and dynamic sensing to bring ease in fabrication and processing.

For the reasons given above, the sensor design should continue to use the modern technology of CDC IC for static pressure measurement, while introducing new processing architecture for dynamic information processing. Under dynamic conditions, we aim to achieve an acquisition rate of 1000 Hz, with very high sensitivity, a higher SNR, and low hysteresis. All of this should be achieved while keeping the requirement for minimal size in mind, as the sensor needs to be small in order to be viable as an artificial skin type element.

4.3 A capacitance based dynamic sensing principle

Our emphasis in this thesis is to achieve multimodality in a way of enabling the sensor for detection of static as well as dynamic tactile forces. Moreover, the construction of such a

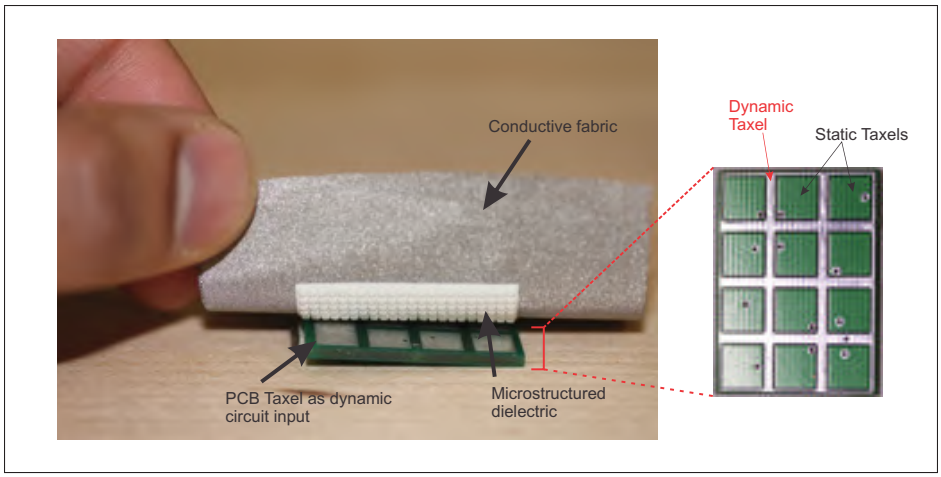

Figure 4.2 Layout of dynamic taxel and sensor formation

sensor must follow all the guidelines as discussed in the sensor requirements. In our design, dynamic and static sensing are both performed using a similar transduction principle, which brings the advantage of greater design flexibility. Sensing elements for static and dynamic events are placed on the same PCB platform and copper layer. Fig. 4.2 shows the design of the sensor presented in this project. In this design, we use the copper surface left around the static taxels presented in the previous chapter. Conductive fabric acts as a common ground-plane of the capacitor, and a micro-structured layer as a dielectric, which are the same for both. In fact, the only difference between the dynamic and static sensing mechanisms occurs at the processing stage, where the dynamic signal is processed by analog circuits, and the static signal is processed by a CDC converter. The fact that the static and dynamic circuits are at least somewhat combined in structure brings great advantages in terms of ease of fabrication and compactness.

In sum, the variable capacitor is formed by a micro-structured dual-layer cone shaped dielectric, and plates are composed of PCB layer and conductive fabric mesh. We receive the dynamic signal in the form of movement of charges, due to the change in capacitance with respect to ground. Any dynamic activity on the sensor's surface, such as flutter or vibration, is reflected by a change in capacitance. Inside the variable capacitance structure, charges are accumulated due to changes in distance Δd. We are able to maximize the change in capacitance by inducing

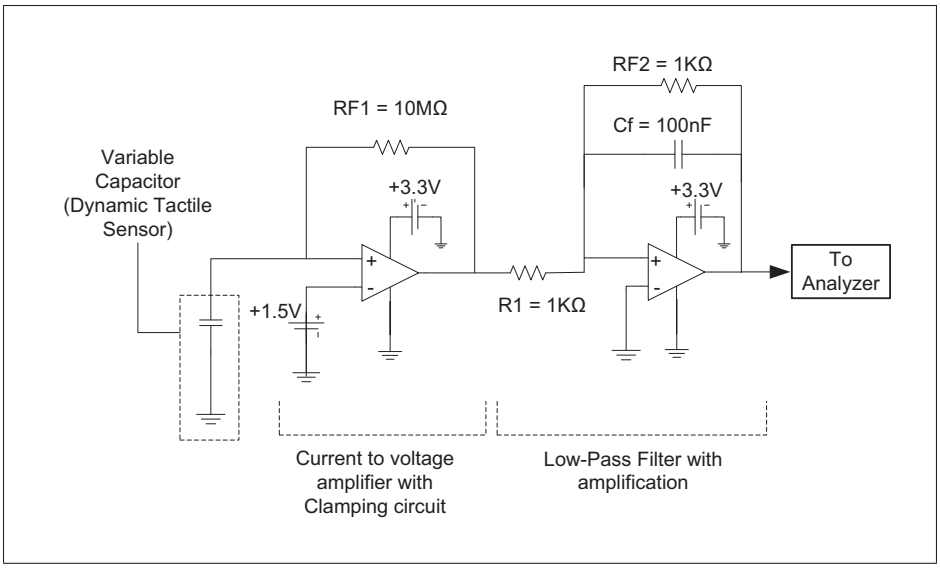

Figure 4.3 The signal processing circuit for dynamic sensing

change in the relative permittivity of the dielectric slab $\Delta\varepsilon_R$ as explained in detail at micro-structured dielectric in section 3.3. Changes in relative permittivity occur when we replace the air between the micro-cones by a relatively higher permittivity material, such as silicone. Such superposed effect results in significant changes in capacitance ΔC, which brings with it a higher displacement of charges. The change in capacitance is given by the equation

$$\Delta C = \varepsilon_0 . \Delta\varepsilon_{Rel} \frac{A}{\Delta d}. \tag{4.1}$$

Where, A is the area of the dynamic taxel on the PCB.

Now, this accumulated charge movement generates a current in scales of micro-amperes to nano-amperes. Hence the first step is to convert that current into the corresponding voltage level and greatly amplify it. This process is done using a charge amplifier. Previous researchers Howe and Cutkosky (1993) and Yamada *et al.* (2002) have used a similar topology for the initial processing of the dynamic signal. In our design, the charge amplifier is connected with reference voltage to get level offset for the signal, in order to remain in the supply voltage range for faithful amplification of the signal. If we do not employ DC level shift of the signal then signal processing would require a negative voltage in order to fulfill amplification in neg-

ative swing. And, negative voltage supply would require special supply and circuitry which could end up with increased bulkiness of sensor. Therefore, the optimal solution is to offset signal up to $\frac{+VDD}{2}$ to accommodate positive swing in $\frac{+VDD}{2}$ to +VDD and negative swing of the amplified signal in +0V to $\frac{+VDD}{2}$ voltage ranges. The output voltage available after the offset-driven charge amplifier stage is given by the equation

$$V_{Out} = -i_{Cap}.R_{F1} + V_{Off}. \tag{4.2}$$

i_{cap} is a very small current, due to charges accumulated at the dynamic taxel after dynamic palpation occurs on the sensor's surface. Also the gain is dependent on the value of R_{F1}, which is considered 10MΩ as shown in Fig. 4.3.

After the charge amplifier, the next step is to filter out the noise and all frequencies above the sampling rate of the analog-to-digital converter (ADC) to avoid lower frequency alias. As per our taxel layout, dynamic taxels are coexisting with static taxels, which are connected to the CDC converter. All CDC converters send a pre-charging wave for the measurements of capacitance. The one we are suing has an excitation signal of 250KHz. This very high frequency wave has to be suppressed in order for filtering to result in a useful spectrum of harmonics. Also, previous researches (Dennerlein *et al.*, 1997; Fagiani *et al.*, 2011; Schmidt *et al.*, 2006b) show that most of the dynamic activity induces harmonics which are below 500 Hz. To abide by the Nyquist criterion, our sampling frequency must be approximately 1000 Hz. Applying a low-pass filter, with a cut-off frequency of 1000 Hz, would suppress most of the high frequencies. Fig. 4.3 shows the configuration of the low pass filter. The output voltage after the filtering stage is given by

$$V_{Fil} = (1 + \frac{(R_{F2}||C_F)}{R_1}).V_{In}. \tag{4.3}$$

R_{F2} and C_f are calculated by the desired frequency. Cut-off frequency $= \frac{1}{2.\pi.R_{F2}.C_f}$ and R_1 is chosen according to equation (4.5) of desired gain at filter stage. Now, replacing V_{In} value by

equation 4.2 gives output voltage at filter

$$V_{Fil} = (-i_{Cap}.R_{F1} + V_{Off}).(1 + \frac{(R_{F2}||C_F)}{R_1}). \tag{4.4}$$

Simplification in terms of gain at filter stage A_{filter} is given by

$$A_{Fil} = V_{Fil}/V_{In} = \frac{(R_1 + R_1.R_{F2}.j.\omega.C_F + R_{F2})}{(1 + R_{F2}.j.\omega.C_F).R_1}. \tag{4.5}$$

After completing this step, our filtered dynamic signal swinging at a baseline of +1.5 VDC is forwarded to the signal analyzer for viewing and further processing.

4.4 Implementation

The dynamic sensor design presented in the previous section was implemented into the System on Chip (SoC). The main benefit of using SoC is that all the useful components are available inside the chip, which is programmed for interconnection in the same manner as Field Programming Gate Arrays (FPGAs). Such inclusion brings flexibility in component selection and great amount of compactness for circuit layout. This technology fits our purpose well, as our current-to-voltage converter and low-pass filters can easily be configured by operational amplifier(op-amp) blocks inside the chip. Recently, Cypress Semiconductors has launched a few range of PSoCs which feature an MCU unit along with programmable sockets on the chip. Moreover, they have a 16-bit CDC converter, with best-in-class accuracy which will be utilized for the static sensing. Hence, this technology is a perfect fit for our needs, and it motivated our use of PSoC for the entire static and dynamic sensing design, which can now be contained inside a single IC. Fig. 4.4 shows the schematic design for processing of dynamic signals inside the Cypress chip.

The first component of this design is a Trans-Impedance Amplifier (TIA), which delivers an op-amp based current-to-voltage conversion with amplification by resistive gain and user-selected bandwidth. The dynamic taxel is connected to the pin of PSoC port 2[3] of an internal TIA,

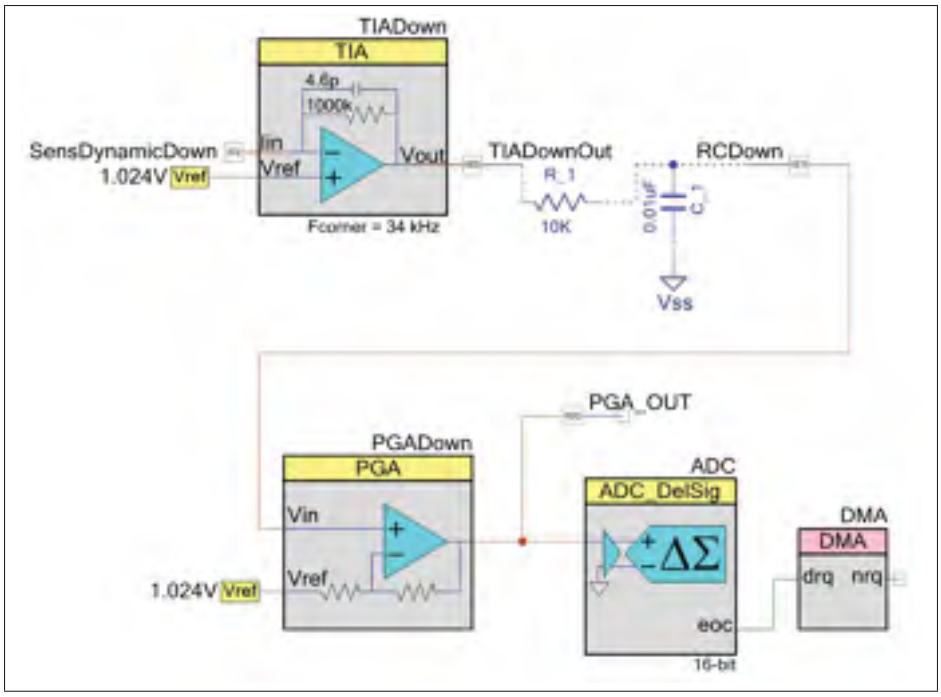

Figure 4.4 Dynamic sensing processing path inside the PSoC chip

and another input pin of the TIA is latched internally with a reference voltage of +1.024VDC. This setup ensures offset of the signal for reliable amplification. We have used the maximum value of feedback resistor for maximum gain with capacitive feedback in parallel. Capacitor on op-amp helps us by delimiting the bandwidth and filtering out higher-order frequencies, which in our case means frequencies above 34KHz selective preset value. The output of the TIA is fed to the first order low-pass filter outside of the chip, where we set the cut-off frequency for the low-pass filter at 1592 Hz. Cut-off frequency of 1592Hz is achieved instead of 1000Hz because of the limited and fixed values of the resistors and capacitors available only. After the next stage of filtering takes place, amplification is applied again along with removal of DC offset with TIA. A Programmable Gain Amplifier (PGA) is used for this purpose. A positive pin of the PGA is connected to the output of the low-pass filter, and a negative pin of the PGA is connected to the same reference voltage of +1.024 VDC to get reliable amplification by keeping wave swing into positive range. The output of the PGA is supplied to the internal 16-bits sigma-delta ADC. The sampling of the ADC is carried out at 2500 Hz, to comply with the

Nyquist criterion for accommodating 1000 Hz of waveform. For rapid data conveying without MCU interference, we used a Direct Memory Access (DMA) channel to transmit data from the ADC to the internal memory of the MCU.

4.5 Optimization of the dynamic taxel distribution

Our current dynamic sensor performs well with its static pressure-sensing taxels and the innovative micro-structured dielectric layer. However, there is still a limit to the sensor's sensitivity, with regards to certain areas on the sensor's surface. We have found that for dynamic palpations covering large areas, the sensor gives a uniform response. However, small size/pin-point dynamic palpations result in a different dynamic responses by the sensor with respect to the palpations' placement. Analysis of the dynamic sensor PCB, shown in Fig. 4.5, reveals that the center of the static taxel areas are the most distant regions for dynamic taxels to reach, which leads to reduced dynamic sensation over these areas. Red markers indicate the areas in which the least dynamic sensitivity is captured. The blue markers in Fig. 4.6 show the points at which maximum dynamic sensitivity is achieved due to the shape of the dynamic taxels. To resolve this irregular response with respect to location, we require a uniform distribution of the dynamic taxels over the entire surface of the PCB. We can not simply make the static taxels smaller to avoid this problem, or introduce a separate layer with another layer of dielectric. Either of these approaches would only add complexity and falsify our claim that coexistence on the same copper layer can be achieved. The best solution we found is actually to change the shape of the dynamic taxel. This will result in the static taxels being approximately the same size, but with small traces of dynamic taxel being integrated within them. This intrusion of dynamic taxel into the static taxels reduces the size of each static taxel fractionally, but overall a more uniform distribution of dynamic taxel will benefit us by providing additional areas for dynamic sensing. So, we redistributed the dynamic taxel in a way that would reach most areas of the PCB with a smaller trace design. To this end, we have tested two new designs where dynamic taxel is designed with small traces into static ones. Fig. 4.6(a) shows that static taxels are redesigned with wedge shaped dynamic taxel traces on all four sides. Fig. 4.6(b) displays

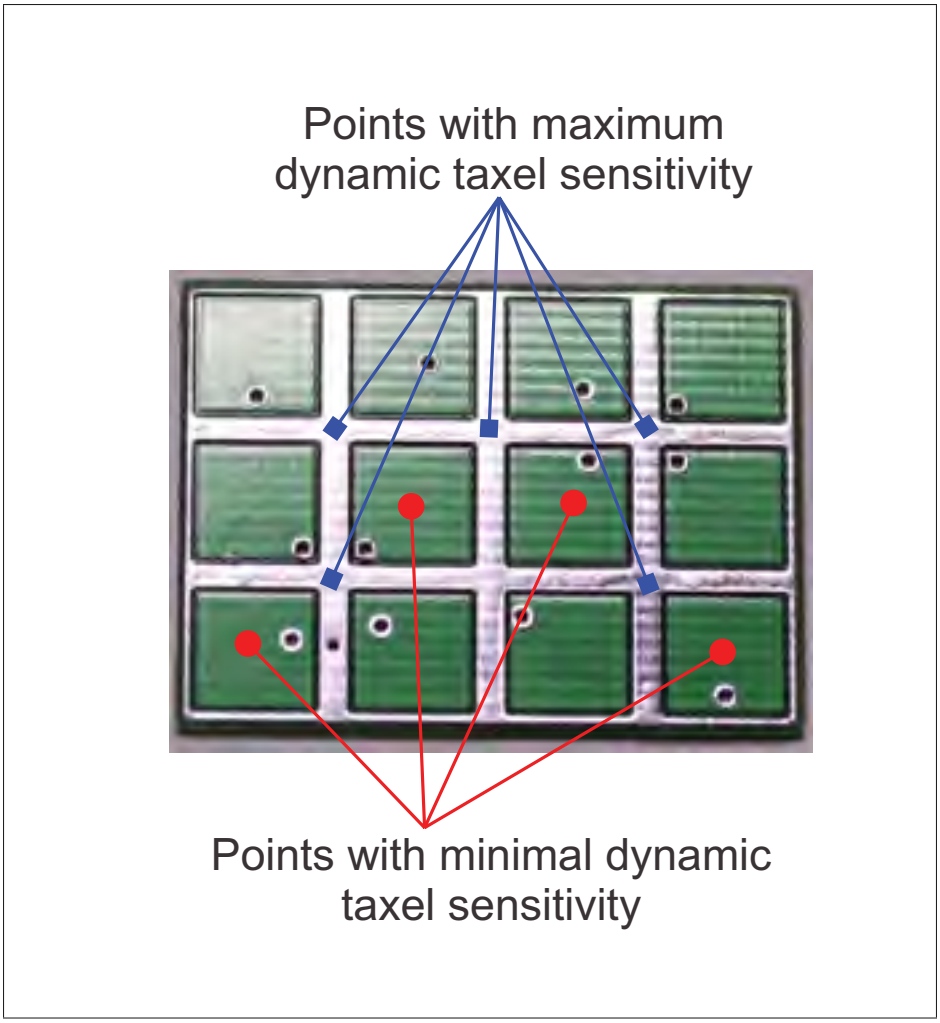

Figure 4.5 Uneven dynamic taxel sensitivity at different areas of the PCB

a more complex design, wherein both static and dynamic taxels are overlaid to cover similar areas of the PCB surface.

Title/Properties	Square Taxel	Design A	Design B
Area of dynamic taxel(mm^2)	236.540	261.164	276.573
Area of static taxel(mm^2)	363	308.621	223.614
% Area covered by dynamic taxel	35.84%	39.57%	41.91%
% Area covered by static taxel	55%	46.76%	33.88%
% Area used by space between taxels	9.16%	13.67%	24.21%

Table 4.1 Comparison of the size of static and dynamic taxels

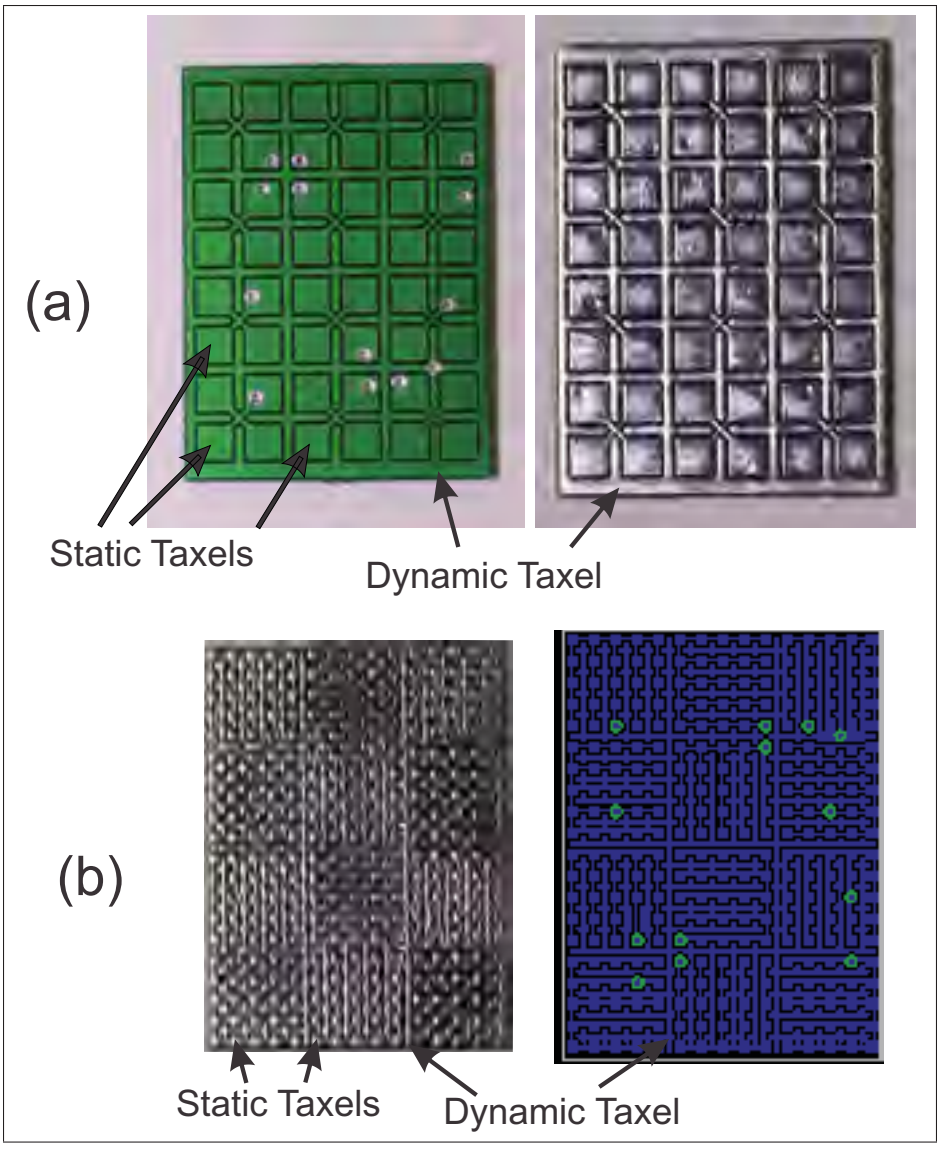

Figure 4.6 Design for dynamic taxels fringed into static taxels

Although, the objective here is to maintain the size of the respective area of the both static and dynamic taxels, this was hard to achieve at drawing stage. These both designs led to a slightly increased area of the dynamic taxel with the consequence of a reduced one for the static taxels. Table 4.1 shows the size comparison of taxel layouts with reference to Fig. 4.6. We should note that we also lose some amount of overall sensitive area, as it must be used as space for clearance between the static and dynamic taxels.

Title/Properties	Square Taxel	Design A	Design B
Dynamic Taxel capacitance C_{At1N}	20.4	24.3	25.6
Static Taxel capacitance C_{At1N}	12	12.5	13.5
% Increase in dynamic taxel area(mm^2)	-	10.41	16.95
% Decrease in static taxel area(mm^2)	-	-14.98	-38.4
% Change in dynamic taxel capacitance	-	19.12	25.49
% Change in static taxel capacitance	-	4.17	12.5

Table 4.2 Comparison of the capacitance of static and dynamic taxels

To provide context for equation 4.1, the structural capacitance of taxels with respect to the ground fabric, as shown in Fig. 4.2, is directly proportional to the area of the taxels. Our assumption states that there must be a similar proportional increment in the capacitance of the dynamic taxels, and a respective decrease in static taxel capacitance. Table 4.2 shows the measured capacitance for static and dynamic taxels of all prototypes. Note that this table falsifies our prediction of proportional increase. Our analysis of these results reveals that the increase in capacitance of the dynamic taxels is greater than the increment in area of these taxels, whereas the decrease in the area of static taxels results in an increased capacitance, rather than a decline. These conflicting results can be explained by a phenomenon of capacitance known as the capacitance's edge effect, which will prove to be instrumental to the creation of our final design.

4.6 Capacitance edge effect's impact in the design of the sensor

A definition of the edge effect of a capacitor is provided by Chew and Kong (1980), which states that the electric field between capacitance plates is not restricted by the edges of the plates, but there is some amount of field which exist outside of the plate area and returns to the other plate of the capacitor. This effect adds some extra capacitance to the device, which is above the capacitance defined by equation 1.1 wherein A is the shadowed area between plates and d is the distance between plates. Implementation of this property of the capacitor could result in an enhanced capacitance of the structure, which will enhance dynamic sensing capabilities and improve the overall sensitivity of the sensor.

Regarding a circular disk capacitor, Nishiyama and Nakamura (1993) proves that there is a significant amount of capacitance defined by the edge effect when the d/A aspect ratio is above unity. Scott and Curtis (1939) gives an explanation for this which is included in equation 4.6. Their results distinctly show that the fringing field is mainly affected by the ratio of d/A, when rectangular plates have a perimeter of length l, width w, thickness of dielectric b and $\mu\mu_f$ denotes edge capacitance per centimeter.

$$\begin{aligned} C_e = {} & \frac{1.113l}{2\pi^2}\left\{1+\ln\left[1+\frac{\pi w}{2b}+\ln\left(1+\frac{\pi w}{2b}\right)\right]\right\} \\ & +\frac{1.113w}{2\pi^2}\left\{1+\ln\left[1+\frac{\pi l}{2b}+\ln\left(1+\frac{\pi l}{2b}\right)\right]\right\}\mu\mu_f \end{aligned} \tag{4.6}$$

In another study Leus and Elata (2004), the significant difference in capacitance, as defined using approximate measurements of capacitance, is shown to be due to fringing fields in actuators. Equation 4.7 represents the formula for calculating the fringing field with respect to the results of finite elements simulations by ANSYS. This study considered a parallel plate capacitor with zero plate thickness where h is gap between plates, t is plate thickness, and w is the width of the plate.

$$C = \varepsilon\frac{w}{h}\left[1+\frac{h}{\pi w}+\frac{h}{\pi w}\ln\left(\frac{2\pi w}{h}\right)+\frac{h}{\pi w}\ln\left(1+\frac{2t}{h}+2\sqrt{\frac{t}{h}+\frac{t^2}{h^2}}\right)\right] \tag{4.7}$$

The first term $\varepsilon\frac{w}{h}(1+\frac{h}{\pi w})$ of the equation defines the capacitance of simple parallel-plate capacitor, where as remaining logarithmic terms in the equation define extra capacitance due to edge effect. The equation clearly shows a direct proportional relation between width w which is perimeter of plate and the edge effect of capacitance.

From previous researchers, we know that an increase in the perimeter of the plates, while the aspect ratio d/A is above 1, will increase the overall capacitance of the structure. This explains the experiment of more uniform dynamic taxel distribution over the entire PCB area

with increased capacitance effect. Hence, we can advantage our sensor with that capacitance's edge effect to acquire uniform dynamic taxel distribution with increased sensitivity.

4.7 Results of the dynamic sensor

The sensors were mounted on the phalangers of the 3-fingered adaptive Robotiq gripper, as shown in Figure 4.5. We tested the sensors by attempting to have them recognize vibrations applied to their surfaces. Getting the sensors to accurately sense vibrations that correspond to the frequency of a supplied waveform is one way to validate the accuracy of our sensor to measure dynamic events. Here, the vibrations were applied with a Mark-II haptuator designed by Vincent Hayward (2015). The haptuator can deliver vibrations that correspond exactly to the frequency of the supplied waveform. The idea is for our sensor to detect change of capacitance on dynamic taxel according to the specific vibration frequency that the haptuator applies to its surface. And transmit that change of capacitance by 16-bits number through processing circuits to the computer for further analysis.

We began by pinch-grasping the haptuator with the distal phalanges of the gripper's fingers as shown in Fig. 4.7. We then deactivated the robotic arm, to ensure that it did not generate any vibrations that might interfere with those of the haptuator during the actual experiment. The next step was to use the function generator to supply the haptuator with a wave frequency range measuring between 1 and 500 Hz, as that is the functional range of measurement of the sensors. During this step we tested sensors with two separate waveforms with respective frequencies of 100 Hz and 450 Hz one after another, in order to test the system's functionality at both a low and a high frequency level. The haptuator successfully applied the vibrations corresponding to each wave frequency to the sensor, which then generated dynamic data and sent the data through the communication interface to the computer. Fig. 4.8 shows a visualization of the dynamic data that were picked up by one of the sensors. The plot in the upper half of the visualization window displays the acquired dynamic signal from the sensor, and the plot in the lower half shows the Fast Fourier Transform (FFT) spectrum analysis of the captured waveform.

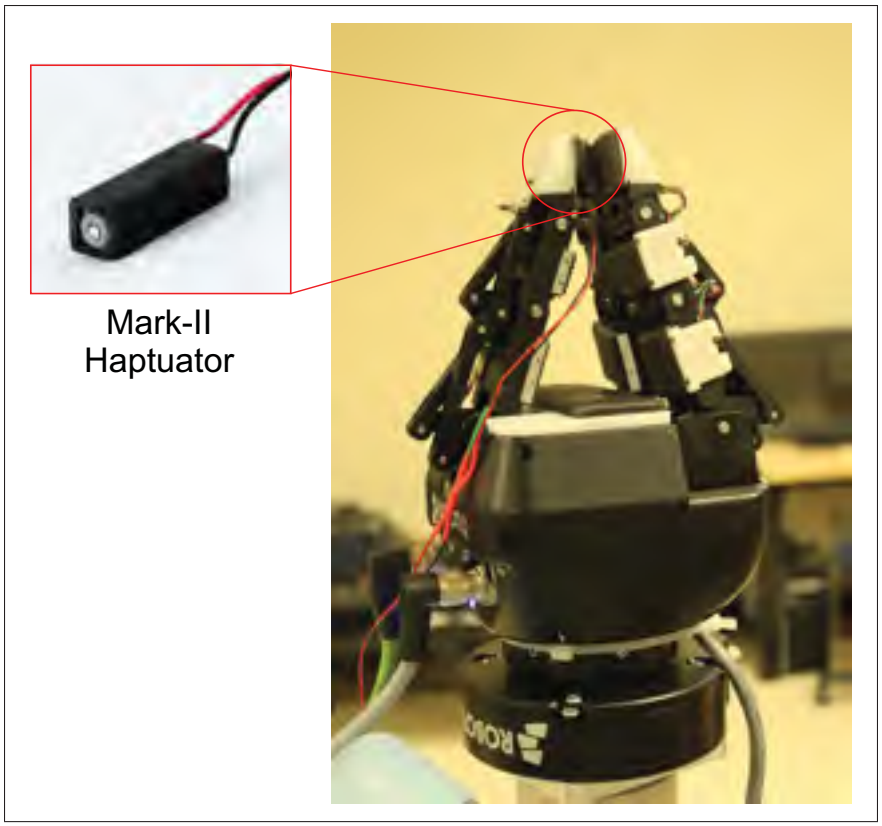

Figure 4.7 Experimental setup for validation of dynamic sensor

The results shown in Figure 4.6 clearly show that the dynamic sensor has acquired vibrations applied by the haptuator. Also, the FFT spectrum denotes the power lobes, which are center at 100 Hz in Fig. 4.8(a) and 450 Hz in Fig. 4.8(b).

We also validated the functionality of our sensor design by comparing its level of sensitivity to that of the FA mechanoreceptors found in healthy human skin. As stated in Merzenich and Harrington (1969) and Sherrick Jr (1953), the human sensory apparatus exhibits optimal sensory capabilities around 250Hz of vibrations. However, a minimal threshold of intensity must be met in order for humans to detect vibrations at all.

As a part of an experiment by another PhD thesis by Florant (2014) that is outside the scope of this thesis, we found that humans could not detect vibrations applied by the haptuator when haptuator is driven below driving voltage of +0.25V peak to peak at 250Hz. Continuing in the

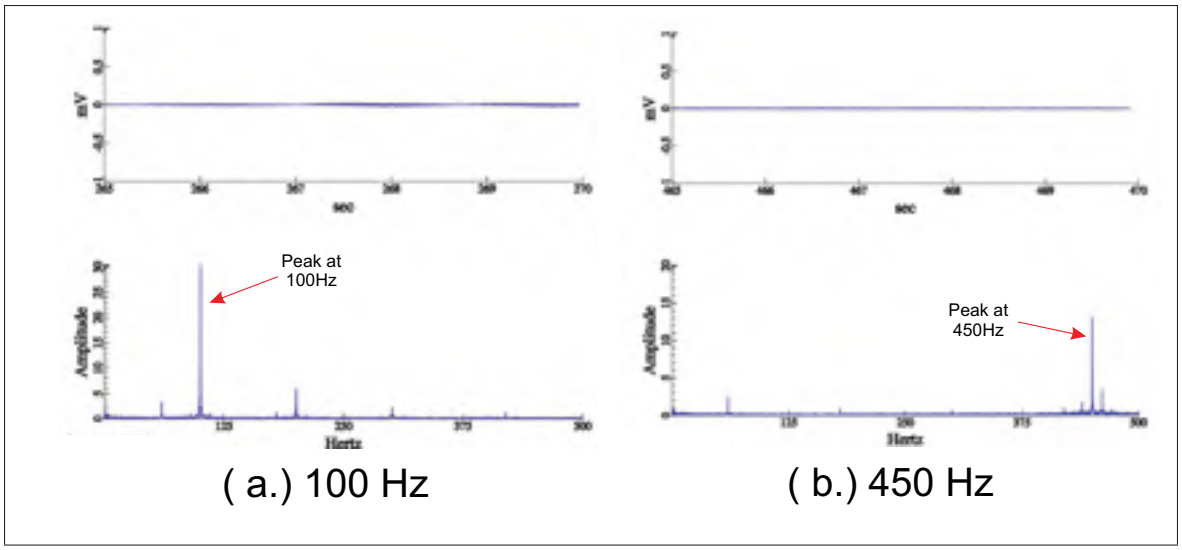

Figure 4.8 Response of the dynamic sensor to vibrations applied by the haptuator

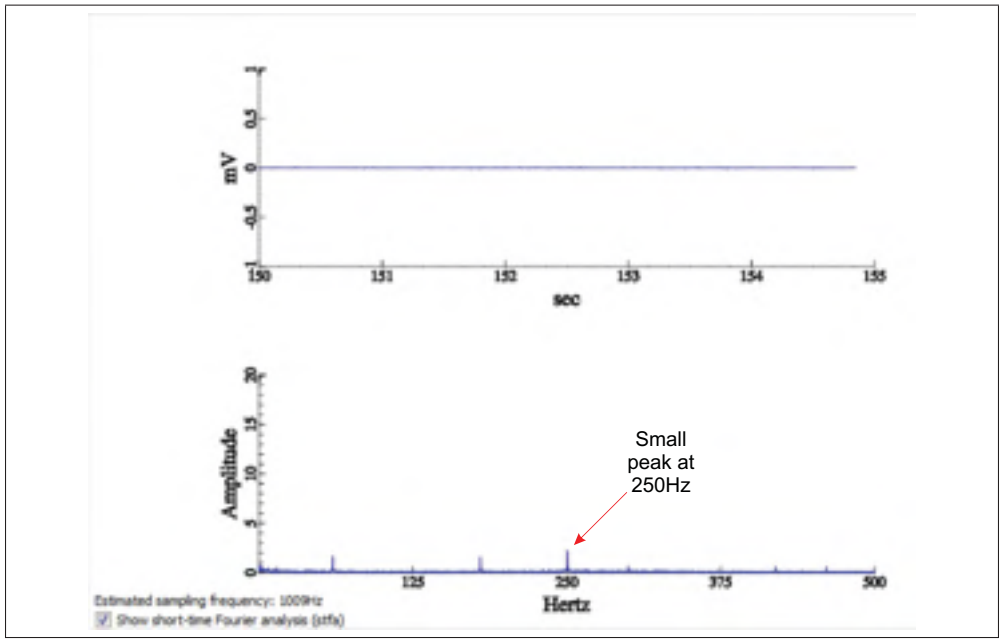

Figure 4.9 Response of the dynamic sensor for very low intensity vibration

directions of comparing level of sensitivity with reference to human, we had used the same set up of previous experiment shown in Fig. 4.7. We applied 250Hz frequency of vibrations by

haptuator and continue to reduce the intensity by decreasing biasing voltage of the haptuator upto +0.25V peak to peak.

Our test succeeded in verifying the minimal sensitivity of our sensor compared to human, because when we set the haptuator to vibrate at an intensity level below the human sensory threshold, our sensor was still able to capture the dynamic activity of the vibrations as in Fig. 4.9. As we see in Fig. 4.9, there is no activity on the top graph because our scale is too large to display the nuances of the sensor's acquisitions. So it falsely appears as a completely straight line. The FFT spectrum, on the other hand, clearly indicates a small peak at 250 Hz, which shows the sensor successfully detected a dynamic activity at this frequency and intensity level.

4.8 Conclusion

This chapter explained the importance and properties of the dynamic tactile sensor whereas most of the pressure based tactile sensors falls short at dynamic events detection. We have used same capacitive sensing principle for development of static as well as dynamic sensor. Such tactic has given ease of development and assistance in compact fabrication compared to current multimodal sensors. The design and fabrication part displays the layout of the dynamic taxel which is designed in the isolation space between static taxels so that static sensitivity will not shrink while novel dynamic sensitivity is being added. For the even distribution, we experimented the different geometrical distribution of the dynamic taxel to achieve uniform dynamic sensitivity on the sensor surface. Such maneuver for dynamic taxel redistribution resulted in increased dynamic sensitivity due to capacitance's edge effect. At the end, we have conceived a dynamic tactile sensor which illustrates better sensitivity around optimal sensory capability bandwidth region. The performance comparison exhibits that the sensor can sense the vibrations beyond human hand's dynamic sensitivity threshold which acclaims it as a better dynamic tactile sensing unit.

CHAPTER 5

UTILIZATION OF MULTIMODAL TACTILE SENSORS

5.1 Introduction

The main goal of this thesis is to develop a better multimodal tactile sensor. We aim to mimic most of the essential functionalities of human mechanoreceptors, as described in chapter 1. Based on these requirements, we designed a relatively better static sensor in chapter 3, and enhanced its capabilities with the addition of dynamic sensing, as detailed in chapter 4. After fine-tuning the parameters to accomplish better sensing, the next step was to test the sensor in real-world grasping and manipulation tasks. In doing so, we attempted to fit our tactile sensors to the fingers of three different robotic hand platforms, as detailed in section 5.1. Fig. 5.1 shows the tactile sensors applied to a prosthetic hand from Kinova Inc., OpenHand from Yale University and an industrial gripper from Robotiq Inc. We decided to use the Robotiq gripper for our experiments because of its greater functionality: it has a wide range of grasping motions, and its fingers are adaptable for a variety of maneuvers, providing precise and powerful grasping. We continued our experiments with precision grasp by setting the gripper to the pinch mode. We did this by following the specific grasp algorithm, which emphasizes the static and dynamic sensor's significance to the experiment, as described in section 5.2. The results of the experiments are shown in the trends in section 5.3, according to the tactile sensor, force sensor and consolidated versions.

In recent years, there has been a keen interest in developing mechanical hands that can perform with similar dexterity and grasp ability as the human hand (Mattar, 2013). Researchers have designed a variety of structures to act as a mechanical hand; however, from the perspective of grasp stability, all of the artificial hands are still far from the performance level of the human hand. The main reason for this gap is the lack of tactile sensing, a feature that is crucial to evaluating grasp stability. We are now able to partially fill that gap with the tactile sensors that have been integrated with robotic hands, as shown in Fig. 5.1. However, the mere addition of a

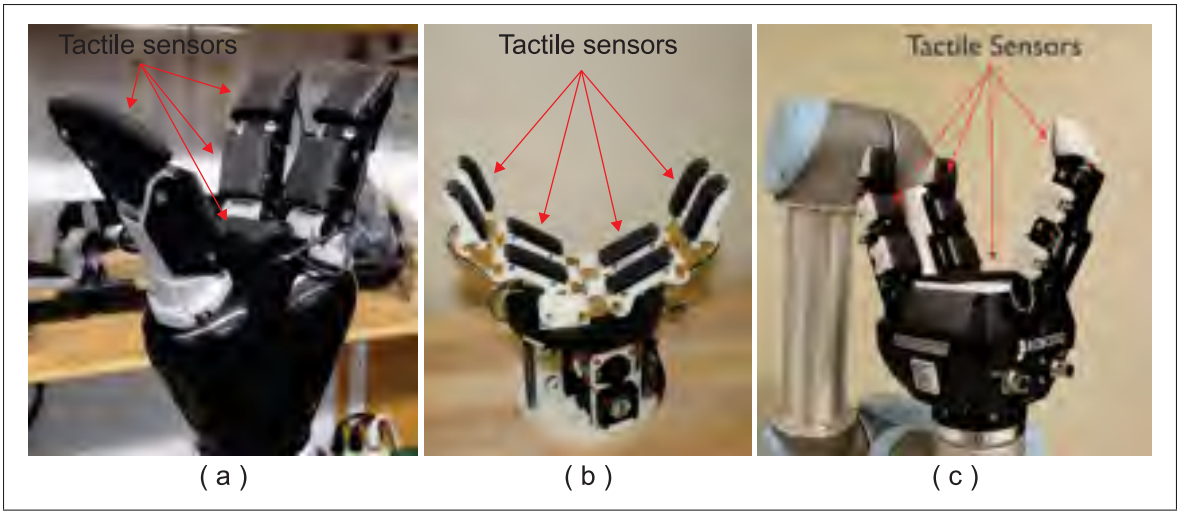

Figure 5.1 Tactile sensors made at ETS CoRo lab mounted on the (a)Kinova Prosthetic hand, (b)Open Hand by Yale university and (c)Industrial gripper by RobotiQ

better tactile sensor to the mechanical hand structure is not sufficient to evaluate grasp stability. We must also develop an index that will allow the robot to predict the outcome of the grasp attempt.

A grasp stability index has been conceived through numerous methods, by combining aspects of visual feedback, tactile feedback (Dang and Allen, 2014; Hyttinen *et al.*, 2015; Haschke, 2015) and advanced machine learning. The main objective of all these previous attempts was to evaluate the grasp quality, so as to avoid unstable manipulation in unstructured environments. Their results demonstrate that such feedback can indeed be used to develop an index for estimating the grasp quality, and that this index is useful for helping the robot to judge the stability of a maneuver.

Several researchers (Sanz *et al.*, 1998; Leeper *et al.*, 2012) have tried to solve the problem of grasp assessment by developing an index based on visual feedback of the grasps. Vision is clearly an important aspect of solving this problem, but, at least when one considers the human grasp-detection ability, vision tends to be the first step; tactile sensation follows, and it makes up the majority of the information that is used for grasp assessment.

We believe it is important to use tactile sensors as well as vision when addressing this problem. Visual feedback improves the planning of a manipulation strategy, and helps with the verification of object displacement with and without grasping, because of its ability to provide an overview of the grasping environment. However, vision alone cannot provide details about tactile features such as initial contact, contact pressure, and incipient slip. Also, it does not allow the robot to recognize properties such as the object's weight and center of mass.

Other researchers (Hyttinen *et al.*, 2015; Bekiroglu *et al.*, 2011) have attempted to incorporate machine learning when predicting grasp outcome. The problem with this approach is with the nature of the artificial intelligence algorithms. The machine comes up with its own decision based on the set of the pre-defined inputs, but the researcher has no way of evaluating the way in which the decision was reached. For example, (Dang and Allen, 2012) has fed a model of the object (including its tactile information) to the algorithm, to allow it to recognize the object with vision and apply the optimal grasp. However, no information is given apart from a predefined grasp database of the same object for the particular orientation of the grasp, and after the algorithm calculates and evaluates the grasp based on its internal methods, the results show that the obtained predictions are not accurate. Moreover, the researcher has no way of knowing how to change the machine learning algorithm to improve the grasp prediction process.

Another approach to machine learning involves the Columbia Grasp Database(CGDB), which consists of information on nearly 8000 everyday objects and 250,000 grasps detail with variety of robotic arms and hands. Goldfeder and Allen (2011) have combined visual feedback with the CGDB to evaluate the optimal orientation for grasping an object. Such a combination significantly improves the grasp performance, by providing a detailed view of the object and unstructured environment with a camera and the CGDB. However, this technique cannot be used with compliant and elastic objects, as the application of force can result in almost infinite shape patterns. Furthermore, machine learning methods have not yet been optimized for anonymous objects. For instance, the problem with the methods used in Dang and Allen (2012); Hyttinen *et al.* (2015); Haschke (2015) is that they all are very object-specific. Again,

the unknown processing of the neural networks, and the inability to improve the results, returns us to the same fundamental problem of machine learning.

At this point, machine learning techniques are still the most promising way to solve the grasp assessment problem, despite having specific processing constraints and undefined computation – yet we do not believe we should give up on deterministic methods just yet. There are clearly some ways in which a more "rational" hand-written rule system makes more sense, as the method can be more clearly correlated with that of the human tactile apparatus. We do not aim, through our exploration of deterministic methods, to present a more viable alternative; we simply hope to gain a better understanding of the factors that contribute to accurate grasp assessment. Future work will probably integrate machine learning with the deterministic index of tactile data, as this will likely result in the best grasp prediction methods.

5.2 Grasp Stability approach

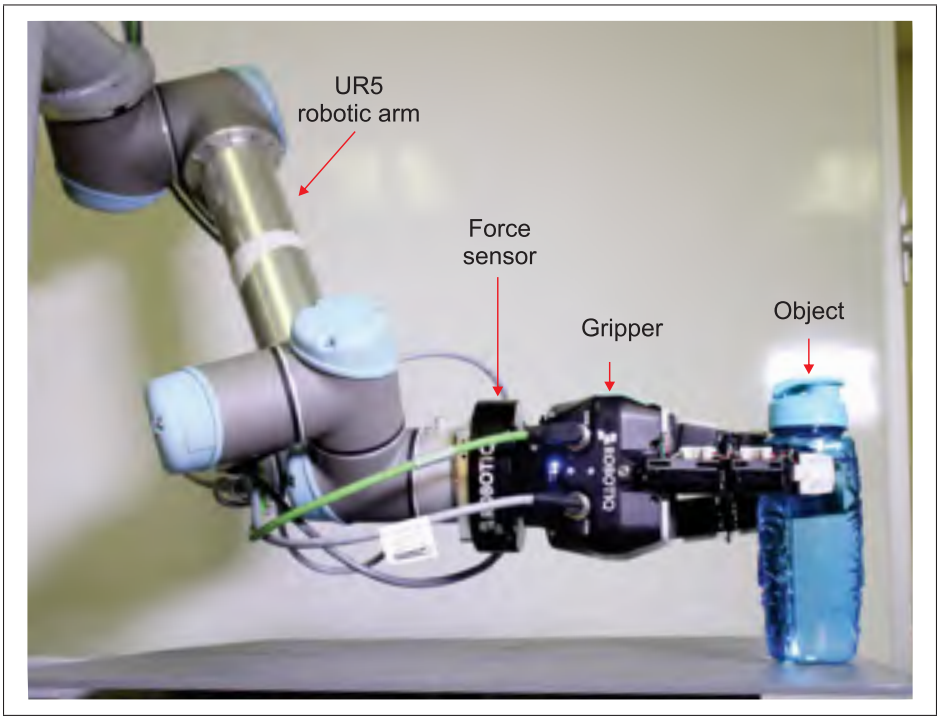

Figure 5.2 Experimental setup for the grasp assessment

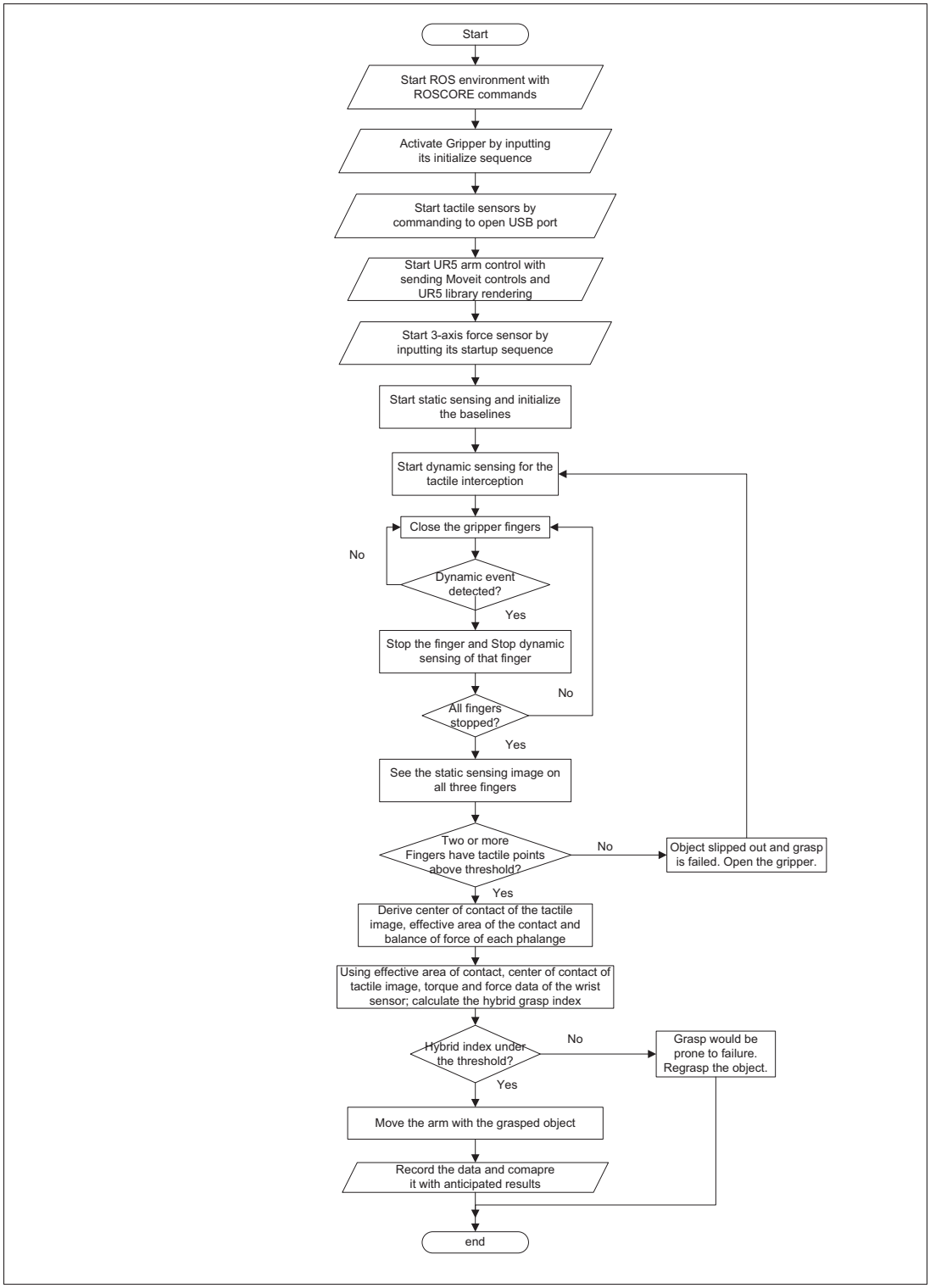

Figure 5.3 Process algorithm for the grasp assessment

Our grasp stability approach mainly operates by using the tactile sensor's feedback to determine the response of the hand that will provide the best grasp. We have designed the entire system on a Robot Operating System (ROS) environment. Fig. 5.2 shows the setup of the experiment. The robotic gripper is equipped with our tactile sensors. As shown in Fig. 5.1(c), the gripper is mounted on the mechanical arm of a Universal Robot (UR5) with coupling of a 6-axis wrist force sensor. The wrist force sensor delivers the details of the object's weight distribution by force sensing, and the distance between the center of mass and the center of contact by the torque values. Sometimes the objects are manipulated in such a way that the center of mass of the object is not aligned with the center of grip. This imbalance results in the turning of the object, due to its weight distribution, and is a major reason for grasp failure. Our belief is that consideration of the force and torque, along with more standard grasp-related tactile information, will reflect in a more cognizant model (and dataset pattern).

Fig. 5.3 illustrates the algorithm of the grasp assessment experiment. The first stage of the grasp sequence is to initialize all the components of the experiment and consolidate their libraries at the ROS interface. Once the communication between ROS and all the components of the experiment has been established, the next step is to place an object in the proximity of the gripper fingers for the precision grasp test. During the initialization sequence for this step, we put fingers of the gripper in pinch mode.

After positioning the object, we begin closing the gripper while continuously monitoring the dynamic activity with the tactile sensor. As soon as any dynamic activity occurs on any one of the fingers, we halt the corresponding finger's motion, so as not to displace the object, and continue to close the rest of the fingers until they register any dynamic activities. At this point, static sensing could have been used instead to detect initial contact, due to its high sensitivity. However, as discussed in chapter 3, each static sensor is working at a 15 Hz refresh rate. Since there are three sensors working at a time, bandwidth sharing would bring the data refresh rate less than 15Hz, which could lead the fingers to move or crush the object because of the slow feedback loop. Therefore, we used dynamic sensing to detect the initial touch events.

After successfully stopping the fingers at the initial contact threshold, the fingers were closed slightly more to exert an adequate force for grasping. Meanwhile, using the static force sensor to continuously monitor the pressure feedback allowed us to determine the finger actuation up to a predefined threshold for particular object. The data from the static sensor give us details of the contact area and force distribution on the finger taxels during the grasp. Note that contact is detected above a certain contact threshold on the opposing fingers of the gripper, in order to proceed with reliable grasping evaluation.

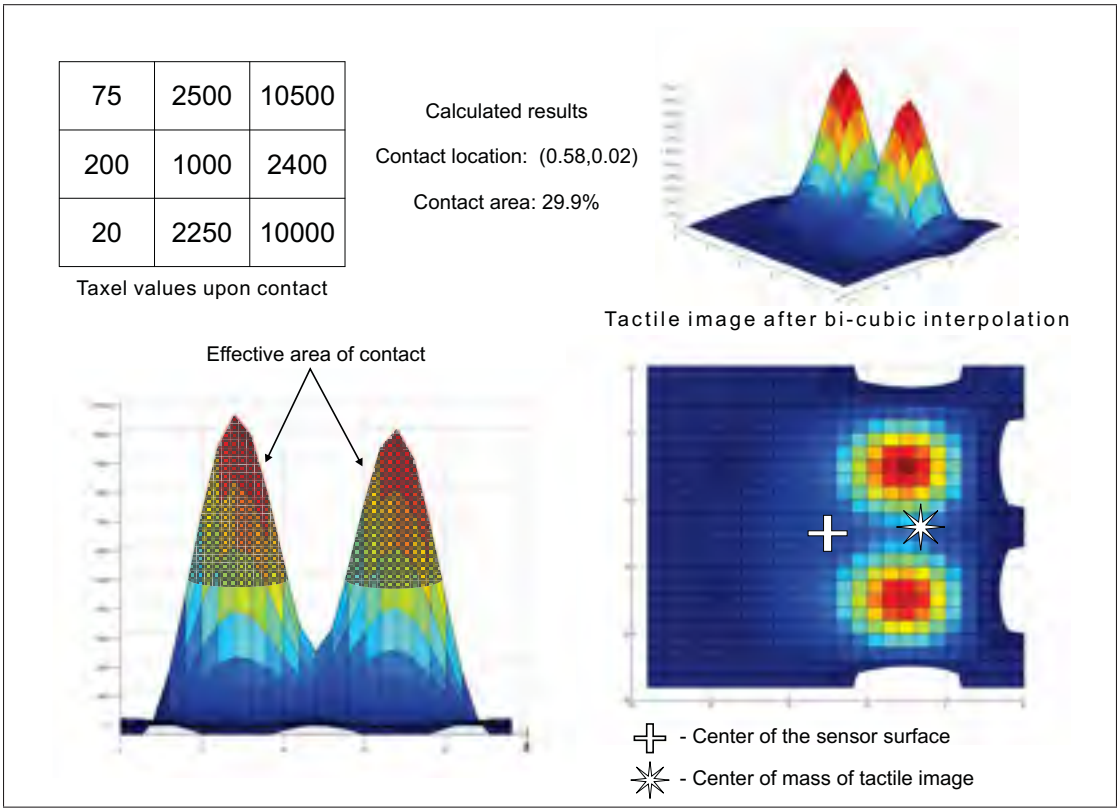

Figure 5.4 Illustration of center of mass of the tactile image and effective contact area

At this moment, the object is grasped between the fingers, and we have the tactile image of all the finger phalanges in the form of static pressure data; but these raw data do not allow us to come to any conclusions regarding grasp stability. We used two factors to analyze the information in detail: the center of mass of the tactile image, and the area of contact on the

sensor surface, as illustrated in Fig. 5.4. We decided to use these factors for our grasp evaluation index because they correlate to situations that occur when a human attempts to grasp an object. For instance, when a a grasp attempt that involves only the very tip of the finger will form a minimal contact area with a relatively large object, the grasp attempt is likely to fail. By contrast, when picking up a large item with the whole hand, the larger contact area results in a better grip and higher probability for grasp success.

The details of static pressure are given by

$$A = \begin{pmatrix} a_{1,1} & a_{1,2} & a_{1,3} \\ a_{2,1} & a_{2,2} & a_{2,3} \\ a_{3,1} & a_{3,2} & a_{3,3} \end{pmatrix}, B = \begin{pmatrix} b_{1,1} & b_{1,2} & b_{1,3} \\ b_{2,1} & b_{2,2} & b_{2,3} \\ b_{3,1} & b_{3,2} & b_{3,3} \end{pmatrix} \text{ and } C = \begin{pmatrix} c_{1,1} & c_{1,2} & c_{1,3} \\ c_{2,1} & c_{2,2} & c_{2,3} \\ c_{3,1} & c_{3,2} & c_{3,3} \end{pmatrix}. \quad (5.1)$$

Where, A, B and C are tactile sensors on the 3 different finger's distal phalanges.

To find the center of contact based on the 3 x 3 matrix of taxel data, one could perform a simple analysis using only each individual taxel as the contact peak. For the added accuracy and resolution, we follow the bi-cubic interpolation of the n^{th} level for each sensor's data matrix. The bi-cubic interpolation is given by the equations below.

$$f(x,y) = \sum_{i=1}^{i=3} \sum_{j=1}^{j=3} a_{(i,j)} x^i y^j \quad (5.2)$$

$$\partial_x f(x,y) = \sum_{i=1}^{i=3} \sum_{j=1}^{j=3} i a_{(i,j)} x^{i-1} y^j \quad (5.3)$$

$$\partial_y f(x,y) = \sum_{i=1}^{i=3} \sum_{j=1}^{j=3} j a_{(i,j)} x^i y^{j-1} \quad (5.4)$$

$$\partial_{xy} f(x,y) = \sum_{i=1}^{i=3} \sum_{j=1}^{j=3} a_{(i,j)} x^{i-1} y^{j-1} \quad (5.5)$$

Where their derivatives coefficients are derived by the equations as follows.

$$\partial_x f(x,y) = \frac{f(x+1,y) - f(x-1,y)}{2} \tag{5.6}$$

$$\partial_y f(x,y) = \frac{f(x,y+1) - f(x,y-1)}{2} \tag{5.7}$$

$$\partial_{xy} f(x,y) = \frac{f(x+1,y+1) - f(x-1,y) - f(x,y-1) + f(x,y)}{4} \tag{5.8}$$

This bi-cubic interpolated 3D spectrum is used to find the center values in the X and Y directions on the sensor plane. The best way to determine the center, even in a multi-peak scenario, is to compare it with half of its overall integral value in the X and Y axis. Therefore, we get two arrays for the bi-cubic interpolated data matrix, given by the following equations,

$$A_x = \sum_{i=1}^{3n} a_{x,i} \; and \; A_y = \sum_{i=1}^{3n} a_{i,y}. \tag{5.9}$$

Now, according to the centroid mean value calculations, the center value of these arrays is equal to the half of the integral value of the total spectrum. Therefore, a comparison of half of the total integral value of the tactile image is given by,

$$\frac{Sum}{2} = \frac{\sum_{i=1}^{i=3n} \sum_{j=1}^{j=3n} a_{i,j}}{2}. \tag{5.10}$$

and integral array of X and Y direction for the sensor matrix if given by,

$$f(x) = \int_0^{3n} A_y.dy \; and \; f(y) = \int_0^{3n} A_x.dx. \tag{5.11}$$

Comparing the $\frac{Sum}{2}$ value, with the closest value of the integral of array from the equations 5.11, gives us the center of contact in the X and Y directions for each sensor.

We believe that the effective contact area is also an important factor for judging grasp stability. Normally, a point/small contact would have relatively small contact area compared

to surface contact. Eventually the contact area is in direct proportion to the friction. Tremblay and Cutkosky (1993) shows that slippage or turning of the object during grasp occurs because of small friction and small contact area. A certain level of force with better contact area are the two factors which contribute to grasp success. So that we should consider the a certain force threshold while finding the effective area of the contact. Another reason for the same is that our dielectric is compliant and soft. So that when a high pressure stimuli is applied on the sensor surface, it shrinks the sensor skin a bit and the object surface around the strong contact also touches the sensor surface and contributes a light contact to pressure distribution map. Therefore, to remove those regions of partial contact, it is necessary to filter the sensor's pressure spectrum above a certain threshold. From that detail, we can derive the effective contact area on the sensor's surface, even for multiple contact situations. The effective contact area is given by the equation

$$Effective\ Area\ of\ contact = \frac{Number\ of\ points\ above\ threshold}{Total\ sensing\ points\ on\ the\ sensor\ surface} \tag{5.12}$$

From the information collected by the tactile sensor, in the forms of center of contact location, effective contact area, weight (in the form of force), and distance between the center of mass and center of contact (by torque), we have derived the plots that are scrutinized in the following section.

5.3 Results

We recorded the tactile sensing data for 17 different objects, as illustrated in Fig. 5.5, with 61 total grasp attempts in different object orientations. We attempted to achieve the grasps in such a way that the center of mass of the object is kept away from the center of the grasp. This type of grasp attempt generated a similar number of failed and successful grasps, which was achieved by the process algorithm shown in Fig. 5.3.

The first set of data that is selected for grasp assessment is the relation between the center of contact to its contact area on the fingers. Our hypothesis is that if a grasp attempt features a

Figure 5.5 Objects used for grasp assessment experiment

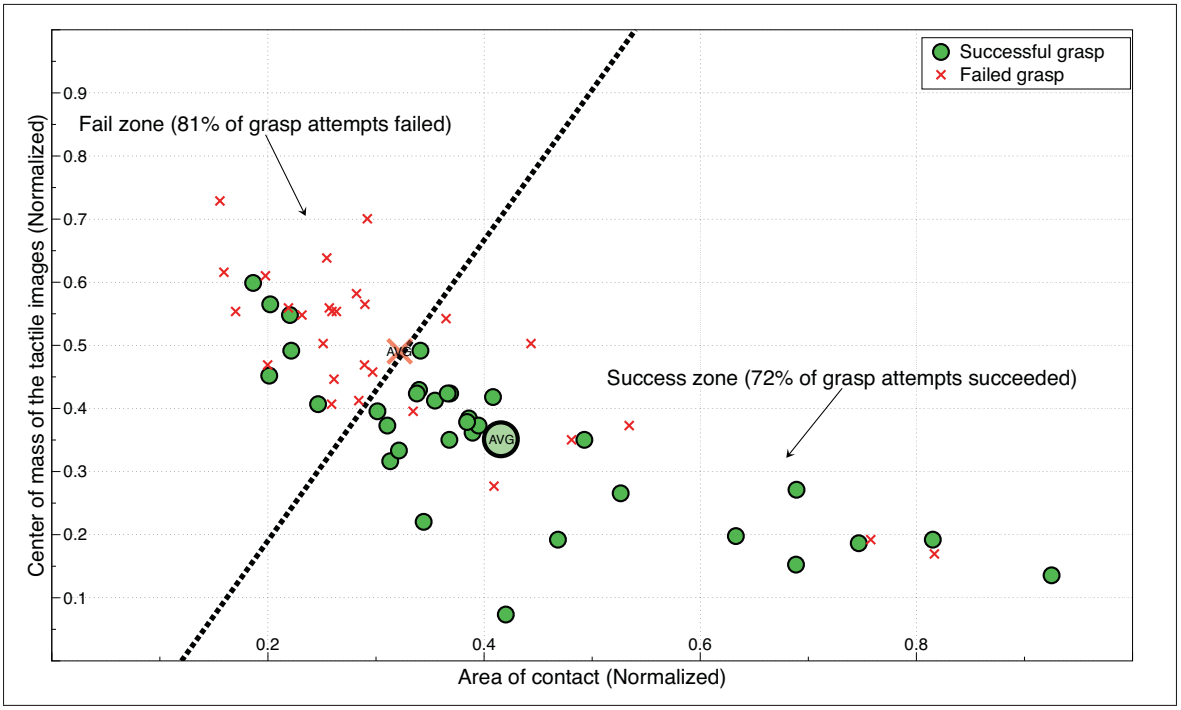

Figure 5.6 Illustration of center contact location and effective contact area after calculations

center of contact that is far from the center of taxels, as well as a relatively small area of contact, the grasp attempt is more likely to fail. As can be seen from Fig. 5.6, more failed grasps are dispersed near higher contact location values and lower contact area values, whereas more successful grasps are found in the region of higher contact areas and smaller distances between the two centers. We have approximated a line for dividing the results into two regions. Based on an evaluation of the 61 grasp attempts, the region of likely-successful grasps are predicted to be successful 72% of the time, and the region of likely-failed grasps are predicted to fail 81% of the time.

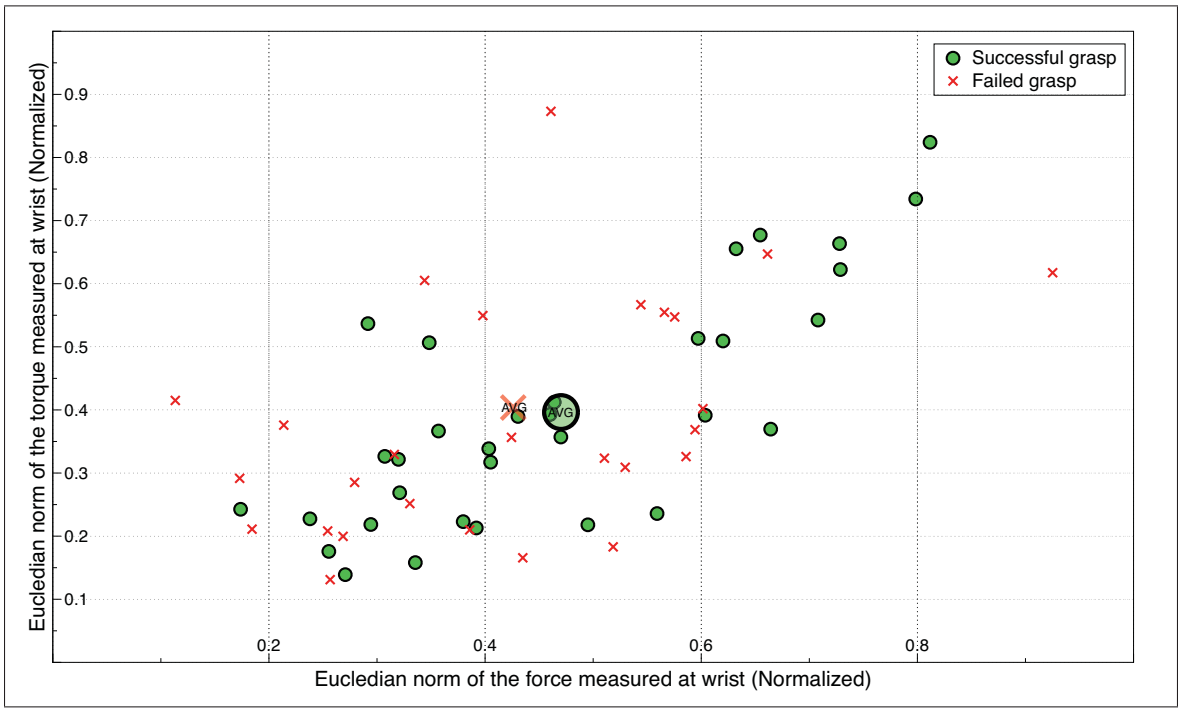

Figure 5.7 Wrist force sensor data analysis for grasp assessment

The grasp assessment is not only limited by the object's palpation; it is also affected by the object's individual properties, such as weight and contact location. During the experiment, we found that the same object, when grasped with the same force, can deliver different results based on the object's weight distribution in the pinch grasp. Therefore, we decided that we also needed to take into account the weight of the object, and the center of mass of the object

relative to the grasping point. The graph shown in Fig. 5.7 corresponds to the force and torque induced by grasping, derived from 6-axis wrist force sensor. Analysis of the graph does not allow us to draw any conclusions, as the data are randomly dispersed, and we cannot observe any specific region or relation.

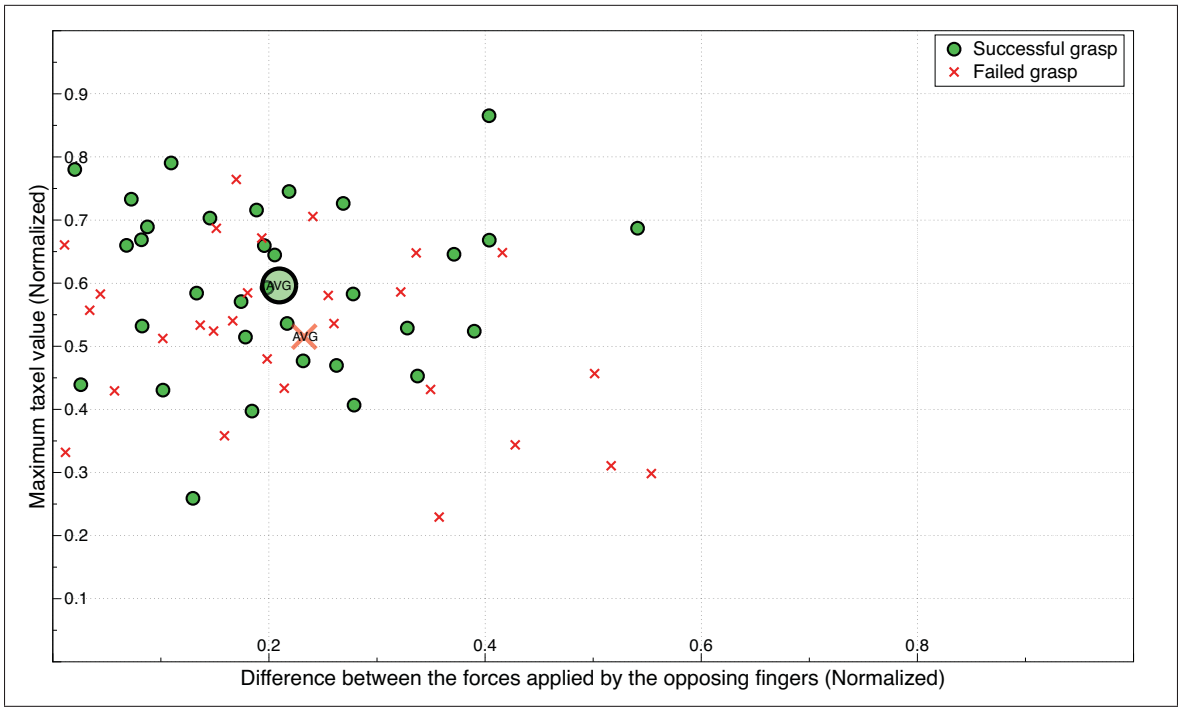

Figure 5.8 Balance of the force to the maximum force in the grasp

Another assumption, and one that we based on human hand grasping strategies, is that the pinch grasp normally has equal and opposing forces from the corresponding pinch grasp fingers. So, a stable grasp should have a balance of forces, which means that the deviation between forces of opposing taxels should be closed to zero. Accordingly, we plotted the maximum force of the grasp to the balance of the force in the grasp, as shown in Fig. 5.8. The graph shows mixed results, and no specific behaviour was found by the investigation of balance of the force details of tactile sensor data.

Some data distribution patterns were found in Fig. 5.6, regarding the correlation of contact location to the tactile image area. However, the rest of the graphs, which are based on the object's properties of weight to the weight distribution during grasping in Fig. 5.7, and the balance of the weight in 5.8, do not illustrate any pattern for grasp estimation. All of these plots have no specific zone that is decoupled, and the four other variables are dispersed entirely at random. Grasp assessment is a multi-featured and sophisticated process that depends on multiple factors. Therefore, we can not declare the anticipated behavior of the grasp based solely on the tactile sensor data shown in Fig. 5.6. Instead, we must also consider other aspects of the object properties: weight and its distribution.

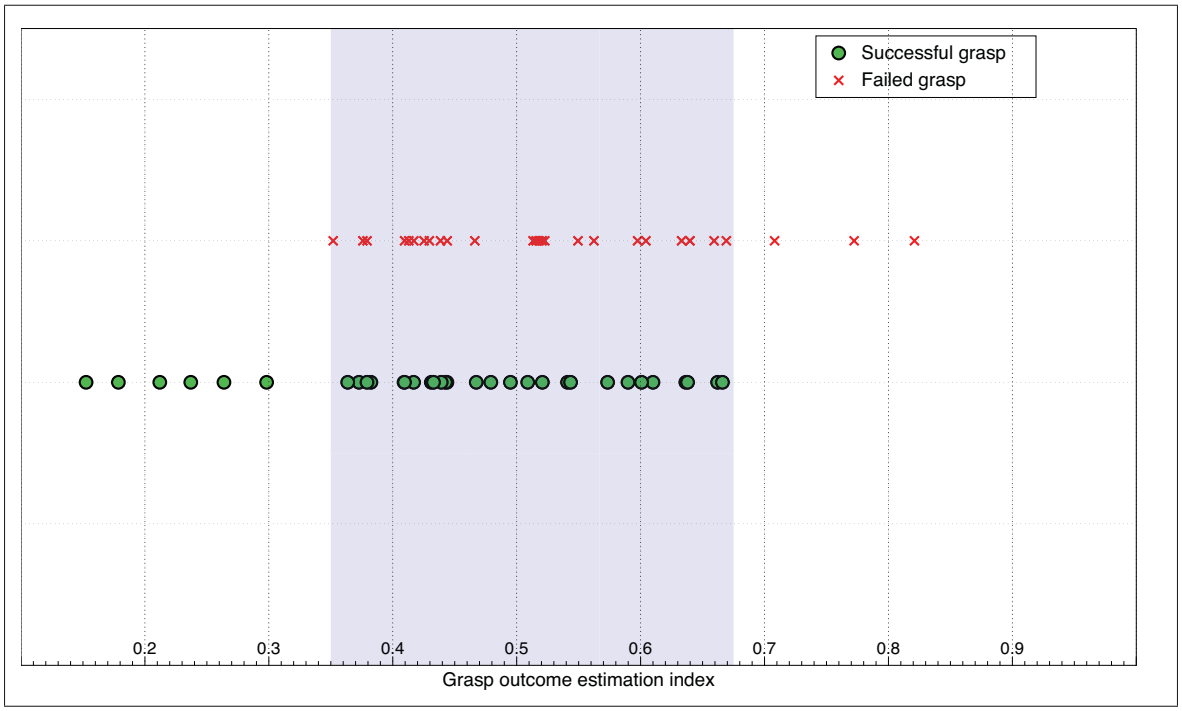

Figure 5.9 Consolidated data of force sensor and tactile sensor for the grasp assessment

For added accuracy of grasp assessment, we conceived the idea of a hybrid index, by including tactile as well as object property information for calculation of the grasp index. The index is useful because it takes all of these trade-offs into account. This grasp index provides a

prediction for the grasp attempt based on six factors: the details of contact area, distance between center of contact to center of phalanger, force, torque, balance of the force during grip and maximum tactile force of the grip. By considering all these factors, we arrived at set of numbers that are normalized between 0 and 1. We normalize them by taking the average score between 0 and 1 for each factor. Generally, a value close to 0 is likely to succeed, and close to 1 is likely to fail. Based on those details we conceived a trend for the grasp assessment model, which is shown in Fig. 5.9.

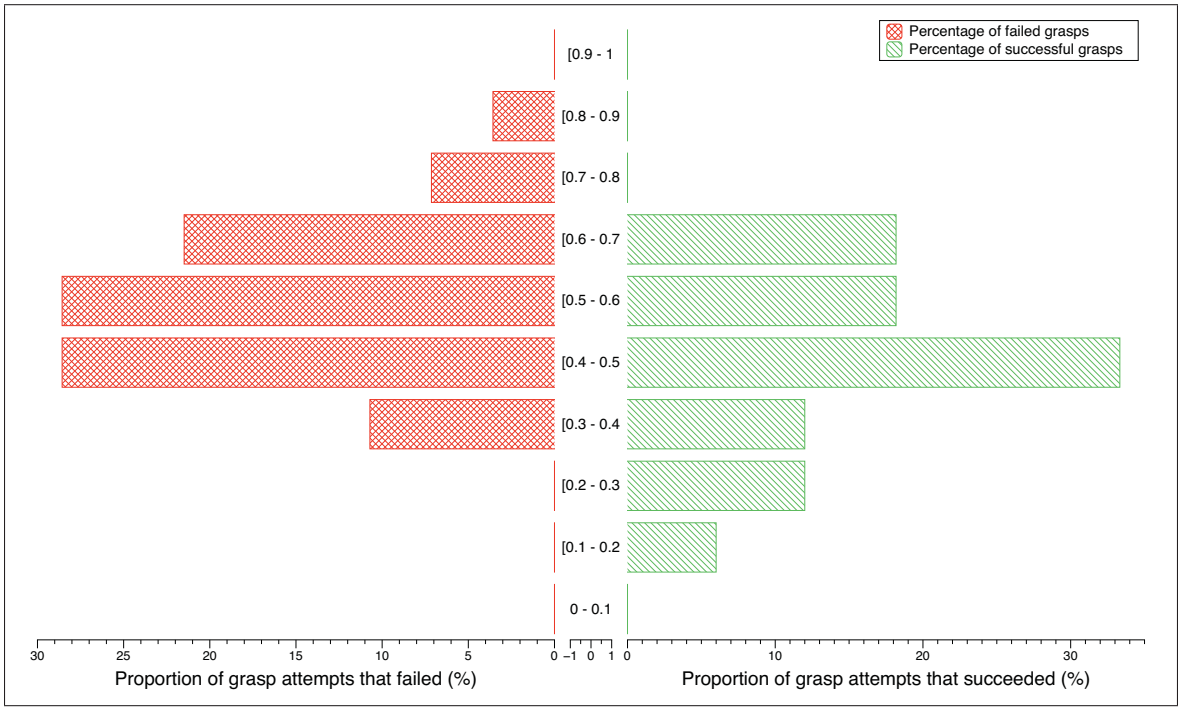

Figure 5.10 Grasp distribution based on the index with their proportions

The successful grasps have a low distance of center of contact, higher area, small torque to force ratio, and low reading for balance of force. Failed grasps have the opposite characteristics. Similar to our anticipated profile for the normalized index, it clearly shows a pattern where successful grasps are randomly distributed close to the index value of 0, and failed ones are close to the index value of 1. Fig. 5.10, which shows a percentage distribution of the failed

grasps to the successful grasps according to their population, also fosters the claim as a generic model for the grasp estimation. However, there is no certainty about the grasp outcome in the huge middle zone, shaded in blue in Fig. 5.9, where no prediction for the outcome could be made due to its transient profile.

Although we have made partial decoupling for the grasp estimation, it is inferior to many existing models that are based on machine learning. However, whereas machine learning involves a completely ciphered neural algorithm based on the pre-defined object properties and details of the grasp environment, our model is more manageable and easy to reconfigure to replicate the results. Bekiroglu *et al.* (2011) has succeeded in grasp estimation with around 86% accuracy, with pre-defined details and known objects. In contrast, we have not used any pre-defined repository for determining the index of grasp estimation. Hence, our deterministic model is easy to use for other sensors, unlike machine learning methods, which are very hard to migrate to another system.

5.4 Conclusion

Chapter 5 presents a deterministic method of estimating grasp stability on the basis of real-time independent data of the tactile image and object properties. Such 'rational' hand-written rules explicitly reveal the predicted outcome of the grasp, based on the grasp index with the instantaneous parameters. The index is able to roughly filters the grasp factors and predict the pattern for success and failure. However we are not claiming it as an alternative to the best available tool, which is machine learning. Unlike the cryptic functioning of machine learning, this chapter presents a deterministic model that enables researchers to trace and tweak data to improve the performance of the estimation algorithm. We are convinced that using machine learning to make a more complex index will definitely help, but this work was valuable to show that certain factors have an impact on grasping, and with our simple approach we were still able to develop a relatively accurate method for estimating the outcome of the grasp attempt.

Although we have achieved good results by including six factors in our index, we believe the inclusion of more input parameters, such as tactile information about surface friction and orientation of the fingertips during grasping, could improve the predictions. Since the inclusion of more factors is likely to increase the accuracy, ultimately this index could be applicable to many more real-world objects.

In future work, we would aim to combine the generic algorithm's details with our present index, to obtain a complex index for predicting the grasps that are presently ambiguous. More precise results could be obtained by feeding more parameters on the tactile side, such as dynamic sensing details and enhanced spatial resolution. The assistance of a vision system, for making the system aware of the object's mass distribution, would greatly diminish the number of failed grasps. We believe that synchronizing all of the positive aspects of machine learning with 'rational' method presented in this chapter will solve the problem of reliable grasp estimation.

CONCLUSION

This thesis presented a multimodal tactile sensor that is based on the capacitive sensing principle, and with a dielectric that includes geometrical and compositional modifications to enhance the sensitivity of the sensor.

Following the biological aspects of tactile sensitivity of the human hand that were discussed in chapter 1, we have listed the essential features to be considered in the design of an artificial tactile sensory apparatus. A repository was formulated based on the properties, performance and distribution of the human tactile cells (mechanoreceptors), and we gave an overview of a variety of sensors that researchers have developed with diverse transduction techniques. Some of the most popular tactile sensing alternatives are described in chapter 2 in the review of literature. Each of these competitors illustrates their distinct pros and cons based on their functionality. During the development of our sensor, we have considered the features of these commercial alternatives and sorted out the essential parameters to be used as the benchmarks for future fabrication.

Chapter 3 presented the implementation of the static type of tactile sensor. The capacitance-based tactile unit was developed by building an innovative dual-layered micro-structured dielectric. We then fabricated the sensor and tested its performance. Based on the review given in chapter 2, all the typical constraints of a dielectric material are addressed by the use of a micro-structured design, and by filling the silicone with the high relative-permittivity nanocomposites. The resulting tactile sensor, with its soft dielectric, displays excellent sensitivity to forces ranging from 10^{-3}N to 15 N.

After accomplishing the pressure-sensing capability, our next goal was to introduce a dynamic-sensing capability that is highly sensitive and has an adequate bandwidth. The addition of dynamic sensing was an important aspect of our sensor, to the significance of dynamic sensing to human tactility. With reference to the multimodal sensors presented in chapter 2, our sensor is based on the same capacitance-sensing principle, which adds ease of construction and compactness to the sensor's design. Our dynamic sensor, which we presented in chapter 4, has

the ability to capture dynamic tactile sensations such as vibrations, slippage and initial contact. Moreover, the goal of uniform sensitivity prompted us to redesign the dynamic taxels, which gave us an increased capacitance effect for dynamic sensing due to the augmented influence of the capacitor's edge effect.

Finally, chapter 5 described the use of the tactile sensor for grasping and manipulation tasks. These were accomplished using the closed loop precision grasp system. An unstable grasp was improved with the generic 'rational' algorithm, executed on ROS by incorporating multimodal feedback from the sensors along with the properties of object, specifically, its weight, and the distribution of its weight during the grip. The hand-written rule-based algorithm exhibited convincing results for estimation of the grasp outcome. In addition, this method circumvented the 'blackbox' estimation behavior of the typical grasp-assessment system, by evaluating the grasp properties through real-time parameters. Such a virtue means that unlike the pre-determined database of machine learning, the method presented in chapter 5 is object-independent.

Further research could be conducted to improve grasp and manipulation performance by designing application-specific tactile sensors. Based on our experience with the grasping experiments performed in chapter 5, future sensors could be upgraded with multiple dynamic taxels, more spatial resolution, and a more compliant sensor structure. The use of more than one dynamic taxel could be helpful for active noise filtering, similar to how headphones achieve noise canceling. An optimized spatial resolution (2mm) could give a more accurate contact location on the sensor's surface, which is quite effective for evaluating a precision grasp. Our current sensor is capable of measuring milli-newton range forces; but in the real world, such hyper-sensitivity has not proven itself to be very significant when it comes to routine grasping and manipulation of objects in everyday life. One might therefore exchange a bit of the sensitivity for increases in spatial and temporal resolution, a trade-off that might allow the sensor to deliver details about tactile contact in a faster and more accurate manner. Lastly, future developments might produce a flexible tactile sensor. This is a viable assumption, as our dielectric is already soft and compliant, and a flexible PCB could be formed with polyimide films. A flexible sensor is an asset for the curved geometries of advanced robotic hands.

From the software point of view, a variety of grasping algorithms could be developed with the data from the multimodal feedback to improve the robotic hand's performance. One could use the high sensitivity of the static sensor to determine the geometrical details of fragile objects, and thus improve the grasp strategy. The sensor's feedback could be integrated with the positions of the robotic fingers to model the shape and size of an object that is being encountered for the first time. Dynamic sensors can also be applied to derive surface information, such as friction and smoothness. A neural system with a texture-recognition algorithm can open new dimensions for the assessment of objects based on surface properties. The multimodal tactile sensor can be combined with a haptic interface to convey a sense of touch through prosthetic limbs. Finally, from the perspective of the sensor network, node expansion capabilities are possible through use of wireless communication ICs in the sensor design.

As we hope that artificial tactile sensors will eventually match the human tactile apparatus, they must perform with multimodal tactile sensitivity in a way that is similar to the human tactile sensory apparatus. The tactile sensor will surely evolve further with the emergence of novel technologies. Nevertheless, the sensor presented in this thesis has marked a stepping stone for future research and development.

BIBLIOGRAPHY

Akasofu, K. and M. R. Neuman. 1991. "A thin-film variable capacitance shear force sensor for medical and robotics applications". In *Engineering in Medicine and Biology Society, 1991. Vol. 13: 1991., Proceedings of the Annual International Conference of the IEEE*. p. 1601–1602. IEEE.

Alirezaei, H., A. Nagakubo, and Y. Kuniyoshi. 2009. "A tactile distribution sensor which enables stable measurement under high and dynamic stretch". In *3D User Interfaces, 2009. 3DUI 2009. IEEE Symposium on*. p. 87–93. IEEE.

Almassri, A. M., W. Wan Hasan, S. Ahmad, A. Ishak, A. Ghazali, D. Talib, and C. Wada. 2015. "Pressure Sensor: State of the Art, Design, and Application for Robotic Hand". *Journal of Sensors*.

Baldyga, J., W. Orciuch, L. Makowski, K. Malik, G. Özcan-Taskin, W. Eagles, and G. Padron. 2008. "Dispersion of nanoparticle clusters in a rotor-stator mixer". *Industrial & Engineering Chemistry Research*, vol. 47, n° 10, p. 3652–3663.

Bekiroglu, Y., R. Detry, and D. Kragic. 2011. "Learning tactile characterizations of object- and pose-specific grasps". In *Intelligent Robots and Systems (IROS), 2011 IEEE/RSJ International Conference on*. p. 1554–1560. IEEE.

Blank, A., A. M. Okamura, and K. J. Kuchenbecker. 2010. "Identifying the role of proprioception in upper-limb prosthesis control: Studies on targeted motion". *ACM Transactions on Applied Perception (TAP)*, vol. 7, n° 3, p. 15.

Bloor, D., K. Donnelly, P. Hands, P. Laughlin, and D. Lussey. 2005. "A metal–polymer composite with unusual properties". *Journal of Physics D: Applied Physics*, vol. 38, n° 16, p. 2851.

Burgess, P. and E. Perl. 1973. Cutaneous mechanoreceptors and nociceptors. Iggo, A., editor, *Somatosensory System*, volume 2 of *Handbook of Sensory Physiology*, p. 29-78. Springer Berlin Heidelberg. ISBN 978-3-642-65440-4. doi: 10.1007/978-3-642-65438-1_3. <http://dx.doi.org/10.1007/978-3-642-65438-1_3>.

Carpi, F., D. De Rossi, and R. Kornbluh, 2008. *Dielectric elastomers as electromechanical transducers: Fundamentals, materials, devices, models and applications of an emerging electroactive polymer technology*.

Castelli, F. 2002. "An integrated tactile-thermal robot sensor with capacitive tactile array". *Industry Applications, IEEE Transactions on*, vol. 38, n° 1, p. 85–90.

Cheng, M., X. Huang, C. Ma, and Y. Yang. 2009. "A flexible capacitive tactile sensing array with floating electrodes". *Journal of Micromechanics and Microengineering*, vol. 19, n° 11, p. 115001.

Cherney, E. 2005. "Silicone rubber dielectrics modified by inorganic fillers for outdoor high voltage insulation applications". *Dielectrics and Electrical Insulation, IEEE Transactions on*, vol. 12, n° 6, p. 1108–1115.

Chew, W. C. and J. A. Kong. 1980. "Effects of fringing fields on the capacitance of circular microstrip disk". *Microwave Theory and Techniques, IEEE Transactions on*, vol. 28, n° 2, p. 98–104.

Choi, B., H. R. Choi, and S. Kang. Aug 2005a. "Development of tactile sensor for detecting contact force and slip". In *Intelligent Robots and Systems, 2005. (IROS 2005). 2005 IEEE/RSJ International Conference on*. p. 2638-2643.

Choi, B., H. R. Choi, and S. Kang. 2005b. "Development of tactile sensor for detecting contact force and slip". In *Intelligent Robots and Systems, 2005.(IROS 2005). 2005 IEEE/RSJ International Conference on*. p. 2638–2643. IEEE.

Chorley, C., C. Melhuish, T. Pipe, and J. Rossiter. 2009. "Development of a tactile sensor based on biologically inspired edge encoding". In *Advanced Robotics, 2009. ICAR 2009. International Conference on*. p. 1–6. IEEE.

Chung, S., I. Kim, and S. Kang. 2004. "Strong nonlinear current–voltage behaviour in perovskite-derivative calcium copper titanate". *Nature materials*, vol. 3, n° 11, p. 774–778.

Clement, R., K. Bugler, and C. Oliver. 2011. "Bionic prosthetic hands: a review of present technology and future aspirations". *The surgeon*, vol. 9, n° 6, p. 336–340.

Cotton, D. P., P. H. Chappell, A. Cranny, N. M. White, and S. P. Beeby. 2007. "A novel thick-film piezoelectric slip sensor for a prosthetic hand". *Sensors Journal, IEEE*, vol. 7, n° 5, p. 752–761.

Cutkosky, M. R. and J. M. Hyde. 1993. "Manipulation control with dynamic tactile sensing". In *6th international symposium on robotics research, Hidden Valley, Pennsylvania*.

Cutkosky, M. R., R. D. Howe, and W. R. Provancher. 2008. Force and tactile sensors. *Springer Handbook of Robotics*, p. 455–476. Springer.

Dahiya, R. S. and M. Valle. 2008. "Tactile sensing for robotic applications". *Sensors, Focus on Tactile, Force and Stress Sensors*, p. 298–304.

Dahiya, R. S., G. Metta, M. Valle, and G. Sandini. 2010. "Tactile sensing—from humans to humanoids". *Robotics, IEEE Transactions on*, vol. 26, n° 1, p. 1–20.

Dang, H. and P. K. Allen. 2012. "Learning grasp stability". In *Robotics and Automation (ICRA), 2012 IEEE International Conference on*. p. 2392–2397. IEEE.

Dang, H. and P. K. Allen. 2014. "Stable grasping under pose uncertainty using tactile feedback". *Autonomous Robots*, vol. 36, n° 4, p. 309–330.

Dang, Z., Y. Lin, H. Xu, C. Shi, S. Li, and J. Bai. 2008. "Fabrication and dielectric characterization of advanced BaTiO3/polyimide nanocomposite films with high thermal stability". *Advanced Functional Materials*, vol. 18, n° 10, p. 1509–1517.

Dargahi, J. and S. Najarian. 2004. "Human tactile perception as a standard for artificial tactile sensing—a review". *The International Journal of Medical Robotics and Computer Assisted Surgery*, vol. 1, n° 1, p. 23–35.

Dellon, E., K. Keller, V. Moratz, and A. Dellon. 1995. "The relationships between skin hardness, pressure perception and two-point discrimination in the fingertip". *The Journal of Hand Surgery: British & European Volume*, vol. 20, n° 1, p. 44–48.

Dennerlein, J. T., P. A. Millman, and R. D. Howe. 1997. "Vibrotactile feedback for industrial telemanipulators". In *Sixth Annual Symposium on Haptic Interfaces for Virtual Environment and Teleoperator Systems, ASME International Mechanical Engineering Congress and Exposition*. p. 189–195.

Dubey, V. N. and R. M. Crowder. 2006. "A dynamic tactile sensor on photoelastic effect". *Sensors and Actuators A: Physical*, vol. 128, n° 2, p. 217–224.

Ehrsson, H., A. Fagergren, and H. Forssberg. 2001. "Differential fronto-parietal activation depending on force used in a precision grip task: an fMRI study". *Journal of Neurophysiology*, vol. 85, n° 6, p. 2613–2623.

Fagiani, R., F. Massi, E. Chatelet, Y. Berthier, and A. Akay. 2011. "Tactile perception by friction induced vibrations". *Tribology International*, vol. 44, n° 10, p. 1100–1110.

Fearing, R., A. Rise, and T. Binford. 1987. "A Tactile sensing finger tip for a dextrous hand". In *Cambridge Symposium_Intelligent Robotics Systems*. p. 378–387. International Society for Optics and Photonics.

Fishel, J., V. J. Santos, G. E. Loeb, et al. 2008. "A robust micro-vibration sensor for biomimetic fingertips". In *Biomedical Robotics and Biomechatronics, 2008. BioRob 2008. 2nd IEEE RAS & EMBS International Conference on*. p. 659–663. IEEE.

Florant, D. 2014. "Développement d'un appareil haptique transmettant par pression des évènements tactiles extéroceptifs". PhD thesis, École de technologie supérieure.

Gasulla, M., X. Li, and G. Meijer. 2005. "The noise performance of a high-speed capacitive-sensor interface based on a relaxation oscillator and a fast counter". *Instrumentation and Measurement, IEEE Transactions on*, vol. 54, n° 5, p. 1934–1940.

Goeger, D., N. Ecker, and H. Woern. 2009. "Tactile sensor and algorithm to detect slip in robot grasping processes". In *Robotics and Biomimetics, 2008. ROBIO 2008. IEEE International Conference on*. p. 1480–1485. IEEE.

Goldfeder, C. and P. K. Allen. 2011. "Data-driven grasping". *Autonomous Robots*, vol. 31, n° 1, p. 1–20.

Guillemet-Fritsch, S., T. Lebey, M. Boulos, and B. Durand. 2006. "Dielectric properties of CaCu3Ti4O12 based multiphased ceramics". *Journal of the European Ceramic Society*, vol. 26, n° 7, p. 1245–1257.

Halata, Z. and K. Baumann. 2008. Anatomy of receptors. Grunwald, M., editor, *Human Haptic Perception: Basics and Applications*, p. 85-92. Birkhäuser Basel. ISBN 978-3-7643-7611-6. doi: 10.1007/978-3-7643-7612-3_6. <http://dx.doi.org/10.1007/978-3-7643-7612-3_6>.

Haschke, R. 2015. Grasping and manipulation of unknown objects based on visual and tactile feedback. Carbone, G. and Fernando Gomez-Bravo, editors, *Motion and Operation Planning of Robotic Systems*, volume 29 of *Mechanisms and Machine Science*, p. 91-109. Springer International Publishing. ISBN 978-3-319-14704-8. doi: 10.1007/978-3-319-14705-5_4. <http://dx.doi.org/10.1007/978-3-319-14705-5_4>.

Heyneman, B. and M. R. Cutkosky. 2014. "Slip Classification for Dynamic Tactile Array Sensors".

Ho, C., W.-S. Su, C.-F. Hu, C.-M. Lin, W. Fang, and F.-L. Yang. 2010. "A flexible, highly-sensitive, and easily-fabricated carbon-nanotubes tactile sensor on polymer substrate". In *2010 10th IEEE International Conference on Solid-State and Integrated Circuit Technology*. p. 1388–1391.

Ho, V. A., D. V. Dao, S. Sugiyama, and S. Hirai. 2011. "Development and analysis of a sliding tactile soft fingertip embedded with a microforce/moment sensor". *Robotics, IEEE Transactions on*, vol. 27, n° 3, p. 411–424.

Hoshi, T. and H. Shinoda. 2006. "Robot skin based on touch-area-sensitive tactile element". In *Robotics and Automation, 2006. ICRA 2006. Proceedings 2006 IEEE International Conference on*. p. 3463–3468. Ieee.

Howe, R. D. and M. R. Cutkosky. 1989. "Sensing skin acceleration for slip and texture perception". In *Robotics and Automation, 1989. Proceedings., 1989 IEEE International Conference on*. p. 145–150. IEEE.

Howe, R. D. and M. R. Cutkosky. 1993. "Dynamic tactile sensing: Perception of fine surface features with stress rate sensing". *Robotics and Automation, IEEE Transactions on*, vol. 9, n° 2, p. 140–151.

Hu, X., X. Zhang, M. Liu, Y. Chen, P. Li, W. Pei, C. Zhang, and H. Chen. 2014. "A flexible capacitive tactile sensor array with micro structure for robotic application". *Science China Information Sciences*, vol. 57, n° 12, p. 1–6.

Huang, Y., B. Xiang, X. Ming, X. Fu, and Y. Ge. 2008. "Conductive mechanism research based on pressure-sensitive conductive composite material for flexible tactile sensing". In *Information and Automation, 2008. ICIA 2008. International Conference on*. p. 1614–1619. IEEE.

Hwang, E.-S., J.-H. Seo, and Y.-J. Kim. 2006. "A polymer-based flexible tactile sensor for normal and shear load detection". In *Micro Electro Mechanical Systems, 2006. MEMS 2006 Istanbul. 19th IEEE International Conference on*. p. 714–717. IEEE.

Hyttinen, E., D. Kragic, and R. Detry. 2015. "Learning the Tactile Signatures of Prototypical Object Parts for Robust Part-based Grasping of Novel Objects". In *IEEE International Conference on Robotics and Automation*.

Ito, Y., Y. Kim, C. Nagai, and G. Obinata. 2011. "Contact state estimation by vision-based tactile sensors for dexterous manipulation with robot hands based on shape-sensing". *Int. J. Adv. Robot. Syst*, vol. 8, n° 4, p. 225–234.

Jaimes, A. and N. Sebe. 2007. "Multimodal human–computer interaction: A survey". *Computer vision and image understanding*, vol. 108, n° 1, p. 116–134.

Kato, Y., T. Mukai, T. Hayakawa, and T. Shibata. 2007. "Tactile sensor without wire and sensing element in the tactile region based on EIT method". In *Sensors, 2007 IEEE*. p. 792–795. IEEE.

Khastgir, D. and K. Adachi. 1999. "Piezoelectric and dielectric properties of siloxane elastomers filled with bariumtitanate". *Journal of Polymer Science Part B: Polymer Physics*, vol. 37, n° 21, p. 3065–3070.

Khastgir, D. and K. Adachi. 2000. "Rheological and dielectric studies of aggregation of barium titanate particles suspended in polydimethylsiloxane". *Polymer*, vol. 41, n° 16, p. 6403–6413.

Kleinhans, G. 2015. "The skin as a sense and communication organ". <http://www.skin-care-forum.basf.com/docs/default-source/Copyright/skin-care-forum_list-of-copyright-holders.pdf?sfvrsn=4>.

Koskinen, E. 2008. "Optimizing tactile feedback for virtual buttons in mobile devices". PhD thesis, Helsinki University of Technology.

Kyberd, P. J., C. Wartenberg, L. Sandsjö, S. Jönsson, D. Gow, J. Frid, C. Almström, and L. Sperling. 2007. "Survey of upper-extremity prosthesis users in Sweden and the United Kingdom". *JPO: Journal of Prosthetics and Orthotics*, vol. 19, n° 2, p. 55–62.

Lederman, S. J. and R. L. Klatzky. 2009. "Haptic perception: A tutorial". *Attention, Perception, & Psychophysics*, vol. 71, n° 7, p. 1439–1459.

Lee, H.-K., J. Chung, S.-I. Chang, and E. Yoon. 2008. "Normal and shear force measurement using a flexible polymer tactile sensor with embedded multiple capacitors". *Microelectromechanical Systems, Journal of*, vol. 17, n° 4, p. 934–942.

Lee, M. H. and H. R. Nicholls. 1999. "Review Article Tactile sensing for mechatronics—a state of the art survey". *Mechatronics*, vol. 9, n° 1, p. 1–31.

Leeper, A. E., K. Hsiao, M. Ciocarlie, L. Takayama, and D. Gossow. 2012. "Strategies for Human-in-the-loop Robotic Grasping". In *Proceedings of the Seventh Annual ACM/IEEE International Conference on Human-Robot Interaction*. (New York, NY, USA 2012), p. 1–8. ACM.

Leineweber, M., G. Pelz, M. Schmidt, H. Kappert, and G. Zimmer. 2000. "New tactile sensor chip with silicone rubber cover". *Sensors and Actuators A: Physical*, vol. 84, n° 3, p. 236–245.

Leus, V. and D. Elata. 2004. "Fringing field effect in electrostatic actuators". *Technion-Israel Institute of Technology Technical Report No. ETR-2004-2*.

Lin, C. H., T. W. Erickson, J. Fishel, N. Wettels, G. E. Loeb, et al. 2009. "Signal processing and fabrication of a biomimetic tactile sensor array with thermal, force and microvibration modalities". In *Robotics and Biomimetics (ROBIO), 2009 IEEE International Conference on*. p. 129–134. IEEE.

Liu, B. and M. Shaw. 2001. "Electrorheology of filled silicone elastomers". *Journal of Rheology*, vol. 45, n° 3, p. 641–657.

Loomis, J. M. and S. J. Lederman. 1986. "Tactual perception". *Handbook of perception and human performances*, vol. 2, p. 2.

Maggiali, M., G. Cannata, P. Maiolino, G. Metta, M. Randazzo, and G. Sandini. 2008. "Embedded distributed capacitive tactile sensor". In *11th Mechatronics Forum Biennial International Conference*. Citeseer.

Mannsfeld, S., B. Tee, R. Stoltenberg, C. Chen, S. Barman, B. Muir, A. Sokolov, C. Reese, and Z. Bao. 2010. "Highly sensitive flexible pressure sensors with microstructured rubber dielectric layers". *Nature Materials*, vol. 9, n° 10, p. 859–864.

Mattar, E. 2013. "A survey of bio-inspired robotics hands implementation: New directions in dexterous manipulation". *Robotics and Autonomous Systems*, vol. 61, n° 5, p. 517 - 544.

Mayol-Cuevas, W., J. Juarez-Guerrero, and S. Munoz-Gutierrez. 1998. "A first approach to tactile texture recognition". In *Systems, Man, and Cybernetics, 1998. 1998 IEEE International Conference on*. p. 4246–4250. IEEE.

Mazid, A. M. and R. A. Russell. 2006. "A robotic opto-tactile sensor for assessing object surface texture". In *Robotics, Automation and Mechatronics, 2006 IEEE Conference on*. p. 1–5. IEEE.

Merzenich, M. and T. Harrington. 1969. "The sense of flutter-vibration evoked by stimulation of the hairy skin of primates: Comparison of human sensory capacity with the responses of mechanoreceptive afferents innervating the hairy skin of monkeys". *Experimental Brain Research*, vol. 9, n° 3, p. 236-260.

Mindtrans. 2015. "Advanced robotic/ prosthetic Hands/Arms". <http://mindtrans.narod.ru/hands/hands.htm>.

Nghiem, B. T., I. C. Sando, R. B. Gillespie, B. L. McLaughlin, G. J. Gerling, N. B. Langhals, M. G. Urbanchek, and P. S. Cederna. 2015. "Providing a Sense of Touch to Prosthetic Hands". *Plastic and Reconstructive Surgery*, vol. 135, n° 6, p. 1652–1663.

Nicholls, H. R. and M. H. Lee. 1989. "A survey of robot tactile sensing technology". *The International Journal of Robotics Research*, vol. 8, n° 3, p. 3–30.

Nishiyama, H. and M. Nakamura. 1993. "Capacitance of disk capacitors". *Components, Hybrids, and Manufacturing Technology, IEEE Transactions on*, vol. 16, n° 3, p. 360–366.

Park, Y.-L., C. Majidi, R. Kramer, P. Bérard, and R. J. Wood. 2010. "Hyperelastic pressure sensing with a liquid embedded elstomer". *Journal of Micromechanics and Microengineering*, vol. 20, n° 12.

Park, Y., K. Chau, R. Black, and M. Cutkosky. 2007. "Force sensing robot fingers using embedded fiber Bragg grating sensors and shape deposition manufacturing". In *Robotics and Automation, 2007 IEEE International Conference on*. p. 1510–1516. Ieee.

Peng, J. and M. Lu. 2015. "A Flexible Capacitive Tactile Sensor Array with CMOS Readout Circuits for Pulse Diagnosis".

Peratech, h. l. "QTC^{TM} Material Science". <http://www.peratech.com/qtc-science.html>.

Pressure Profile Systems, I. "RoboTouch/DigiTacts tactile sensors by PPS". <http://www.pressureprofile.com/>.

Provancher, W. R. 2003. "On tactile sensing and display". PhD thesis, Citeseer.

Pyun, S., Y. Jin, and G. Lee. 2002. "Dielectric properties of Pb (Mg1/3Nb2/3) O3-PbTiO3/polyurethane 0–3 composites". *Journal of materials science letters*, vol. 21, n° 3, p. 243–244.

Qi, L., B. Lee, W. Samuels, G. Exarhos, and S. Parler Jr. 2006. "Three-phase percolative silver–BaTiO3–epoxy nanocomposites with high dielectric constants". *Journal of applied polymer science*, vol. 102, n° 2, p. 967–971.

Randall, C., S. Miyazaki, K. More, A. Bhalla, and R. Newnham. 1992. "Structural-property relationships in dielectrophoretically assembled BaTiO3 nanocomposites". *Materials Letters*, vol. 15, n° 1, p. 26–30.

Rao, Y., S. Ogitani, P. Kohl, and C. Wong. 2001. "Novel polymer–ceramic nanocomposite based on high dielectric constant epoxy formula for embedded capacitor application". *Journal of Applied Polymer Science*, vol. 83, n° 5, p. 1084–1090.

Raspopovic, S., M. Capogrosso, F. M. Petrini, M. Bonizzato, J. Rigosa, G. Di Pino, J. Carpaneto, M. Controzzi, T. Boretius, E. Fernandez, et al. 2014. "Restoring natural sensory feedback in real-time bidirectional hand prostheses". *Science translational medicine*, vol. 6, n° 222, p. 222ra19–222ra19.

Romano, J. M., S. R. Gray, N. T. Jacobs, and K. J. Kuchenbecker. 2009. "Toward tactilely transparent gloves: Collocated slip sensing and vibrotactile actuation". In *EuroHaptics conference, 2009 and Symposium on Haptic Interfaces for Virtual Environment and Teleoperator Systems. World Haptics 2009. Third Joint*. p. 279–284. IEEE.

Sanz, P. J., A. P. Del Pobil, J. M. Inesta, and G. Recatala. 1998. "Vision-guided grasping of unknown objects for service robots". In *Robotics and Automation, 1998. Proceedings. 1998 IEEE International Conference on*. p. 3018–3025. IEEE.

Schmidt, P. A., E. Maël, and R. P. Würtz. 2006a. "A sensor for dynamic tactile information with applications in human–robot interaction and object exploration". *Robotics and Autonomous Systems*, vol. 54, n° 12, p. 1005–1014.

Schmidt, P. A., E. Maël, and R. P. Würtz. 2006b. "A sensor for dynamic tactile information with applications in human–robot interaction and object exploration". *Robotics and Autonomous Systems*, vol. 54, n° 12, p. 1005 - 1014.

Schmitz, A., M. Maggiali, L. Natale, B. Bonino, and G. Metta. 2010. "A tactile sensor for the fingertips of the humanoid robot iCub". In *In IEEE/RSJ International Conference on Intelligent Robots and Systems*.

Schmitz, A., P. Maiolino, M. Maggiali, L. Natale, G. Cannata, and G. Metta. 2011. "Methods and Technologies for the Implementation of Large-Scale Robot Tactile Sensors". *Robotics, IEEE Transactions on*, , p. 1–12.

Scott, A. H. and H. Curtis. 1939. "Edge correction in the determination of dielectric constant". *Journal of Research*, p. 747–775.

Shen, Y., E. Cherney, and S. Jayaram. 2004. "Electric stress grading of composite bushings using high dielectric constant silicone compositions". In *Electrical Insulation, 2004. Conference Record of the 2004 IEEE International Symposium on*. p. 320–323. IEEE.

Sherrick Jr, C. E. 1953. "Variables affecting sensitivity of the human skin to mechanical vibration.". *Journal of Experimental Psychology*, vol. 45, n° 5, p. 273.

Shimojo, M., A. Namiki, M. Ishikawa, R. Makino, and K. Mabuchi. 2004. "A tactile sensor sheet using pressure conductive rubber with electrical-wires stitched method". *Sensors Journal, IEEE*, vol. 4, n° 5, p. 589–596.

Stassi, S., V. Cauda, G. Canavese, and C. F. Pirri. 2014. "Flexible tactile sensing based on piezoresistive composites: a review". *Sensors*, vol. 14, n° 3, p. 5296–5332.

Stillman, B. C. 2002. "Making sense of proprioception: the meaning of proprioception, kinaesthesia and related terms". *Physiotherapy*, vol. 88, n° 11, p. 667–676.

Su, W.-S., C.-F. Hu, C.-M. Lin, and W. Fang. 2010. "Development of a 3D distributed carbon nanotubes on flexible polymer for normal and shear forces measurement". In *Micro Electro Mechanical Systems (MEMS), 2010 IEEE 23rd International Conference on*. p. 615–618. IEEE.

Surapaneni, R., Q. Guo, Y. Xie, D. Young, and C. Mastrangelo. 2013. "A three-axis high-resolution capacitive tactile imager system based on floating comb electrodes". *Journal of Micromechanics and Microengineering*, vol. 23, n° 7, p. 075004.

Tanaka, Y., Y. Horita, A. Sano, and H. Fujimoto. 2011. "Tactile sensing utilizing human tactile perception". In *World Haptics Conference (WHC), 2011 IEEE*. p. 621–626. IEEE.

Tenzer, Y., L. P. Jentoft, and R. D. Howe. 2014. "Inexpensive and easily customized tactile array sensors using mems barometers chips". *IEEE Robotics and Automation Magazine*.

Teshigawara, S., K. Tadakuma, A. Ming, M. Ishikawa, and M. Shimojo. 2010. "High sensitivity initial slip sensor for dexterous grasp". In *Robotics and Automation (ICRA), 2010 IEEE International Conference on*. p. 4867–4872. IEEE.

Thanh-Vinh, N., N. Binh-Khiem, H. Takahashi, K. Matsumoto, and I. Shimoyama. 2014. "High-sensitivity triaxial tactile sensor with elastic microstructures pressing on piezoresistive cantilevers". *Sensors and Actuators A: Physical*, vol. 215, p. 167–175.

Tise, B. 1988. "A compact high resolution piezoresistive digital tactile sensor". In *Robotics and Automation, 1988. Proceedings., 1988 IEEE International Conference on*. p. 760–764. IEEE.

Toledo, C., L. Leija, R. Munoz, A. Vera, et al. 2009. "Upper limb prostheses for amputations above elbow: A review". In *Health Care Exchanges, 2009. PAHCE 2009. Pan American*. p. 104–108. IEEE.

Tomer, V. and C. Randall. 2008. "High field dielectric properties of anisotropic polymer-ceramic composites". *Journal of Applied Physics*, vol. 104, n° 7, p. 074106–074106.

Tremblay, M. R. and M. R. Cutkosky. 1993. "Estimating friction using incipient slip sensing during a manipulation task". In *Robotics and Automation, 1993. Proceedings., 1993 IEEE International Conference on*. p. 429–434. IEEE.

Ulmen, J. and M. Cutkosky. 2010. "A robust, low-cost and low-noise artificial skin for human-friendly robots". In *Robotics and Automation (ICRA), 2010 IEEE International Conference on*. p. 4836–4841. IEEE.

Vallbo, Å. B., R. Johansson, et al. 1984. "Properties of cutaneous mechanoreceptors in the human hand related to touch sensation". *Hum Neurobiol*, vol. 3, n° 1, p. 3–14.

Van Boven, R. W. and K. O. Johnson. 1994. "The limit of tactile spatial resolution in humans Grating orientation discrimination at the lip, tongue, and finger". *Neurology*, vol. 44, n° 12, p. 2361–2361.

Vatani, M., E. D. Engeberg, and J.-W. Choi. 2013. "Force and slip detection with direct-write compliant tactile sensors using multi-walled carbon nanotube/polymer composites". *Sensors and Actuators A: physical*, vol. 195, p. 90–97.

Vincent Hayward, X. D. 2015. "Tactile Labs Inc.". <http://www.tactilelabs.com/products/haptics/haptuator-mark-ii-v2/>.

Vinogradov, A. and F. Holloway. 1999. "Electro-mechanical properties of the piezoelectric polymer PVDF". *Ferroelectrics*, vol. 226, n° 1, p. 169–181.

Walsh, L. D., J. L. Taylor, and S. C. Gandevia. 2014. Proprioceptive mechanisms and the human hand. *The Human Hand as an Inspiration for Robot Hand Development*, p. 123–141. Springer.

Wang, L., T. Ding, and P. Wang. 2009. "Thin flexible pressure sensor array based on carbon black/silicone rubber nanocomposite". *IEEE Sensors Journal*, vol. 9, n° 9, p. 1130–1135.

Wang, Y., K. Xi, G. Liang, M. Mei, and Z. Chen. 2014. "A flexible capacitive tactile sensor array for prosthetic hand real-time contact force measurement". In *Information and Automation (ICIA), 2014 IEEE International Conference on*. p. 937–942. IEEE.

Wang, Y., Y. Wang, S. Patel, and D. Patel. 2006. "A layered reference model of the brain (LRMB)". *Systems, Man, and Cybernetics, Part C: Applications and Reviews, IEEE Transactions on*, vol. 36, n° 2, p. 124–133.

Weiss, K. and H. Woern. 2004. "Tactile sensor system for an anthropomorphic robotic hand". In *IEEE International conference on manipulation and grasping IMG*.

Weiß, K. and H. Wörn. 2005. "The working principle of resistive tactile sensor cells". In *Mechatronics and Automation, 2005 IEEE International Conference*. p. 471–476. IEEE.

Westling, G. and R. S. Johansson. 1987. "Responses in glabrous skin mechanoreceptors during precision grip in humans". *Experimental Brain Research*, vol. 66, n° 1, p. 128–140.

Wettels, N., D. Popovic, V. J. Santos, R. S. Johansson, and G. E. Loeb. 2007. "Biomimetic tactile sensor for control of grip". In *Rehabilitation Robotics, 2007. ICORR 2007. IEEE 10th International Conference on*. p. 923–932. IEEE.

Wettels, N., J. Fishel, and G. Loeb. 2014. Multimodal tactile sensor. Balasubramanian, R. and Veronica J. Santos, editors, *The Human Hand as an Inspiration for Robot Hand Development*, volume 95 of *Springer Tracts in Advanced Robotics*, p. 405-429. Springer International Publishing. ISBN 978-3-319-03016-6. doi: 10.1007/978-3-319-03017-3_19. <http://dx.doi.org/10.1007/978-3-319-03017-3_19>.

Yamada, Y., T. Maeno, I. Fujimoto, T. Morizono, and Y. Umetani. 2002. "Identification of incipient slip phenomena based on the circuit output signals of PVDF film strips embedded in artificial finger ridges". In *Proceedings of the SICE Annual Conference*. p. 3272–3277.

Yoneda, Y., K. Sakaue, and H. Terauchi. 2000. "Dielectric Investigation of BaTiO3 Thin-Film Capacitor". *Japanese Journal of Applied Physics*, vol. 39, p. 4839.

Yousef, H., M. Boukallel, and K. Althoefer. 2011. "Tactile sensing for dexterous in-hand manipulation in robotics—A review". *Sensors and Actuators A: physical*, vol. 167, n° 2, p. 171–187.

Yussof, H. B., M. Ohka, H. Suzuki, N. Morisawa, and J. Takata. 2008. "Tactile Sensing-Based Control Architecture in Multi-Fingered Arm for Object Manipulation.". *Engineering Letters*, vol. 16, n° 2, p. 236–247.

Zhang, T., H. Liu, L. Jiang, S. Fan, and J. Yang. 2013. "Development of a flexible 3-D tactile sensor system for anthropomorphic artificial hand". *Sensors Journal, IEEE*, vol. 13, n° 2, p. 510–518.